

# Identification of CYP2E1-dependent Genes Involved in Carbon Tetrachloride-induced Hepatotoxicity

YANG LEI

楊 磊

A Thesis Submitted in Partial Fulfillment of the  
Requirements for the Degree of  
Master of Philosophy  
in  
Biochemistry

©The Chinese University of Hong Kong

August, 2001

The Chinese University of Hong Kong holds the copyright of this thesis. Any person(s) intending to use a part or whole of the materials in the thesis in a proposed publication must seek copyright release from the Dean of the Graduate School.



## ACKNOWLEDGEMENTS

I would like to express my sincere heartfelt thank to Prof. Lee Sau Tuen Susanna, my supervisor, for providing me a precious opportunity to conduct research in her well-equipped laboratory and for her insightful direction on my research work.

I would appreciate Prof. Tsang Sau Cheuk David and Prof. Cheung Wing Tai for their generous permission for me to use the facilities and equipment in their laboratories.

Particular thanks are due to Dr. Tian Li for her valuable advice and great help on my research project. I also would like to thank Ms. Lee Wan Chi and Ms. Lee Yun Ling for their technical assistance and for helping me to purchase chemicals, Ms. Lee Wing Sum, Mr. Lee Yiu Fai, and other colleagues who work in Science Center 294 for teaching me to use experimental equipment in this laboratory.

Special thanks should be expressed to my dear parents, fiancée, and younger brother for their encouragement and constant support throughout my study.

## ABSTRACT

Carbon tetrachloride (CCl<sub>4</sub>) was once widely used as industrial and household cleaning fluid, organic solvent and anthelmintic drug. Minor uses of CCl<sub>4</sub> as household reagent and fire extinguishers still exist in some developing countries. Previous studies demonstrated that exposure to CCl<sub>4</sub> could cause liver injury in both human and rodents. It is known that CYP2E1, an isoform of P450, is generally considered responsible for CCl<sub>4</sub>-induced hepatotoxicity. Our previous studies using CYP2E1-null mice further confirmed the involvement of CYP2E1 in CCl<sub>4</sub>-induced liver injury.

Although by now we have already obtained some basic information about the biochemical mechanism of CCl<sub>4</sub>-induced hepatotoxicity, the exact molecular mechanism of this process is still poorly understood. In this study, fluorescent differential display (FDD) and CYP2E1-null mice were used to identify the spectrum of CYP2E1-dependent genes involved in this process. Identification the spectrum of CYP2E1-dependent genes involved in CCl<sub>4</sub>-induced liver injury is the first major step toward the understanding of the molecular mechanism of this process.

After 2, 6, 12, 24 and 48 hr CCl<sub>4</sub> treatment, it was found that serum ALT and AST activities, two indicators of liver injury, increased from 6 to 48 hr, reached a maximum at 24 hr, and then declined at 48 hr after CCl<sub>4</sub> treatment in *cyp2e1*<sup>+/+</sup> but not *cyp2e1*<sup>-/-</sup> mice indicating that CCl<sub>4</sub>-induced liver injury occur in a time-dependent manner. Since maximum liver injury was induced by CCl<sub>4</sub> in *cyp2e1*<sup>+/+</sup> mice after 24 hr treatment, liver RNA samples from both *cyp2e1*<sup>+/+</sup> and *cyp2e1*<sup>-/-</sup> mice after 24 hr CCl<sub>4</sub> treatment were used to perform the FDD RT-PCR analysis.



In this study, three different primer combinations (AP 5 and ARP 2, AP 5 and ARP 4, and AP 5 and ARP 7) were used for FDD analysis. Thirty-four cDNA fragments showing differentially expressed patterns after CCl<sub>4</sub> treatment were excised for characterization. Thirty cDNA fragments were successfully reamplified and subcloned and twenty-eight (93%) of them were successfully sequenced. Among them, twenty-five (83%) cDNA fragments were identified as known genes. Three cDNA fragments showed remarkable homology to mouse ESTs.

Due to the time limitation, Northern blot analysis was performed to confirm the differential expression patterns of only sixteen cDNA fragments. Till now, the differential expression patterns of four cDNA fragments (ADRP, RPL3,  $\gamma$ -actin and MUP) shown on FDD gels were confirmed by Northern blot analysis. The expression of ADRP, RPL3 and  $\gamma$ -actin was up-regulated while MUP expression was down-regulated in the livers of CCl<sub>4</sub>-treated *cyp2e1*<sup>+/+</sup> but not *cyp2e1*<sup>-/-</sup> mice indicating that these four genes are all CYP2E1-dependent genes involved in CCl<sub>4</sub>-induced liver injury. Data from the time course study (2, 6, 12, 24 and 48 hr) showed that the expression of these four identified genes in *cyp2e1*<sup>+/+</sup> mice after exposure to CCl<sub>4</sub> from 2 to 48 hr was time-dependent and in different manners. Tissue distribution study revealed that these four identified genes showed different degree of constitutive expression in various tissues indicating that they might have different roles in different tissues. The involvement of these four genes in CCl<sub>4</sub>-induced liver injury is a novel finding. Future studies are needed to investigate their roles in CCl<sub>4</sub>-induced liver injury.

## 摘 要

四氯化碳 (CCl<sub>4</sub>) 曾廣泛用作工業和家用清洗液，有機溶劑和殺蟲劑。作為家用試劑及滅火劑，CCl<sub>4</sub> 的少量使用在一些發展中國家仍然存在。以前的研究證實 CCl<sub>4</sub> 可導致人類和啮齒類的肝損傷。P450 的一種異構體，CYP2E1 一般被認為負責 CCl<sub>4</sub> 誘導的肝毒性。我們以前使用 CYP2E1 “無效” 小鼠的研究進一步證實 CYP2E1 與 CCl<sub>4</sub> 誘導的肝損傷有關。

雖然到目前為止我們已經對 CCl<sub>4</sub> 誘導的肝毒性的生物化學機制有了基本的了解，但是對於與此過程相關的準確的分子機制仍然所知甚少。在本研究中，熒光差異顯示 (FDD) 和 CYP2E1 “無效” 小鼠被用來尋找和鑑定與此過程相關的 CYP2E1 依賴性基因。尋找和鑑定與 CCl<sub>4</sub> 誘導的肝損傷相關的 CYP2E1 依賴性基因是了解這一過程的準確分子機制的第一步。

用 CCl<sub>4</sub> 處理 2, 6, 12, 24 和 48 小時後，發現肝損傷的兩個指示物，血清 ALT 和 AST 的活動水平在 *cyp2e1*<sup>+/+</sup> 小鼠中，從 CCl<sub>4</sub> 處理後的 6 到 48 小時逐步升高，在 24 小時達到最大值，然後在 48 小時開始下降，而在 *cyp2e1*<sup>+/+</sup> 小鼠中無此變化，表明 CCl<sub>4</sub> 誘導的肝損傷是以時間依賴性的方式發生的。由於在 *cyp2e1*<sup>+/+</sup> 小鼠中，CCl<sub>4</sub> 誘導的最大肝損傷出現在 CCl<sub>4</sub> 處理後的 24 小時，因此來自 CCl<sub>4</sub> 處理 24 小時後的 *cyp2e1*<sup>+/+</sup> 和 *cyp2e1*<sup>-/-</sup> 小鼠的肝 RNA 樣品被用來進行 FDD-RT PCR 分析。

在本研究中，三種不同的引物組合 (AP 5 和 ARP 2, AP 5 和 ARP 4, AP 5 和 ARP 7) 被用於 FDD 分析。三十四條經過 CCl<sub>4</sub> 處理後表現出差異表達模式的

cDNA 片段被切取用於鑑定。三十條 cDNA 片段被成功的再擴增和克隆，其中的二十八條（93%）被成功的測序。二十五條（83%）cDNA 片段被鑑定為已知的基因。三條 cDNA 片段（10%）則顯示出和小鼠 EST 明顯同源的序列。

由於時間限制，只有十六條 cDNA 片段的差異表達模式被用於 Northern blot 分析。到目前為止，四條 cDNA 片段（ADRP, RPL3,  $\gamma$ -actin 和 MUP）的差異表達模式被證實與 FDD 膠上表現出的差異表達模式相同。在  $\text{CCl}_4$  處理的 *cyp2e1*<sup>+/+</sup> 小鼠而非 *cyp2e1*<sup>-/-</sup> 小鼠的肝中，ADRP, RPL3 和  $\gamma$ -actin 的表達是正調控的，而 MUP 的表達則是負調控的，表明這四個基因都是與  $\text{CCl}_4$  誘導的肝損傷有關的 CYP2E1 依賴性基因。來自時序性（2, 6, 12, 24 和 48 小時）研究的數據表明在用  $\text{CCl}_4$  處理 *cyp2e1*<sup>+/+</sup> 小鼠後的 2 到 48 小時過程中，這四個基因的表達是時間依賴性的，並且以不同的方式進行。組織分布研究揭示這四個基因在多種組織中表現出不同程度的構建性表達，表明它們也許在不同的組織中有不同的作用。這四個基因與  $\text{CCl}_4$  誘導的肝損傷有關是一個新的發現，關於它們在此過程中的作用需要進一步的研究。

## TABLE OF CONTENTS

<b>Acknowledgements</b>	<b>i</b>
<b>Abstract</b>	<b>ii</b>
<b>Abstract (Chinese Version)</b>	<b>iv</b>
<b>Table of Contents</b>	<b>vi</b>
<b>List of Abbreviations</b>	<b>xii</b>
<b>List of Figures</b>	<b>xiii</b>
<b>List of Tables</b>	<b>xviii</b>
<b>Chapter 1 Literature review</b>	<b>1</b>
1.1 Carbon tetrachloride (CCl <sub>4</sub> )	1
1.2 Major uses of CCl <sub>4</sub>	1
1.3 Potential human exposure pathways to CCl <sub>4</sub>	2
1.4 Toxicity of CCl <sub>4</sub>	3
1.5 Mechanism of CCl <sub>4</sub> -induced hepatotoxicity	5
1.6 Role of CYP2E1 involved in CCl <sub>4</sub> -induced hepatotoxicity	7
1.7 Definite proof of the involvement of CYP2E1 in CCl <sub>4</sub> -induced hepatotoxicity by CYP2E1-null mouse <i>in vivo</i> model	10
1.8 Identification of CYP2E1-dependent genes involved in CCl <sub>4</sub> -induced hepatotoxicity by fluorescent differential display (FDD)	11
1.9 Objectives of the study	14

<b>Chapter 2</b>	<b>Materials and methods</b>	<b>16</b>
2.1	Animals and treatments	16
2.1.1	Materials	16
2.1.2	Methods	16
2.2	Serum alanine aminotransferase (ALT) and aspartate aminotransferase (AST) analyses	17
2.2.1	Materials	17
2.2.2	Methods	17
2.2.2.1	Serum preparation	17
2.2.2.2	Activity determination	18
2.3	Tail-genotyping by PCR	18
2.3.1	Materials	18
2.3.2	Methods	20
2.3.2.1	Preparation of genomic DNA from mouse tail	20
2.3.2.2	PCR reaction	20
2.4	Total RNA isolation	21
2.4.1	Materials	21
2.4.2	Methods	21
2.5	DNase I treatment	23
2.5.1	Materials	23
2.5.2	Methods	23
2.6	Reverse transcription of mRNA and amplification by fluorescent PCR amplification	26

2.6.1	Materials	27
2.6.2	Methods	27
2.7	Fluorescent differential display (FDD)	28
2.7.1	Materials	28
2.7.2	Methods	28
2.8	Excision of differentially expressed cDNA fragments	29
2.8.1	Materials	29
2.8.2	Methods	29
2.9	Reamplification of differentially expressed cDNA fragments	34
2.9.1	Materials	34
2.9.2	Methods	34
2.10	Subcloning of reamplified cDNA fragments	36
2.10.1	Materials	36
2.10.2	Methods	37
2.11	Purification of plasmid DNA from recombinant clones	39
2.11.1	Materials	39
2.11.2	Methods	39
2.12	DNA sequencing of differentially expressed cDNA fragments	40
2.12.1	Materials	40
2.12.2	Methods	40
2.12.3	BLAST search against the GenBank DNA databases	41
2.13	Northern blot analysis of differentially expressed cDNA fragments	41
2.13.1	Formaldehyde gel electrophoresis of total RNA	41



2.13.1.1	Materials	42
2.13.1.2	Methods	42
2.13.2	Preparation of cDNA probes for hybridization	42
2.13.2.1	EcoRI digestion of cDNA inserts from plasmid DNA	42
2.13.2.1.1	Materials	42
2.13.2.1.2	Methods	43
2.13.2.2	Purification of DNA from agarose gel	43
2.13.2.2.1	Materials	43
2.13.2.2.2	Methods	43
2.13.2.3	DIG labeling of cDNA	44
2.13.2.3.1	Materials	44
2.13.2.3.2	Methods	44
2.13.3	Hybridization	45
2.13.3.1	Materials	45
2.13.3.2	Methods	45
<b>Chapter 3</b>	<b>Results</b>	<b>47</b>
3.1	Liver morphology	47
3.2	Serum ALT and AST activities	47
3.3	Tail-genotyping by PCR	51
3.4	DNase I treatment	51
3.5	FDD RT-PCR and excision of differentially expressed cDNA fragments	51
3.6	Reamplification of excised cDNA fragments	61

3.7	Subcloning of reamplified cDNA fragments	61
3.8	DNA sequencing of subcloned cDNA fragments	69
3.9	Confirmation of differentially expressed patterns by Northern blot analysis	106
3.10	Temporal expression of differentially expressed genes	113
3.11	Tissue distribution of differentially expressed genes	117
<b>Chapter 4 Discussion</b>		<b>125</b>
4.1	Liver morphology and serum ALT and AST activities	126
4.2	Identification of CYP2E1-dependent genes involved in CCl <sub>4</sub> -induced hepatotoxicity	127
4.3	Functional roles of the identified differentially expressed genes	129
4.3.1	Fragment B4	129
4.3.2	Fragment C12	130
4.3.3	Fragment B13	131
4.3.4	Fragment A5	132
4.4	Temporal expression of differentially expressed genes	133
4.4.1	Fragment B4	133
4.4.2	Fragment C12	134
4.4.3	Fragment B13	134
4.4.4	Fragment A5	135
4.5	Tissue distribution of differentially expressed genes	136
4.5.1	Fragment B4	136

4.5.2	Fragment C12	136
4.5.3	Fragment B13	137
4.5.4	Fragment A5	137
4.5.5	Roles of the identified genes involved in CCl <sub>4</sub> -induced hepatotoxicity	138
4.6	Normalization of Northern blot analysis	138
4.7	Limitations of FDD technique to identify differentially expressed genes	138
4.8	Future studies	139
4.8.1	Investigation of the differential expression patterns of the identified genes in acetaminophen-induced liver injury	139
4.8.2	Dot blot analysis	140
4.8.3	DNA microarray	140
	<b>References</b>	<b>141</b>

## LIST OF ABBREVIATIONS

ADRP	Adipose differentiation-related protein
Anti-AP	Polyclonal antibody against digoxigenin
AP	Anchored primer
ARP	Arbitrary primer
BCIP	5-bromo-4-chloro-3-indolyl-phosphate
BLAST	Basic Local Alignment Search Tool
bp	Basepair
CCl <sub>4</sub>	Carbon tetrachloride
cDNA	Complementary deoxyribonucleic acid
cm	Centimeter
FDD	Fluorescent differential display
g	Gram
γ-actin	Cytoplasmic gamma-actin
GAPDH	Glyceraldehyde-3-phosphate dehydrogenase
hr	Hour
kg	Kilogram
LB	Luria-Bertani
μl	Microlitre
μM	Micromolar
min	Minute
ml	Millilitre
mM	Millimolar
MUP	Major urinary protein
NaCl	Sodium chloride
NBT	Nitroblue tetrazolium chloride
ng	Nanogram
nm	Nanometer
Oligo(dT)	Oligopolydeoxythymidine
PCR	Polymerase chain reaction
pg	Picogram
RNA	Ribonucleic acid
RPL3	Ribosome protein L3
rpm	Round per minute
RT-PCR	Reverse transcription-polymerase chain reaction
sec	Second
SDS	Sodium dodecyl sulfate
SSC	Sodium chloride/sodium citrate buffer
TMR	Tetramethylrhodamine
Tris-HCl	Tris (hydroxymethyl) aminomethane/hydrochloric acid
UGDH	UDP-glucose dehydrogenase
V	Voltage
W	Watt
X-Gal	5-bromo-4-chloro-3-indolyl-β-D-thiogalactoside

## LIST OF FIGURES

		Page
Figure 1.1	Summary of the mechanism of CCl <sub>4</sub> -induced liver injury.	6
Figure 1.2	Schematic diagram to show the procedure of FDD method.	13
Figure 2.1	The schematic representation of the genomic organization of CYP2E1 gene and the strategy of PCR primer design for <i>cyp2e1</i> <sup>+/+</sup> and <i>cyp2e1</i> <sup>-/-</sup> mice.	19
Figure 2.2	Flowchart showing the overall strategy to identify differentially expressed genes by FDD RT-PCR.	22
Figure 2.3	GenomyxLR™ DNA electrophoresis system.	30
Figure 2.4	GenomyxSC™ fluorescent imaging scanner.	31
Figure 2.5	Band Excision Workstation for fluorescent differential display.	33
Figure 2.6	Schematic diagram to show the reamplification of the cDNA fragment by PCR and the reconstruction of priming site using full-length M13 reverse (-48) 24-mer and T7 promoter 22-mer primers.	35
Figure 2.7	Restriction map and multiple cloning site of the pT-Adv vector.	38
Figure 3.1	Liver morphology of <i>cyp2e1</i> <sup>+/+</sup> and <i>cyp2e1</i> <sup>-/-</sup> mice treated with corn oil (CTL) or CCl <sub>4</sub> for 2, 6, 12, 24 and 48 hr.	48
Figure 3.2	Serum ALT and AST activities in <i>cyp2e1</i> <sup>+/+</sup> and <i>cyp2e1</i> <sup>-/-</sup> mice after 24 hr exposure to 1 ml/kg CCl <sub>4</sub> i.p. injection.	49
Figure 3.3	Serum ALT and AST activities in <i>cyp2e1</i> <sup>+/+</sup> and <i>cyp2e1</i> <sup>-/-</sup> mice after 2, 6, 12, 24 and 48 hr exposure to 1 ml/kg CCl <sub>4</sub> i.p. injection.	52
Figure 3.4	Tail-genotyping of <i>cyp2e1</i> <sup>+/+</sup> and <i>cyp2e1</i> <sup>-/-</sup> mice used for FDD RT-PCR analysis (A) and time course study (B).	53
Figure 3.5	Electrophoretic separation of total liver RNAs after DNase I treatment on a 1% agarose gel containing 1x MOPS and 2.2 M formaldehyde with ethidium bromide staining.	54
Figure 3.6	Gel A: Fluorescent differential display of liver RNAs from <i>cyp2e1</i> <sup>+/+</sup> and <i>cyp2e1</i> <sup>-/-</sup> mice treated with corn oil (CTL) or CCl <sub>4</sub> for 24 hr.	56

	Page	
Figure 3.7	Gel B: Fluorescent differential display of liver RNAs from <i>cyp2e1</i> <sup>+/+</sup> and <i>cyp2e1</i> <sup>-/-</sup> mice treated with corn oil (CTL) or CCl <sub>4</sub> for 24 hr.	58
Figure 3.8	Gel C: Fluorescent differential display of liver RNAs from <i>cyp2e1</i> <sup>+/+</sup> and <i>cyp2e1</i> <sup>-/-</sup> mice treated with corn oil (CTL) or CCl <sub>4</sub> for 24 hr.	60
Figure 3.9	Reamplification of cDNA fragments excised from FDD gels A, B and C (Part A).	63
Figure 3.10	Reamplification of cDNA fragments excised from FDD gels A, B and C (Part B).	64
Figure 3.11	EcoRI restriction enzyme digestion of recombinant clones containing inserts A2, A5, B7, B8, C2, C11, B9 and B10.	68
Figure 3.12	EcoRI restriction enzyme digestion of recombinant clones containing inserts A1, A4 and B4.	70
Figure 3.13	EcoRI restriction enzyme digestion of recombinant clones containing inserts B4, B5, B6, C4 and C7.	71
Figure 3.14	EcoRI restriction enzyme digestion of recombinant clones containing inserts B2, B11, B12, B13, C3, C5, C6 and C8.	72
Figure 3.15	EcoRI restriction enzyme digestion of recombinant clones containing inserts C12, C8, C10, C13, C14, C15, C16 and C9.	73
Figure 3.16	Sequencing comparison between cDNA fragment A1 and <i>Mus musculus</i> hemopexin.	77
Figure 3.17	Sequencing comparison between cDNA fragment A4 and <i>Mus musculus</i> t-complex protein 1 (TCP1).	78
Figure 3.18	Sequencing comparison between cDNA fragment A5 and mouse major urinary protein (MUP).	79
Figure 3.19	Sequencing comparison between cDNA fragment B2 and <i>Mus musculus</i> guanine nucleotide binding protein, beta-2.	80
Figure 3.20	Sequencing comparison between cDNA fragment B4 and mouse adipose differentiation-related protein (ADRP).	81



	Page
Figure 3.21 Sequencing comparison between cDNA fragment B5 and his-tagged-multidrug resistance glycoprotein.	82
Figure 3.22 Sequencing comparison between cDNA fragment B6 and rat GAP-associated protein (P190).	83
Figure 3.23 Sequencing comparison between cDNA fragment B7 and <i>Mus musculus</i> integrin linked kinase (ILK).	84
Figure 3.24 Sequencing comparison between cDNA fragment B8 and ribosomal protein S10.	85
Figure 3.25 Sequencing comparison between cDNA fragment B9 and fatty acid binding protein, intestine (FABPI).	86
Figure 3.26 Sequencing comparison between cDNA fragment B10 and <i>Mus musculus</i> clusterin (CLU).	87
Figure 3.27 Sequencing comparison between cDNA fragment B11 and <i>Rattus norvegicus</i> phospholipase C, gamma 1 (PLCG1).	88
Figure 3.28 Sequencing comparison between cDNA fragment B12 and mouse EST.	89
Figure 3.29 Sequencing comparison between cDNA fragment B13 and mouse cytoplasmic gamma-actin ( $\gamma$ -actin).	90
Figure 3.30 Sequencing comparison between cDNA fragment C2 and <i>Rattus norvegicus</i> mRNA for acyl-CoA synthetase 5 (ACS5).	91
Figure 3.31 Sequencing comparison between cDNA fragment C3 and mouse EST.	92
Figure 3.32 Sequencing comparison between cDNA fragment C4 and <i>Mus musculus</i> cullin 1 (CUL1).	93
Figure 3.33 Sequencing comparison between cDNA fragment C5 and mouse DNA for virus-like (VL30) retrotransposon BVL-1.	94
Figure 3.34 Sequencing comparison between cDNA fragment C6 and mouse EST.	95
Figure 3.35 Sequencing comparison between cDNA fragment C7 and <i>Mus musculus</i> COP9, subunit 3 (COPS3).	96

	Page
Figure 3.36 Sequencing comparison between cDNA fragment C9 and mouse cytoplasmic gamma-actin ( $\gamma$ -actin).	97
Figure 3.37 Sequencing comparison between cDNA fragment C10 and mouse fibronectin (FN).	98
Figure 3.38 Sequencing comparison between cDNA fragment C11 and <i>Mus musculus</i> ribosomal protein L3 (RPL3).	99
Figure 3.39 Sequencing comparison between cDNA fragment C12 and <i>Mus musculus</i> ribosomal protein L3 (RPL3).	100
Figure 3.40 Sequencing comparison between cDNA fragment C13 and mouse major histocompatibility complex region.	101
Figure 3.41 Sequencing comparison between cDNA fragment C14 and <i>Mus musculus</i> PK-120 precursor (ITIH-4).	102
Figure 3.42 Sequencing comparison between cDNA fragment C15 and tcp-1=t-complex polypeptide 1 (TCP1).	103
Figure 3.43 Sequencing comparison between cDNA fragment C16 and tcp-1=t-complex polypeptide 1 (TCP1).	104
Figure 3.44 Confirmation of FDD expression pattern of cDNA fragment B4 (adipose differentiation-related protein) by Northern blot analysis.	108
Figure 3.45 Confirmation of FDD expression pattern of cDNA fragment C12 (ribosomal protein L3) by Northern blot analysis.	110
Figure 3.46 Confirmation of FDD expression pattern of cDNA fragment B13 (cytoplasmic gamma-actin) by Northern blot analysis.	111
Figure 3.47 Confirmation of FDD expression pattern of cDNA fragment A5 (major urinary protein) by Northern blot analysis.	112
Figure 3.48 Time-dependent expression pattern of cDNA fragment B4 (adipose differentiation-related protein).	114
Figure 3.49 Time-dependent expression pattern of cDNA fragment C12 (ribosomal protein L3).	115
Figure 3.50 Time-dependent expression pattern of cDNA fragment B13 (cytoplasmic gamma-actin).	116

	Page
Figure 3.51 Time-dependent expression pattern of cDNA fragment A5 (major urinary protein).	118
Figure 3.52 Expression pattern of cDNA fragment B4 (adipose differentiation-related protein) in kidney, heart, spleen, brown fat, white fat and brain (Part I).	119
Figure 3.53 Expression pattern of cDNA fragment B4 (adipose differentiation-related protein) in lung, stomach, intestine, muscle and testis (Part II).	120
Figure 3.54 Expression pattern of cDNA fragment C12 (ribosomal protein L3) in kidney (K), testis (T), brain (B), lung (L), heart (H), intestine (I), stomach (St), spleen (Sp), brown fat (Bf), white fat (Wf) and muscle (Mu).	122
Figure 3.55 Expression pattern of cDNA fragment B13 (cytoplasmic gamma-actin) in kidney (K), testis (T), brain (B), lung (L), heart (H), intestine (I), stomach (St), spleen (Sp), brown fat (Bf), white fat (Wf) and muscle (Mu).	123
Figure 3.56 Expression pattern of cDNA fragment A5 (major urinary protein) in kidney (K), testis (T), brain (B), lung (L), heart (H), intestine (I), stomach (St), spleen (Sp), brown fat (Bf), white fat (Wf) and muscle (Mu).	124

## LIST OF TABLES

	Page
Table 1.1	P450s isoforms of subfamily 1-3 in human, rats and mice. 9
Table 2.1	Sequence of anchored primers (APs) used for the first-strand cDNA synthesis. 25
Table 2.2	Sequence of arbitrary primers (ARPs) used for FDD-PCR reaction. 26
Table 2.3	Possible gene expression patterns on FDD gels. 32
Table 3.1	Serum ALT and AST activities in <i>cyp2e1</i> <sup>+/+</sup> and <i>cyp2e1</i> <sup>-/-</sup> mice after exposure to 1 ml/kg CCl <sub>4</sub> i.p. injection. 50
Table 3.2	CYP2E1-dependent cDNA fragments excised from Gel A. 57
Table 3.3	CYP2E1-dependent cDNA fragments excised from Gel B. 59
Table 3.4	CYP2E1-dependent cDNA fragments excised from Gel C. 62
Table 3.5	Summary of cDNA fragments reamplified from Gel A. 65
Table 3.6	Summary of cDNA fragments reamplified from Gel B. 66
Table 3.7	Summary of cDNA fragments reamplified from Gel C. 67
Table 3.8	Summary of subcloning of cDNA fragments reamplified from Gel A. 74
Table 3.9	Summary of subcloning of cDNA fragments reamplified from Gel B. 75
Table 3.10	Summary of subcloning of cDNA fragments reamplified from Gel C. 76
Table 3.11	Summary of sequence homology of subcloned cDNA fragments. 105
Table 3.12	Summary of Northern blot analyses on sequenced cDNA fragments. 107

## CHAPTER 1: LITERATURE REVIEW

### 1.1 Carbon tetrachloride (CCl<sub>4</sub>)

Carbon tetrachloride (CCl<sub>4</sub>) is a colourless, non-inflammable and heavy liquid that evaporates very easily. CCl<sub>4</sub> has a molecular weight of 153.82 and is soluble in alcohol and acetone and miscible with benzene, ether and chloroform (McGregor and Lang, 1996). Most CCl<sub>4</sub> that escapes to the environment is therefore found as a gas with a characteristic sweet odour (Environmental Protection Agency, 1984).

### 1.2 Major uses of CCl<sub>4</sub>

In the past years, CCl<sub>4</sub> had been used widely as an industrial and household cleaning fluid (McGregor and Lang, 1996). In industry, it was an effective metal-degreaser. CCl<sub>4</sub> was consumed in the synthesis of chlorofluorocarbons (CFCs), which were used as heat transfer agents in refrigerating equipment and as aerosol propellants (Ruprah *et. al.*, 1985). At home, it was used to remove spots from clothing, furniture and carpets. CCl<sub>4</sub> also has been used as an extracting solvent for flowers and seeds, as a component in fire extinguishers, as an anthelmintic and anesthetic, and until 1969, as a waterless shampoo (Recknagel and Glende, 1973; Fleming *et. al.*, 1995; Manno *et. al.*, 1996; McGregor and Lang, 1996).

In 1950s, the acute toxicity of CCl<sub>4</sub> was widely recognized. From then on, CCl<sub>4</sub> manufacture and use have decreased. Because of the international agreements to restrict the use of CFCs in the end of 1980's, which were thought to deplete the earth's protective ozone layer, production of CCl<sub>4</sub> continued to decline since then. However, minor amounts



of CCl<sub>4</sub> are still used as a solvent for oils, fats, lacquers, pesticides, varnishes, rubber, waxes and resins for domestic or industrial purposes in some countries, most of which are developing countries (Fleming *et. al.*, 1995).

### **1.3 Potential human exposure pathways to CCl<sub>4</sub>**

Although CCl<sub>4</sub> does not occur naturally, it is ubiquitous in the environment. Its chemical stability results in an atmospheric half-life of 30-100 years (Fleming *et. al.*, 1995). However, very low background levels of CCl<sub>4</sub> are found in natural environment including air, water, and soil because of past and present releases. Higher levels of CCl<sub>4</sub> are likely to occur only at specific industrial locations where CCl<sub>4</sub> is still used or near chemical waste sites where emissions into air, water, or soil are not properly controlled (Agency for Toxic Substances and Disease Registry, 1994). In these places, the ground-water are more susceptible to be contaminated with CCl<sub>4</sub>.

In industry, workers using CCl<sub>4</sub> or CCl<sub>4</sub>-containing products are at greatest risk exposure to this compound. According to a 1981-1983 survey made by the National Institute for Occupational Safety and Health (NIOSH), it was estimated that 58,000 workers are potentially exposed to CCl<sub>4</sub> in the United States (Agency for Toxic Substances and Disease Registry, 1994). Due to the alcohol inducible mechanisms of CCl<sub>4</sub> metabolism (refer to 1.4), moderate to heavy drinkers and diabetics may be at increased risk of CCl<sub>4</sub>'s adverse effects (Fleming *et. al.*, 1995). Moreover, another possible risk of exposure to CCl<sub>4</sub> is that young children may be exposed when they are playing with the soil contaminated with CCl<sub>4</sub> (Agency for Toxic Substances and Disease Registry, 1994).



In summary, the potential of ground-water contamination (Manno *et. al.*, 1996; Zangar *et. al.*, 2000), the industrial use of CCl<sub>4</sub> and the permission of the household use of CCl<sub>4</sub> in some countries make the exposure to CCl<sub>4</sub> still exist today.

#### 1.4 Toxicity of CCl<sub>4</sub>

CCl<sub>4</sub> readily enters the body by inhalation, ingestion and dermal absorption. Inhalation is the primary route of exposure, with pulmonary absorption in humans estimated to be 60% and, which is also the most frequent cause of poisoning by this chemical in industry (McGregor and Lang, 1996). The rate of absorption through the gastrointestinal tract is rapid and greatly affected by diet (e.g., fat or alcohol in the gut enhances CCl<sub>4</sub> absorption). CCl<sub>4</sub> is also absorbed through the skin, though less readily than by the lungs. Dermal, the liquid is more rapidly absorbed than the vapour, and prolonged skin contact with the liquid can result in systemic effects (Fleming *et. al.*, 1995).

Liver is especially sensitive to CCl<sub>4</sub> and numerous reports indicated that CCl<sub>4</sub> has been shown to produce liver injury including cirrhosis, centrilobular necrosis, fatty degeneration, fatty infiltration and decreased activities of microsomal enzymes that catalyse the oxidation of drugs in various species (Lamson and Wing, 1926; Chaplin and Mannering, 1970; Tomenson *et. al.*, 1995; Padma and Setty, 1999). After exposure to CCl<sub>4</sub>, in mild cases, the liver becomes swollen and tender, and fat builds up inside the organ. In severe cases, liver cells may be damaged or destroyed, leading to a decrease in liver function. Such effects are usually reversible if exposure is not too high or too long (Bruckner *et. al.*, 1986; Chopra *et. al.*, 1972; Recknagel *et. al.*, 1989; Ugazio *et. al.*, 1973). Although liver is the most susceptible to the damage caused by CCl<sub>4</sub> (Gram and Gillette,

1971; Timbrell, 1991; Janbaz and Gilani, 1999), other organs are also suffering from the damage after exposure to CCl<sub>4</sub>. These organs include kidney, lung, testis, adrenal and central nervous system (McGregor and Lang, 1996; Abraham *et. al.*, 1999).

Besides the hepatic effects of CCl<sub>4</sub>, carcinogenic effects have also been studied by some researchers. The Department of Health and Human Services (DHHS) has determined that CCl<sub>4</sub> may reasonably be anticipated to be a carcinogen. The International Agency for Research on Cancer (IARC) has determined that CCl<sub>4</sub> is possibly carcinogenic to humans. The Environmental Protection Agency (EPA) has determined that CCl<sub>4</sub> is a probable human carcinogen (Agency for Toxic Substances and Disease Registry, 1994). Although data on the carcinogenic effects in humans are inconclusive, studies in experimental animals provide convincing evidence that ingestion of CCl<sub>4</sub> increases the risk of liver cancer, in particular, hepatomas and hepatocellular carcinomas. It was revealed that treatment of CCl<sub>4</sub> by mouth could increase the frequency of liver tumours in some species. Studies have not been performed to determine if breathing CCl<sub>4</sub> causes tumours in animals, or whether swallowing or breathing CCl<sub>4</sub> causes tumours in humans, but it should be assumed that CCl<sub>4</sub> could produce cancer (Fleming *et. al.*, 1995). Understanding the carcinogenic effects of CCl<sub>4</sub> in animals can help us to know more about the similar carcinogenic effects of CCl<sub>4</sub> in humans.

Today, cirrhosis of the liver is one of the major health problems in developed countries. It is the fourth leading cause of death in American adults (Rubin and Popper, 1967), about 70% of which is associated with alcoholism. There have many studies of the hepatotoxic responses and the cirrhotic responses particularly in experimental animals. The cirrhotic response in rats dosed twice weekly for five weeks with i. p. injection of CCl<sub>4</sub>

at the dose of 1000 mg/kg body weight is superficially similar to human cirrhosis (Tamayo, 1983). Thus, the liver is grossly nodular, there are signs of portal hypertension and the normal architecture is replaced by nodules by regenerating plates of hepatocytes surrounded by connective tissue septa with proliferated bile ducts. The pathogenesis of CCl<sub>4</sub>-induced cirrhosis seems to involve repeated episodes of focal hepatocyte necrosis, fibrosis resulting from the collapse of the previously existing collagen framework and the regeneration from surviving hepatocytes of nodules within connective tissue septa (McGregor and Lang, 1996). Since the animal model of CCl<sub>4</sub>-induced cirrhosis is remarkably similar to human alcoholic cirrhosis both histologically (Stenger, 1966; Rubin and Popper, 1967) and systemically (McLean et. al., 1969), the understanding of CCl<sub>4</sub>-induced cirrhosis in animals like rats and mice can enable scientists to uncover mechanistic aspects of the cirrhosis in humans.

### **1.5 Mechanism of CCl<sub>4</sub>-induced hepatotoxicity**

Since the discovery of its hepato-and nephrotoxic properties in humans in the early 1920's, when the compound was used as an effective but, unfortunately, often lethal anthelmintic drug, CCl<sub>4</sub> has probably become one of the most widely investigated hepatotoxins (Manno *et. al.*, 1996). The mechanism responsible for the hepatotoxicity of CCl<sub>4</sub> has been the subject of numerous studies during the past decades (Anders, 1988).

The mechanism of CCl<sub>4</sub>-induced liver injury was summarized in Figure 1.1 (Huether and McCance, 1996). In the beginning of CCl<sub>4</sub>-induced liver injury, CCl<sub>4</sub> is converted by an enzyme system in the smooth endoplasmic reticulum (ER) of liver cells into chloromethyl (CCl<sub>3</sub>·), a highly toxic free radical (Recknagel and Ghoshal, 1966; Slater,

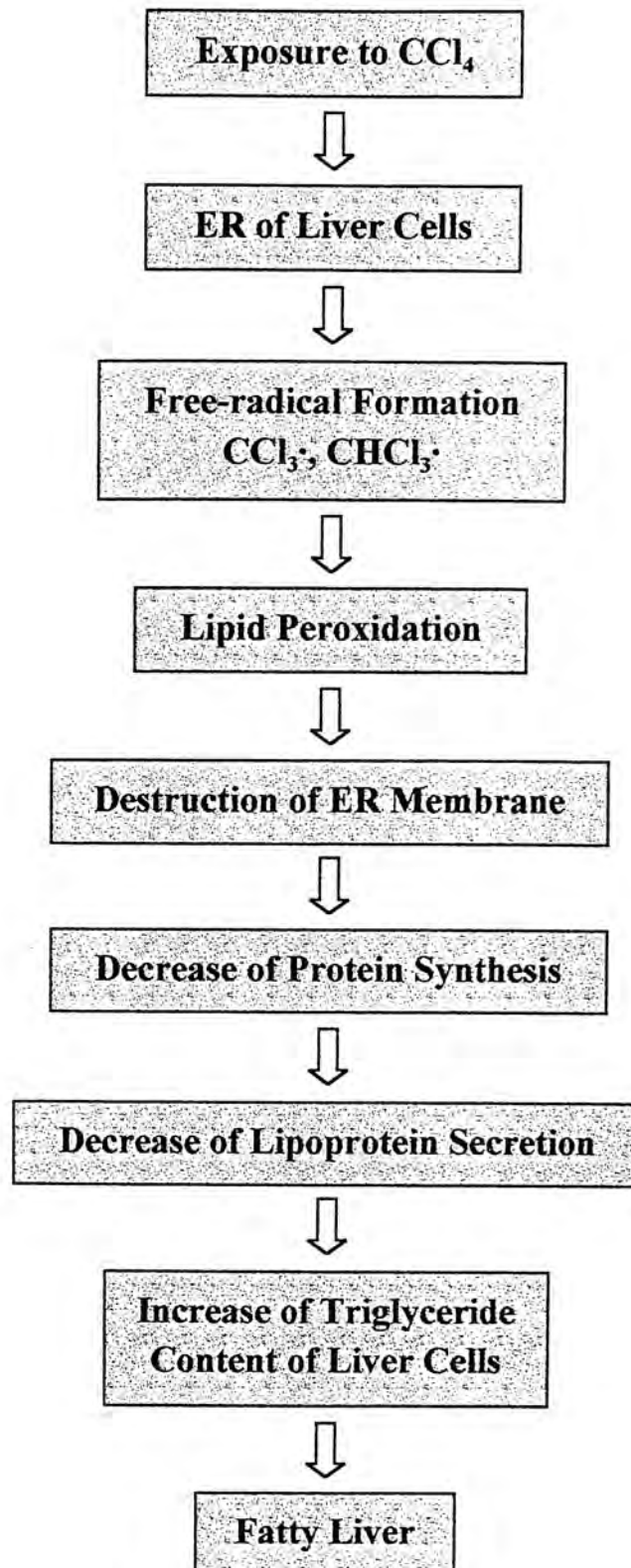


Figure 1.1. Summary of the mechanism of  $\text{CCl}_4$ -induced liver injury (Adapted from Huether and McCane, 1996).

1982). Some of the  $\text{CCl}_3\cdot$  may attack the double allylic hydrogen atoms of polyenoic fatty acids and  $\text{CHCl}_3\cdot$  is generated in these hydrogen abstraction reactions (Holman, 1954). The newly formed  $\text{CCl}_3\cdot$  and  $\text{CHCl}_3\cdot$  rapidly destroy the ER of the liver cell by breaking down the reticulum's lipid component (lipid peroxidation). The lipid molecules accumulate within the cytoplasm, starting within cisternae of the ER. Fatty liver develops because  $\text{CCl}_4$  poisoning blocks the synthesis of lipid-acceptor proteins (apoproteins) that normally bind with triglycerides to form lipoproteins, which are transported out of the cell (Recknagel *et al.*, 1989; Huether and McCance, 1996). The blockage of triglyceride (lipoprotein) secretion begins 10 to 15 minutes after  $\text{CCl}_4$  exposure. Fat droplets that accumulate in cisternae of the ER combine to form larger droplets and fill vacuoles that, in turn, fill the entire cytoplasm. Approximately 10 to 12 hours later, the liver appears grossly enlarged and pale because of the accumulation of fat (Recknagel, 1967; Pencil *et al.*, 1984).

### **1.6 Role of CYP2E1 involved in $\text{CCl}_4$ -induced hepatotoxicity**

Previous studies have demonstrated that cytochrome P450 superfamily (P450s), an enzyme system in the ER of liver cells, is mainly responsible for  $\text{CCl}_4$  bioactivation and metabolism (Recknagel and Glende, 1973). P450s are key detoxification enzymes and catalyse the first step in the biotransformation process with xenobiotics being oxidized to forms that can then be further modified by conjugating enzymes. While P450 enzymes generally carry out detoxification reactions, some xenobiotics are metabolized by these enzymes to forms that are potentially carcinogenic, mutagenic or toxic. Additionally, P450 enzymes may play an important role in the maintenance and degradation of endogenous



molecules that affect growth and other cellular functions (Nebert, 1990; Denison and Whitlock, 1995).

In animals, P450 superfamily is presently known to contain hundreds of members, divided into 68 families. P450 superfamily has undergone divergent evolution, and some of the ancestral genes are probably more than two billion years old (Nebert *et. al.*, 1989). P450s are well-conserved across humans and rodents during the course of long-term evolution. Among the various isoforms of P450 subfamilies 1-3, CYP1A1, CYP1A2, CYP1B1 and CYP2E1 are present in human, rats and mice (Table 1.1).

Among the multiple isoforms of P450s existing in liver, CYP2E1 has been believed to be the primary P450 isoform involved in CCl<sub>4</sub> metabolism and CCl<sub>4</sub>-induced liver injury (Raucy *et.al.*, 1993). By using chemical inducers or inhibitors to induce or inhibit the expression of CYP2E1, the involvement of CYP2E1 in the bioactivation of CCl<sub>4</sub> was supported (Klaassen and Plaa, 1966; Brady *et. al.*, 1991). For example, the hepatotoxicity induced by CCl<sub>4</sub> can be potentiated by administration of ethanol, an inducer of CYP2E1, usually 16-18 hr prior to CCl<sub>4</sub> exposure (Shibayama, 1988; Ray and Mehendale, 1990). Induction of CYP2E1 by other agents such as phenobarbital or polychlorinated biphenyls also increases the extent of CCl<sub>4</sub> metabolism and hence its hepatotoxicity (Tuchweber *et. al.*, 1974; Kluwe *et. al.*, 1982; Lindros *et. al.*, 1990). On the other hand, disulfiram, one of the known CYP2E1 inhibitors, was shown to block the hepatotoxicity mediated by treatment of CCl<sub>4</sub> in rats (Brady *et. al.*, 1991). Inhibition of CYP2E1-mediated metabolism by agents as SKF-525A or chloramphenicol also decreases CCl<sub>4</sub> bioactivation and the resulting hepatotoxicity (Castro *et. al.*, 1974). These studies suggested that CYP2E1 is required in the process of bioactivation of CCl<sub>4</sub> leading to liver injury.



Table 1.1 P450s isoforms of subfamily 1-3 in human, rats and mice (Adapted from Juchau *et. al.*, 1998).

<b>Subfamily</b>	<b>Human</b>	<b>Rat</b>	<b>Mouse</b>
1A	1, 2	1, 2	1, 2
1B	1	1	1
2A	6, 7, 13	1, 2, 3	4, 5, 12
2B	6	1, 2, 3, 12, 15	9, 10, 13
2C	8, 9, 18, 19	6, 7, 11, 12, 13, 22, 23, 24	29
2D	6, 18	1, 2, 3, 4, 5	9, 10, 11, 12, 13
<b>2E</b>	<b>1</b>	<b>1</b>	<b>1</b>
2F	1		2
2G		1	
2J	2	3	
3A	4, 5, 7	1, 2, 9, 18, 23	11, 13, 16

Although the role of CYP2E1 involved in CCl<sub>4</sub>-induced hepatotoxicity has been suggested by studies using CYP2E1 inducers or inhibitors, there are still some shortcomings of these methods. The effects of inducers on CYP2E1 are not specific since other P450s including CYP1A2 can also be induced simultaneously (Sinclair et. al., 2000), therefore it can not be very sure that the increase of hepatotoxicity induced by CCl<sub>4</sub> is fully due to the contribution of CYP2E1 alone.

### **1.7 Definite proof of the involvement of CYP2E1 in CCl<sub>4</sub>-induced hepatotoxicity by CYP2E1-null mouse *in vivo* model**

To further confirm the involvement of CYP2E1 in CCl<sub>4</sub>-induced hepatotoxicity, the CYP2E1-null (*cyp2e1*<sup>-/-</sup>) mouse model which lacks the expression of CYP2E1 was developed in 1996 (Lee et. al., 1996). Lee et. al. isolated a 14.2 kb DNA fragment containing the entire CYP2E1 gene coding sequence from a SV/129 mouse genomic library. Then the homozygous mice were created by the disruption of this gene. There was no obvious external phenotypic difference between the CYP2E1-null mice (*cyp2e1*<sup>-/-</sup>) and their wild-type counterparts (*cyp2e1*<sup>+/+</sup>). Using this direct and *in vivo* animal model, the hepatotoxicity of CCl<sub>4</sub> was assessed by measuring the serum ALT and AST activities and by examining the liver histology (Wong et. al., 1998). In these studies (Wong et. al., 1998), CCl<sub>4</sub> treatment resulted in 422- and 125-fold increases in serum ALT and AST activities respectively in *cyp2e1*<sup>+/+</sup> mice but not *cyp2e1*<sup>-/-</sup> mice. Consistent with the results of serum ALT and AST activities, severe liver injury was observed in *cyp2e1*<sup>+/+</sup> mice but not *cyp2e1*<sup>-/-</sup> mice after CCl<sub>4</sub> treatment. These results conclusively demonstrated that CYP2E1 plays an important role in mediating the hepatic damage following CCl<sub>4</sub> exposure

in these mice. Although it is clear that CYP2E1 is required in CCl<sub>4</sub>-induced hepatotoxicity, the exact molecular mechanism of the involvement of CYP2E1 in CCl<sub>4</sub>-induced liver injury is still unclear.

### **1.8 Identification of CYP2E1-dependent genes involved in CCl<sub>4</sub>-induced hepatotoxicity by fluorescent differential display (FDD)**

Although the biochemical mechanism of CCl<sub>4</sub>-induced liver injury has been well characterized, the molecular mechanism of this process is still poorly understood. Identification of the spectrum of genes involved in CCl<sub>4</sub>-induced liver injury may help us to gain insight into the molecular mechanism of this process.

In the past decade, subtractive hybridization (Travis *et. al.*, 1989; Watson and Margulies, 1996) and electronic subtraction (Adams *et. al.*, 1993; Ito *et. al.*, 1994; Murakawa *et. al.*, 1994; Franco *et. al.*, 1995) were the two main methods to identify the differentially expressed genes. Although by using these two methods, a lot of differentially expressed genes have been identified in various biological processes, there are three main shortcomings of these two methods. These shortcomings are the incomplete recovery, the selection of only under- or over-expressed genes and the tedious screening step, which greatly cumber the further development and application of these methods.

In 1992, a powerful tool, differential display (DD) was developed by Liang and Pardee (Liang and Pardee, 1992). This fast, simple and sensitive method permits the detection of genes whose expression level is up-regulated or down-regulated. Moreover, DD is also able to compare more than two RNA samples simultaneously and is capable to identify differentially expressed genes that are characteristic of a process instead of only a

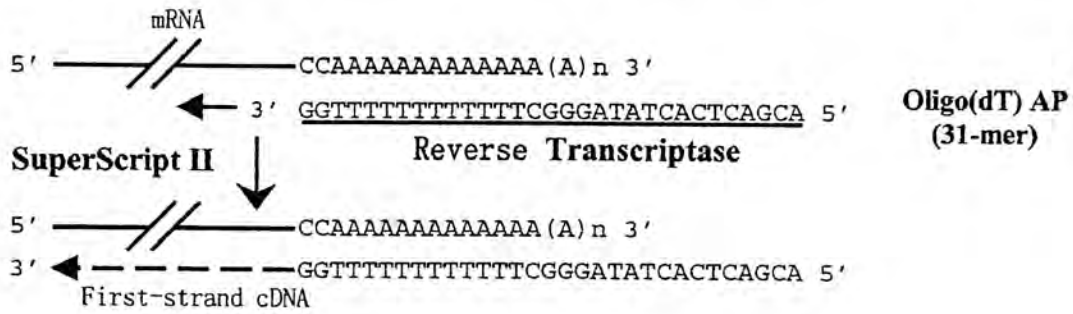
particular cell line (Liang and Pardee, 1992; Zhang *et. al.*, 1998). In this way, it allows the identification and analysis of the expression patterns of previously uncharacterized genes.

A standard protocol of DD method involves the following steps. The isolation of RNAs with high-quality is the first and crucial step which can directly affect the final results of DD. Then the selective reverse transcription of polyadenylated mRNA using specific anchored oligopolydeoxythymidine [oligo(dT)] primers (AP) is carried out to obtain the reverse transcribed cDNA. After that, the subsequent PCR amplification of the cDNA with the same oligo(dT), an arbitrary upstream primer and radioisotopes for labeling the PCR products is conducted to amplify the cDNA fragment. Finally, The radioisotopically labeled products are then separated on a sequencing gel and the differentially expressed fragments will appear on the DD gel (Liang and Pardee, 1992; Velculescu *et. al.*, 1995).

Because of the great hazard and risk to handle and dispose radioisotopes, an alternative approach, fluorescent differential display (FDD), in which the fluoresceins were used for labeling instead of the radioisotopes, was developed to overcome the shortcoming of traditional isotopic DD (Bauer *et. al.*, 1993; Ito *et. al.*, 1994). After the first-strand cDNA strand was synthesized with the anchored primers (APs) in the FDD strategy, the PCR amplification was carried out with the fluorescent tetramethylrodamine (TMR)-labeled AP in combination with the arbitrary primer (ARP). ARP contain sequence which was designed to anneal at sites 5' or upstream of the AP annealing site to convert the first-strand cDNA into one or more truncated cDNA fragments (Figure 1.2). The fluorescent TMR-labeled PCR product was then electrophoresed on a polyacrylamide gel



**I Synthesis of first-strand cDNA fragment (Reverse transcription)**



**II Synthesis of double-strand cDNA fragment (DD-PCR)**

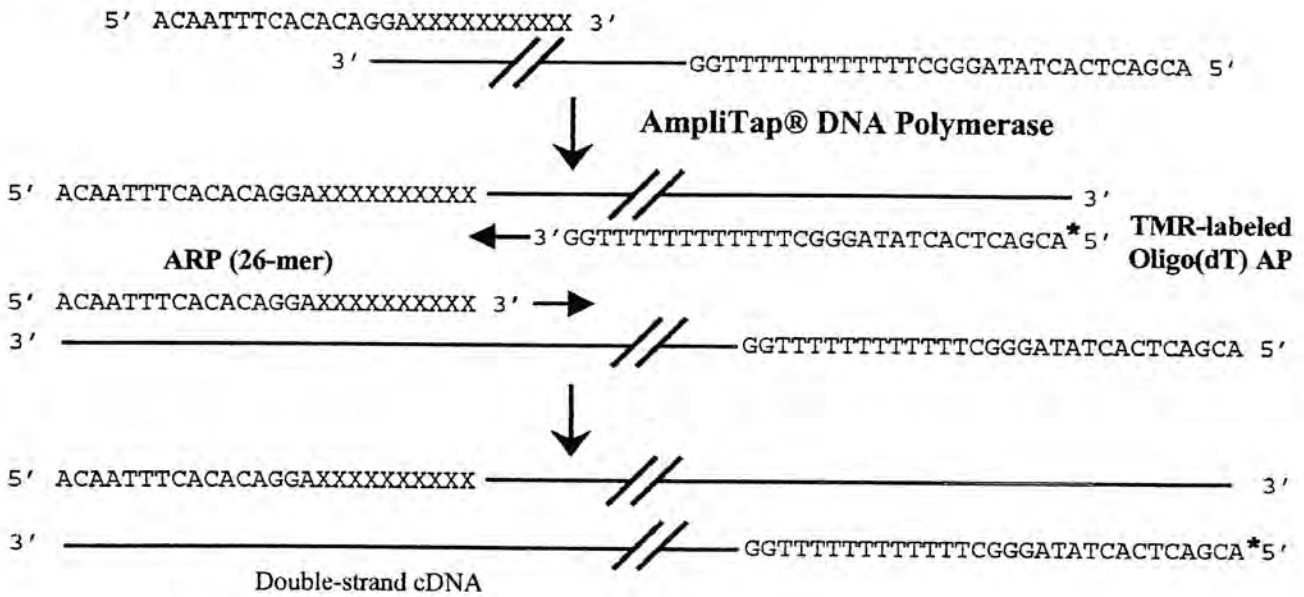


Figure 1.2. Schematic diagram to show the procedure of FDD method. I, synthesis of first-strand cDNA (Reverse transcription); II, synthesis of double-strand cDNA (FDD-PCR). AP, anchored primer; ARP, arbitrary primer (Adapted from fluoroDD manual, Genomyx).

(Bauer *et. al.*, 1993; Ito *et. al.*, 1994) and scanned with a fluorescent scanner to develop and store the gel image.

In summary, FDD allows rapid visualization of a specific banding pattern of partial gene fragments on fluorescent image analyzer by reverse-transcription of mRNA using fluorescent-labeled AP to subsequent PCR with additional ARP. It is a powerful technique for analyzing differences in gene expression that can be useful in identifying both known and novel genes and gene functions. Especially, it is beneficial in analyzing disease states, characterizing pharmacologically active compounds, discovering novel drug targets, and determining the activity of gene therapy agents. By understanding how and when a gene is expressed or repressed, targeted interventions can be developed to achieve the desired effect. By now, differential display has already emerged as one of the most popular methods for gene expression profiling (Cho *et. al.*, 2001).

## 1.9 Objectives of the study

It is necessary to investigate the molecular basis of CCl<sub>4</sub>-induced liver injury since the possibility of exposure to CCl<sub>4</sub> still exists in our daily life. Understanding the molecular mechanism of CCl<sub>4</sub>-induced hepatotoxic effects in rodents will be a basic step for accurate assessment of the human health risks associated with exposure to CCl<sub>4</sub>.

Although our previous studies using CYP2E1-null mice confirmed the involvement of CYP2E1 in CCl<sub>4</sub>-induced hepatotoxicity, the exact molecular mechanism of this process is still poorly understood. Therefore, the aim of this study was to identify the spectrum of genes involved in CCl<sub>4</sub>-induced hepatotoxicity using the CYP2E1-null mouse *in vivo* model and the fluorescent differential display method. Identification of the



spectrum of genes involved in CCl<sub>4</sub>-induced liver injury might help to understand the molecular mechanism of this process.

Since previous biochemical and histological studies have demonstrated that CCl<sub>4</sub>-induced hepatotoxicity occurred in a time-dependent manner, the temporal expression of the identified CYP2E1-dependent genes involved in this process was also investigated. In addition, the tissue distribution of the identified CYP2E1-dependent genes in various tissues was also examined.

The objectives of this study are summarized as follow:

1. To identify CYP2E1-dependent genes involved in CCl<sub>4</sub>-induced liver injury in *cyp2e1*<sup>+/+</sup> and *cyp2e1*<sup>-/-</sup> mice by FDD RT-PCR method.
2. To study the temporal expression (2, 6, 12, 24 and 48 hr) of the identified CYP2E1-dependent genes.
3. To examine the tissue distribution of the identified CYP2E1-dependent genes in kidney, testis, brain, lung, heart, intestine, stomach, spleen, brown fat, white fat and muscle.

## CHAPTER 2: MATERIALS AND METHODS

### 2.1 Animals and treatments

In order to search and identify CYP2E1-dependent genes involved in CCl<sub>4</sub>-induced liver injury, CYP2E1-null mice were used as an *in vivo* animal model.

#### 2.1.1 Materials

Carbon tetrachloride (CCl<sub>4</sub>, 99.8% purity) was obtained from Riedel-de Haën Company (Germany). Corn oil was obtained from Lion and Globe Company (Hong Kong).

#### 2.1.2 Methods

Male *cyp2e1*<sup>+/+</sup> and *cyp2e1*<sup>-/-</sup> mice (20-30 g, 2-3 months) were used for all experiments. Both *cyp2e1*<sup>+/+</sup> and *cyp2e1*<sup>-/-</sup> mice were inbred strains on Sv/129 genetic background (Lee *et. al.*, 1996). A pair of parental stocks of *cyp2e1*<sup>+/+</sup> and *cyp2e1*<sup>-/-</sup> mice was shipped from the National Cancer Institute (National Institutes of Health, USA). They were then bred and reared at the Laboratory Animal Service Center of the Chinese University of Hong Kong on a 12 hr light/dark cycle (light, 06:00-18:00) period. Two to three mice with the same genotypes were housed per cage and provided with ozonated water *ad libitum*.

Mice (3-6 per treatment group) were i.p. injected with 1 ml/kg body weight CCl<sub>4</sub> (10% solution in corn oil). Controls for each group were injected with corn oil vehicle only. After 2, 6, 12, 24 and 48 hr of injection, mice were sacrificed by cervical dislocation and blood was collected. Livers and other tissues were excised, weighed, wrapped in aluminum

foil and immediately frozen and stored in liquid nitrogen until further use for RNA preparation.

## **2.2 Serum alanine aminotransferase (ALT) and aspartate aminotransferase (AST) analyses**

Serum alanine aminotransferase (ALT) and aspartate aminotransferase (AST) are two types of enzymes mainly present in liver and kidney. Both ALT and AST are located in liver cells and will leak out and make their way into the general blood circulation when liver cells are damaged. Therefore, the elevation of ALT and AST activities in blood is generally regarded as marker of liver injury.

### **2.2.1 Materials**

Commercial ALT and AST kits (Cat. No. 59-UV for ALT and 58-UV for AST) were obtained from Sigma Chemical Company (USA).

### **2.2.2 Methods**

#### **2.2.2.1 Serum preparation**

Blood samples were collected from mice and serum was obtained after blood was allowed to clot at room temperature for 30 min. The clotted blood samples were centrifuged at 3,000 rpm at room temperature for 20 min. The supernatant was transferred to a new eppendorf and centrifuged again at 3,000 rpm for 20 min. After the second centrifugation, clear serum was transferred to a new eppendorf and stored at -20°C.

### 2.2.2.2 Activity determination

Total 2  $\mu$ l (for CCl<sub>4</sub>-treated *cyp2e1*<sup>+/+</sup> group) or 35  $\mu$ l (for the other three groups) of serum was used for each assay. The ALT and AST assays were performed according to the manufacturer's directions. The ALT and AST activities were determined enzymatically by the rate of NADH disappearance (Bergmeyer *et. al.*, 1978).

## 2.3 Tail-genotyping by PCR

PCR method was applied to confirm the genotypes of *cyp2e1*<sup>+/+</sup> and *cyp2e1*<sup>-/-</sup> mice used in our studies. A pair of primers for *cyp2e1*<sup>+/+</sup> and *cyp2e1*<sup>-/-</sup> mice each were designed by using the primer design program OLIGO4 (Molecular Biology Insight Inc., CO, USA) as follows for tail genotyping (Figure 2.1). For *cyp2e1*<sup>+/+</sup> mice, the forward primer (FP, CCACCCTCCTCCTCGTAT) was based on exon 1 and the backward primer (BP<sub>1</sub>, GCCAAGGTGCAGTGTGAA) was based on exon 2. The size of expected PCR fragment was 957 bp. For *cyp2e1*<sup>-/-</sup> mice, the forward primer (FP, CCACCCTCCTCCTCGTAT) was the same, but the backward primer (BP<sub>2</sub>, GCCGCCGCATTGCATCAG) was based on the neo gene in place of exon 2. The size of expected PCR fragment was 1.6 kb.

### 2.3.1 Materials

Trizma base (Tris), sodium chloride (NaCl) and ethidium bromide (EtBr) were obtained from Sigma Chemical Company (USA). Proteinase K was obtained from Boehringer Mannheim Company (Germany). EDTA was obtained from Riedel-de Haën (Germany). Magnesium chloride (MgCl<sub>2</sub>), 10x PCR buffer and AmpliTaq<sup>®</sup> enzyme were

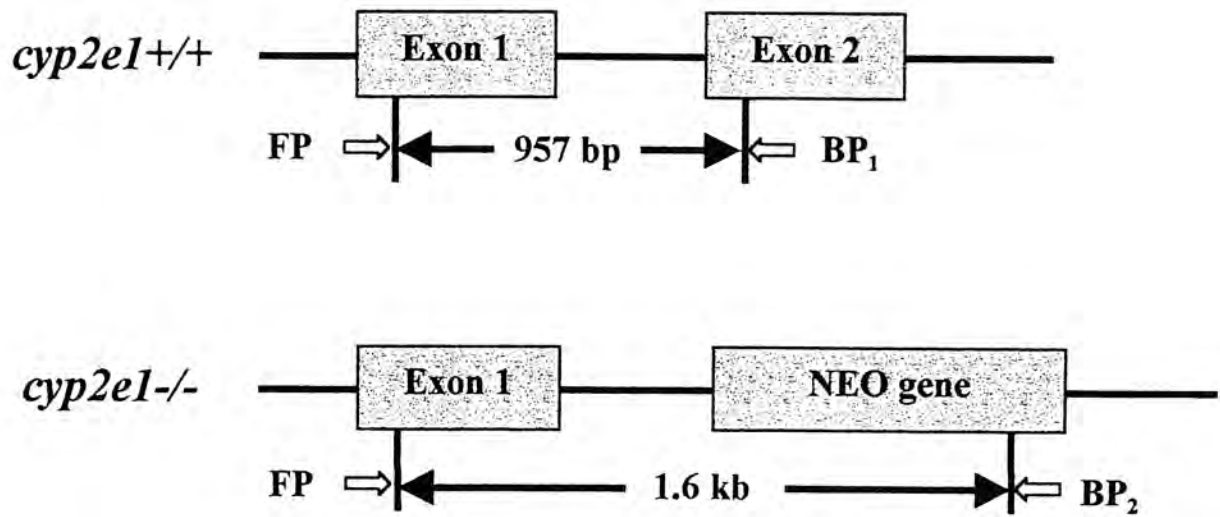


Figure 2.1. The schematic representation of the genomic organization of CYP2E1 gene and the strategy of PCR primer design for *cyp2e1*<sup>+/+</sup> and *cyp2e1*<sup>-/-</sup> mice. In *cyp2e1*<sup>-/-</sup> mice, exon 2 was deleted and replaced by a neo gene fragment. FP represents forward primer; BP<sub>1</sub> and BP<sub>2</sub> represent backward primers.

obtained from Perkin Elmer Company (USA). Agarose, dNTP, DNA markers (100 bp and 1 kb) were obtained from Life Technologies (USA). Oligonucleotides were synthesized and obtained from Life Technologies (USA).

## 2.3.2 Methods

### 2.3.2.1 Preparation of genomic DNA from mouse tail

About 1 cm of mouse tail tip was excised from each group of mice and incubated in 0.5 ml of lysis buffer (0.1 M Tris-HCl, 5 mM EDTA, 0.2 % SDS, 0.2 M NaCl, 100 µg/ml Proteinase K, pH 8.5) at 55°C with shaking for overnight (Laird *et. al.*, 1991). In the next morning these samples were centrifuged at 3,000 rpm for 10 min and supernatant was then transferred into new eppendorfs. After centrifugation at 12,000 g for 10 min, supernatant was transferred to new eppendorfs containing 0.5 ml isopropanol and mixed well by shaking laterally with hands in order to precipitate out DNA strands. Pipette tip was used to pick up and transfer DNA strands to new eppendorfs. Then the DNA pellets were air-dried for 10 min and resuspended in 100 µl of TE buffer (10 mM Tris-HCl, 0.1 mM EDTA, pH 7.5). The samples were then incubated at 37°C for overnight to enhance dissolution of the DNA pellets.

### 2.3.2.2 PCR reaction

For each PCR reaction, 1 µl of 10-fold diluted genomic DNA from mouse tail was used as the templates and was mixed with 1x PCR buffer, 3.75 mM MgCl<sub>2</sub>, 50 µM dNTP, 0.35 µM forward primer, 0.35 µM backward primer and 0.05 unit AmpliTaq<sup>®</sup> enzyme. PCR reaction was performed in a thermal cycler (GeneAmp<sup>®</sup> PCR System 9700). The



thermal cycling profile was as follows: 95°C for 2 min, followed by 34 cycles of 92°C for 15 sec, 55°C for 30 sec, 72°C for 2 min, and followed by final extension at 72°C for 7 min and hold at 4°C. The PCR products were resolved on 1.5% agarose, 0.5x TBE gels.

## 2.4 Total RNA isolation

Isolation of total RNA with high quality is the first but most important step of FDD RT-PCR analysis, which may affect the final experimental results directly. The strategy of FDD RT-PCR analysis is illustrated in Figure 2.2. RNAs were extracted from livers and other tissues from both controls and CCl<sub>4</sub>-treated *cyp2e1*<sup>+/+</sup> and *cyp2e1*<sup>-/-</sup> mice.

### 2.4.1 Materials

Trizol reagent was obtained from Life Technologies (USA). Chloroform, ethanol and isopropanol were obtained from Merck Company (USA). Nuclease-free water was obtained from Promega Company (USA).

### 2.4.2 Methods

Mixture of 0.1 g of tissue and 1 ml of Trizol reagent was homogenized by tissue tearor (Dremel<sup>®</sup>, USA). Then 0.2 ml of chloroform was added into the mixture and it was centrifuged at 12,000 g for 15 min. The supernatant was transferred into a new tube with 0.5 ml of isopropanol. RNA was precipitated at -80°C for overnight. The next day the sample was centrifuged at 12,000 g for 15 min. The pellet was washed with 1 ml of 70% ethanol twice, then air-dried and finally dissolved in appropriate amount of nuclease free

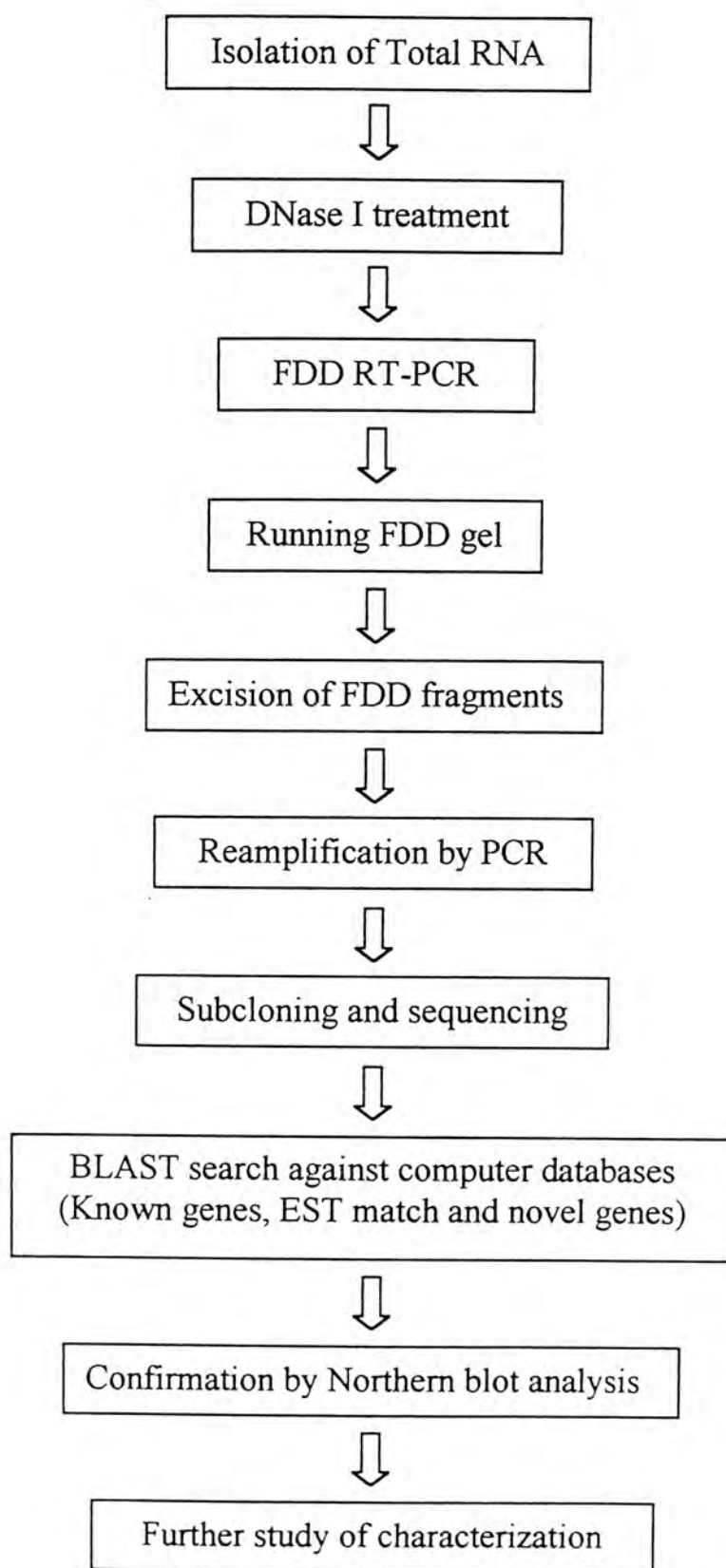


Figure 2.2. Flowchart showing the overall strategy to identify differentially expressed genes by FDD RT-PCR (Martin *et. al.*, 1997).

water. The concentration of the extracted RNA was determined from the absorbance at 260 nm, and the purity of RNA was quantified by the ratio of 260 to 280 nm.

## **2.5 DNase I treatment**

Extreme trace amount of contaminating DNA can be amplified during FDD RT-PCR and result in false positives. Therefore, DNase I digestion of the total RNA samples is essential to be carried out in order to remove the possible contamination of genomic DNA.

### **2.5.1 Materials**

Sodium acetate (NaAc) and ethidium bromide (EtBr) were obtained from Sigma Chemical Company (USA). RNase-free DNase I and nuclease-free water were obtained from Promega Company (USA). Phenol: chloroform: isoamyl alcohol (25: 24: 1, pH 4.7) and agarose were obtained from Life Technologies (USA).

### **2.5.2 Methods**

Fifty micrograms of total RNA was incubated with 1x DNase I buffer, 10 units of RNase-free DNase I at 37°C for 15 min. Fifty microliters of phenol: chloroform: isoamyl alcohol (25: 24: 1, pH 4.7) was added into the reaction and then vortexed vigorously for 1 min. The aqueous phase containing the RNA was separated from the organic phase by centrifuging the mixture at 15,000 g for 5 min. After centrifugation, 50 µl of ethanol and 10 µl of 3 M sodium acetate were added to precipitate the RNA at -80°C for overnight. The RNA pellet obtained by centrifuging at 15,000 g for 15 min and was washed with 70% ethanol, air-dried, and resuspended in 20 µl nuclease free water. The concentration of RNA

was determined from the absorbance at 260 nm. One microliter of the sample was resolved on 1% agarose, 0.5x TBE gel to check the integrity of RNA after DNase I treatment. Only the RNA without noticeable degradation could be used for further analysis.

## **2.6 Reverse transcription of mRNA and fluorescent PCR amplification**

The first-strand cDNA was synthesized by using the HIEROGLYPH kit. There were 12 anchored primers (APs) for reverse transcription of mRNA (Table 2.1) in the kit. Each of the APs had a same piece of sequence as oligo-(dT)<sub>12</sub> which can allow the AP to be anchored to the poly (A<sup>+</sup>) region of mRNA. The difference among the APs was the two-base combinations on the upstream of the poly (A<sup>+</sup>) region. Each respective two-base AP could encompass approximately 1-12 of the mRNA pool constituency and could render approximately 800-1200 different first-strand cDNAs.

There were 20 arbitrary primers (ARPs) in the HIEROGLYPH kit for the FDD-PCR reaction (Table 2.2). The length of the APs and ARPs should be enough to allow for stringent annealing conditions and to prevent the production of nonspecific products (Mou *et. al.*, 1994; Zhao *et. al.*, 1995). Only the fragment between APs and ARPs should be amplified during the course of the FDD RT-PCR.

The fluoroDD kit was used for the fluorescent PCR amplification. This kit contains 12 APs which were identical in DNA sequence to the HIEROGLYPH APs, but were 3'-end labeled with the fluorescent tag, tetramethylrodamine (TMR). Three sets of AP and ARP primer combinations (AP 5 & ARP 2, AP 5 & ARP 4, AP 5 & ARP 7) were used in the present study. All of the FDD RT-PCR reaction was performed in duplicate per sample to verify PCR reproducibility. To minimize the individual animal variability, for each



Table 2.1 Sequence of anchored primers (APs) used for the first-strand cDNA synthesis (Adapted from fluoroDD manual, Genomyx).

AP 1	5' <u>ACGACTCACTATAGGGCTTTTTTTTTTTT</u> <b>GA</b> 3'
AP 2	5' <u>ACGACTCACTATAGGGCTTTTTTTTTTTT</u> <b>GC</b> 3'
AP 3	5' <u>ACGACTCACTATAGGGCTTTTTTTTTTTT</u> <b>GG</b> 3'
AP 4	5' <u>ACGACTCACTATAGGGCTTTTTTTTTTTT</u> <b>GT</b> 3'
AP 5	5' <u>ACGACTCACTATAGGGCTTTTTTTTTTTT</u> <b>CA</b> 3'
AP 6	5' <u>ACGACTCACTATAGGGCTTTTTTTTTTTT</u> <b>CC</b> 3'
AP 7	5' <u>ACGACTCACTATAGGGCTTTTTTTTTTTT</u> <b>CG</b> 3'
AP 8	5' <u>ACGACTCACTATAGGGCTTTTTTTTTTTT</u> <b>AA</b> 3'
AP 9	5' <u>ACGACTCACTATAGGGCTTTTTTTTTTTT</u> <b>AC</b> 3'
AP 10	5' <u>ACGACTCACTATAGGGCTTTTTTTTTTTT</u> <b>AG</b> 3'
AP 11	5' <u>ACGACTCACTATAGGGCTTTTTTTTTTTT</u> <b>AT</b> 3'
AP 12	5' <u>ACGACTCACTATAGGGCTTTTTTTTTTTT</u> <b>CT</b> 3'

Note: The 17 nucleotides of the T7 promoter sequence are underlined and the two-base combinations upstream are bolded.

Table 2.2 Sequence of arbitrary primers (ARPs) used for FDD-PCR reaction  
(Adapted from fluoroDD manual, Genomyx).

ARP 1	5' <u>ACAATTTCACACAGGAC</u> GACTCCAAG 3'
ARP 2	5' <u>ACAATTTCACACAGGAG</u> GCTAGCATGG 3'
ARP 3	5' <u>ACAATTTCACACAGGAG</u> ACCATTGCA 3'
ARP 4	5' <u>ACAATTTCACACAGGAG</u> GCTAGCAGAC 3'
ARP 5	5' <u>ACAATTTCACACAGGA</u> ATGGTAGTCT 3'
ARP 6	5' <u>ACAATTTCACACAGGAT</u> ACAACGAGG 3'
ARP 7	5' <u>ACAATTTCACACAGGAT</u> GGATTGGTC 3'
ARP 8	5' <u>ACAATTTCACACAGGAT</u> GGTAAAGGG 3'
ARP 9	5' <u>ACAATTTCACACAGGAT</u> AAGACTAGC 3'
ARP 10	5' <u>ACAATTTCACACAGGAG</u> ATCTCAGAC 3'
ARP 11	5' <u>ACAATTTCACACAGGA</u> ACGCTAGTGT 3'
ARP 12	5' <u>ACAATTTCACACAGGAG</u> GGTACTAAGG 3'
ARP 13	5' <u>ACAATTTCACACAGGAG</u> TTCACCAT 3'
ARP 14	5' <u>ACAATTTCACACAGGAT</u> TCCATGACTC 3'
ARP 15	5' <u>ACAATTTCACACAGGA</u> CTTTCTACCC 3'
ARP 16	5' <u>ACAATTTCACACAGGAT</u> CGGTCATAG 3'
ARP 17	5' <u>ACAATTTCACACAGGA</u> CTGCTAGGTA 3'
ARP 18	5' <u>ACAATTTCACACAGGAT</u> GTGCTACC 3'
ARP 19	5' <u>ACAATTTCACACAGGAT</u> TTTGGCTCC 3'
ARP 20	5' <u>ACAATTTCACACAGGAT</u> CGATACAGG 3'

Note: The 16 nucleotides of the M13 reverse (-48) sequence are underlined.



group, RNA samples from two different mice per treatment group were used for the FDD RT-PCR analysis. Under the conditions of no reverse transcriptase, negative RT-PCR was carried out to guarantee that no genomic DNA contamination existed.

### 2.6.1 Materials

HIEROGLYPH kit, dNTP mix (1:1:1:1) and fluoroDD kit were obtained from Genomymx (USA). SuperScript II RT buffer, SuperScript II RT enzyme and DTT were purchased from Life Technologies (USA).

### 2.6.2 Methods

Two hundred nanograms of total RNA after DNase I treatment were reverse-transcribed in the presence of 0.2  $\mu$ M AP, 1x SuperScript II RT buffer, 25  $\mu$ M dNTP mix (1:1:1:1), 10 mM DTT and 40 units of SuperScript II RT enzyme. For the negative reverse transcription (RT), no reverse transcriptase was added in the reaction. Reverse transcription (RT) reaction was performed in a thermal cycler (GeneAmp<sup>®</sup> PCR System 9700). The thermal cycling profile was as follows: 42°C for 5 min, 50°C for 50 min, and followed by final extension at 70°C for 15 min and hold at 4°C.

After the first-strand cDNA synthesis, double-strand cDNA was synthesized by PCR. One microliter of RT mixture was used and mixed with 1x PCR buffer, 3.75 mM MgCl<sub>2</sub>, 50  $\mu$ M dNTP mix (1:1:1:1), 0.35  $\mu$ M 5'-ARP, 0.35  $\mu$ M 3'-TMR-AP and 0.5 unit of AmpliTaq enzyme. PCR was performed in a thermal cycler (GeneAmp<sup>®</sup> PCR System 9700). The thermal cycling profile was as follows: 95°C for 2 min, followed by 4 cycles at 92°C for 15 sec, 50°C for 30 sec, and 72°C for 2 min, followed by 30 cycles at 92°C for 15

sec, 60°C for 30 sec, and 72°C for 2 min and followed by final extension at 72°C for 7 min and hold at 4°C.

## **2.7 Fluorescent differential display (FDD)**

### **2.7.1 Materials**

TMR-molecular weight DNA standard marker, fluoroDD loading dye, 5.6% clear denaturing HR-1000 gel, 1x TBE and 0.5x TBE buffers were obtained from Genomyx (USA). Ammonium persulfate and TEMED were purchased from Sigma Chemical Company (USA).

### **2.7.2 Methods**

Following FDD RT-PCR, the TMR-labeled cDNA fragments were separated on a polyacrylamide gel with high resolution under denaturing conditions by electrophoresis. The FDD gel with high resolution was prepared by mixing 70 ml of 5.6% clear denaturing HR-1000 gel with 400  $\mu$ l of freshly prepared 10% ammonium persulfate and 40  $\mu$ l TEMED. After mixing and pouring, the FDD gel was allowed to polymerize for overnight at room temperature.

Four microliters of each FDD PCR product with 1.5  $\mu$ l of fluoroDD loading dye were denatured at 95°C for 2 min. The TMR-molecular weight marker was prepared in the same manner as the FDD PCR products. The lower and upper buffer chambers were filled with 250 ml of 1x TBE buffer and 120 ml of 0.5x TBE buffer respectively. The TMR-labeled PCR products and TMR-molecular weight marker were electrophoresed on a 5.6% denatured polyacrylamide gel at 3000 V, 100 W, 50°C for 4.5 hours using a GenomyxLR™

DNA electrophoresis system (Genomyx, USA) (Figure 2.3). After gel electrophoresis, the gel was dried in the same instrument and the gel image was scanned by the GenomyxSC™ fluorescent imaging scanner (Genomyx, USA) (Figure 2.4).

## **2.8 Excision of differentially expressed cDNA fragments**

Following FDD RT-PCR, only the CCl<sub>4</sub>-responsive and CYP2E1-dependent differentially expressed cDNA fragments showing consistent changes among four different treatment groups were excised from the FDD gels. The possible CCl<sub>4</sub> responsive and CYP2E1-dependent expression patterns of FDD cDNA fragments were indicated in Table 2.3.

### **2.8.1 Materials**

Sterile scalpel blades were obtained from Hecos Company (China).

### **2.8.2 Methods**

To exactly locate the position of the bands with interests, the physical grid (Genomyx, USA) and the Excision Workstation (Genomyx, USA) were used (Figure 2.5). The physical grid was placed on the gel to locate the bands with interests. The gel slice was excised from the FDD gels with a sterile scalpel blade and then transferred into an eppendorf containing 25 µl TE buffer (10 mM Tris-HCl, 1 mM EDTA, pH 7.4). The sample was incubated at 37°C for 1 hr to elute the DNA out of the gel slice, and then stored at -20°C for later use. After the excision of bands, the FDD gel was scanned again to check for the accuracy of band excision.

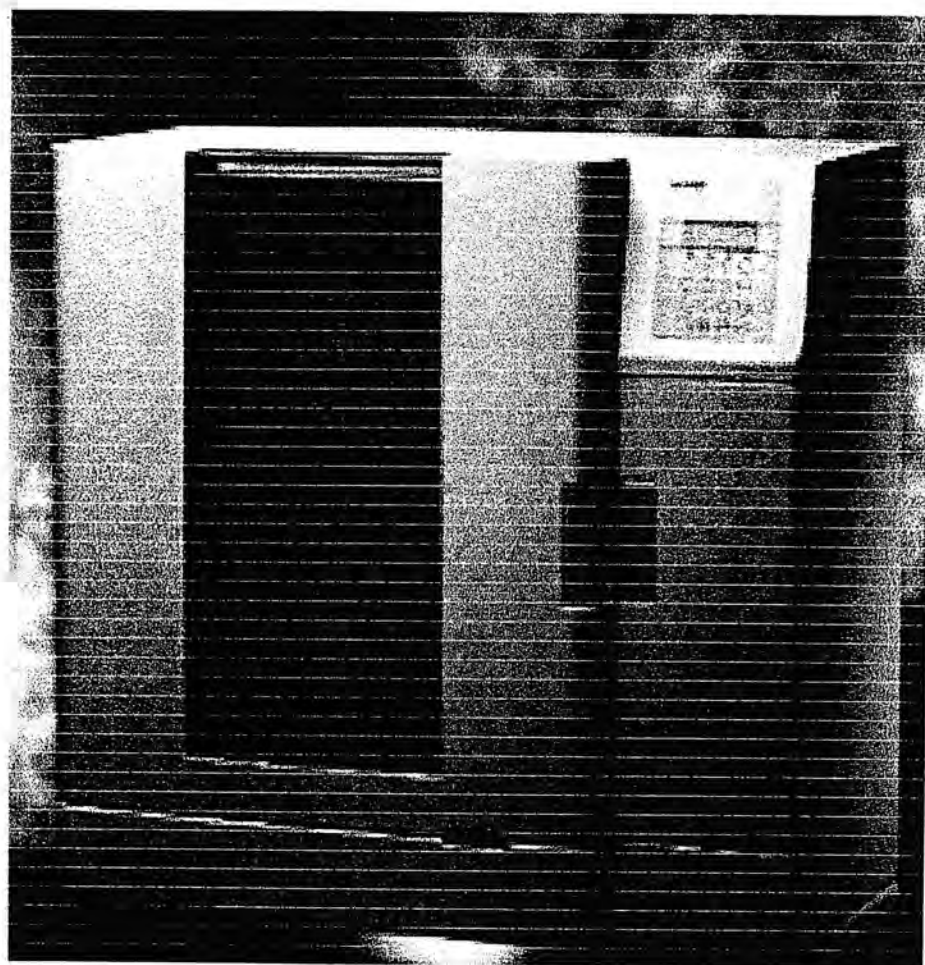


Figure 2.3. GenomyxLR™ DNA electrophoresis system (Genomyx, USA). A complete electrophoresis system possesses full programmability of all electrophoresis run parameters (temperature, voltage, wattage, gel temperature, and run-time). Following electrophoresis, the gel is dried within this instrument which can minimize the requirement for gel fixation and transfer (Adapted from fluoroDD catalogue, Genomyx).



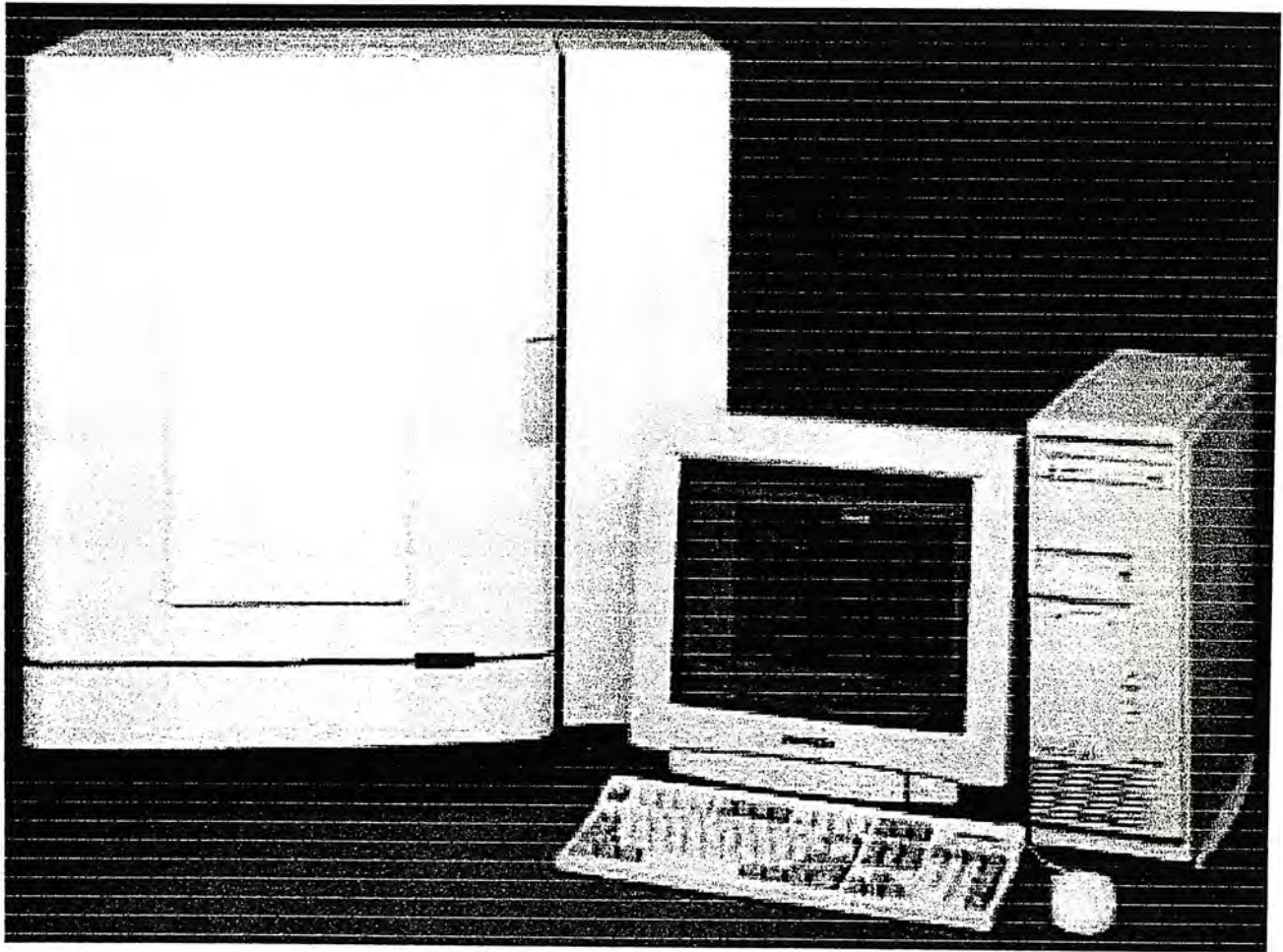


Figure 2.4. GenomyxSC™ fluorescent imaging scanner (Genomyx, USA). The signals from the fluorescent-labeled PCR products are recognized and exported to the computer for the further data analysis (Adapted from fluoroDD catalogue, Genomyx).



Table 2.3 Possible gene expression patterns on FDD gels.

FDD Expression Pattern					
<i>cyp2e1</i> +/+		<i>cyp2e1</i> -/-		Up- or Down-regulated	CYP2E1-dependent
Control	CCl <sub>4</sub>	Control	CCl <sub>4</sub>		
-	+	-	-	Up-regulated	Yes
+	+++	+	+	Up-regulated	Yes
+	-	+	+	Down-regulated	Yes
+++	+	+++	+++	Down-regulated	Yes
-	-	-	+	Down-regulated	Yes
+	+	+	-	Up-regulated	Yes
-	+	-	+	Up-regulated	No
+	-	+	-	Down-regulated	No

+ represents that there is observable expression in this treatment group on the FDD gel, while - means that there is no observable expression in this treatment group on the FDD gel. Number of + represents the level of expression.

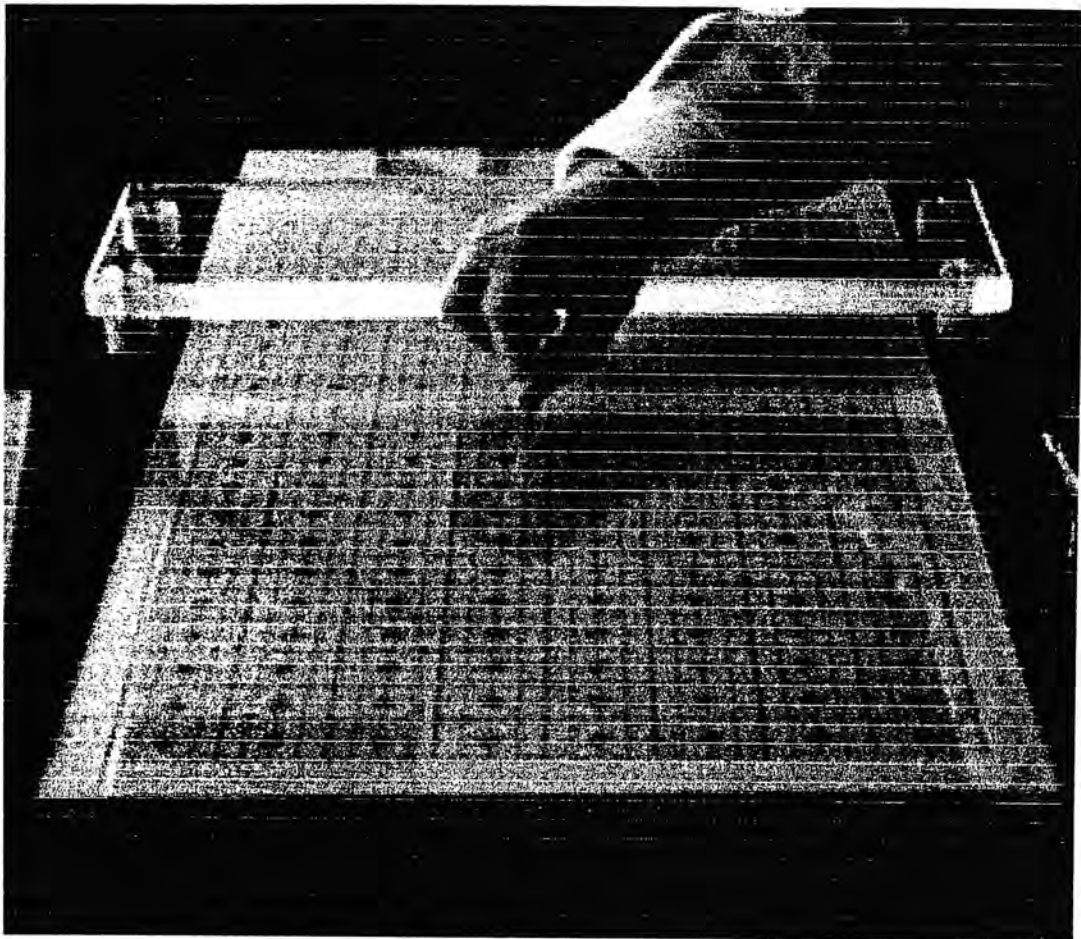


Figure 2.5. Band Excision Workstation for fluorescent differential display. The physical grid is placed on the gel to locate the exact position of bands with interests (Adapted from fluoroDD catalogue, Genomyx).

## 2.9 Reamplification of differentially expressed cDNA fragments

The excised FDD cDNA fragments were reamplified by PCR reaction with two primers, M13 reverse (-48) 24-mer (5' AGCGGATAACAATTTTCACACAGGA 3') primer and T7 promoter 22-mer (5' GTAATACGACTCACTATAGGGC 3') primer. Since each of the ARPs used in FDD RT-PCR incorporated a 16 nucleotides of segment of the M13 reverse (-48) 24-mer priming sequence, direct sequencing from the 5' end of the original transcript could be carried out. On the other hand, since each of the APs used in FDD RT-PCR incorporated 17 nucleotides of segment of the T7 promoter 22-mer priming sequence, direct sequencing from 3' end of the original transcript could also be carried out. The principles of the reamplification by PCR was illustrated in details in Figure 2.6.

### 2.9.1 Materials

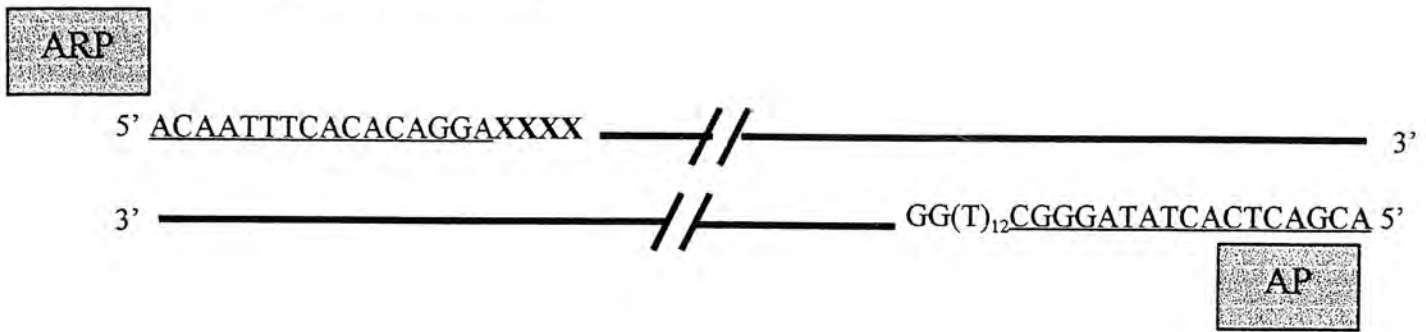
Trizma base was obtained from Sigma Chemical Company (USA). EDTA was obtained from Riedel-de Haën Company (Germany). M13 reverse (-48) 24-mer primer, T7 promoter 22-mer primer and dNTP mix (1:1:1:1) were obtained from Genomymx Company (USA). Magnesium chloride ( $MgCl_2$ ), 10x PCR buffer and AmpliTaq<sup>®</sup> enzyme were obtained from Perkin Elmer Company (USA). Agarose and 100 bp DNA marker were obtained from Life Technologies (USA). Ethidium bromide (EtBr) was obtained from Sigma Chemical Company (USA).

### 2.9.2 Methods

One to six microliters of gel band eluate was used for the reamplification of cDNA fragments by PCR. The eluate was then mixed with 1x PCR buffer, 1.5 mM  $MgCl_2$ , 20  $\mu M$



## I. cDNA fragment excised from the gel



## II. Priming of M13 reverse (-48) 24-mer and T7 promoter 22-mer primers to cDNA fragments

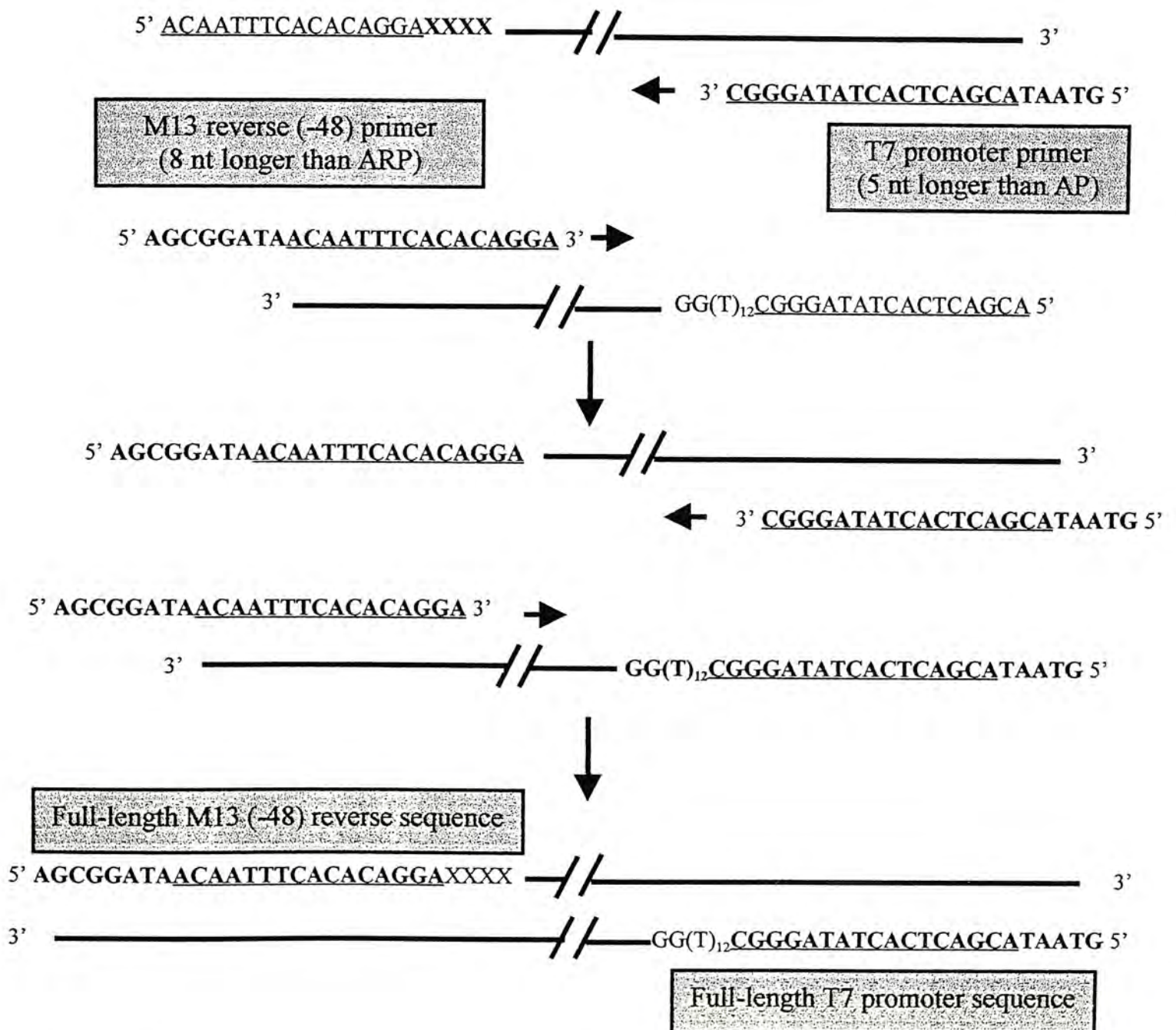


Figure 2.6. Schematic diagram to show the reamplification of the cDNA fragment by PCR and the reconstruction of priming site using full-length M13 reverse (-48) 24-mer and T7 promoter 22-mer primers (Adapted from fluoroDD manual, Genomyx and modified by Lee, 2000). AP, anchored primer; ARP, arbitrary primer; nt, nucleotides. The sequences of M13 reverse (-48) and T7 promoter primers were bolded.

dNTP mix (1:1:1:1), 0.2  $\mu$ M M13 reverse (-48) 24-mer primer, 0.2  $\mu$ M T7 promoter 22-mer primer and 2 units of AmpliTaq<sup>®</sup> enzyme. PCR was performed in a thermal cycler (GeneAmp<sup>®</sup> PCR System 9700). The thermal cycling profile was as follows: 95°C for 2 min, followed by 4 cycles at 92°C for 15 sec, 50°C for 30 sec, and 72°C for 2 min, then followed by 25 cycles at 92°C for 15 sec, 60°C for 30 sec, and 72°C for 2 min and followed by final extension at 72°C for 7 min and hold at 4°C. Ten microliters of reamplified PCR product was then resolved on 1% agarose, 0.5x TBE gel with ethidium bromide staining.

## **2.10 Subcloning of reamplified cDNA fragments**

AdvaTAge<sup>™</sup> PCR cloning system was used to subclone the reamplified cDNA fragments. This cloning system allowed to screen positive recombinant clones by restriction enzyme digestion. Large amount of inserts could be easily obtained and purified from recombinant clones for later labeling as the probe in Northern blot analysis.

### **2.10.1 Materials**

AdvaTAge<sup>™</sup> cloning kit was purchased from Clontech Company (USA). Bactotryptone and yeast extract were obtained from Becton Dickinson Company (USA). X-Gal was obtained from Boehringer Mannheim Company (Germany). Ampicillin, acetic acid, glucose, potassium acetate and sodium chloride (NaCl) were obtained from Sigma Chemical Company (USA). Agarose and phenol: chloroform: isoamyl alcohol (25: 24: 1, pH 4.7) were obtained from Life Technologies (USA). EDTA and SDS were obtained from Riedel-de Haën Company (Germany). EcoRI buffer and EcoRI restriction enzyme were obtained from New England Biolabs (UK).



### 2.10.2 Methods

For the ligation, 1  $\mu$ l of PCR product was mixed with 1x ligation buffer, 50 ng pT-Adv vector and 4 units of T4 DNA ligase. The ligation reaction was performed at 14°C for overnight. Two microliters of ligation mixture was added into 50  $\mu$ l TOP10F' *E. coli* competent cells with 2  $\mu$ l of 0.5 M  $\beta$ -mercaptoethanol. The cell mixture was incubated on ice for 30 min and then heat-shocked for exact 30 sec at 42°C to allow the ligated vector to be transformed into the TOP10F' *E. coli* competent cells. After heat shock, 250  $\mu$ l of SOC medium (2% tryptone, 0.5% yeast extract, 10 mM NaCl, 2.5 mM KCl, 10 mM MgCl<sub>2</sub>, 10 mM MgSO<sub>4</sub>, 20 mM glucose) was added into the cell mixture and shaken at 37°C for 1 hour at 225 rpm in a rotary shaking incubator (Lab-Line, USA). The cell mixture was then spread on a LB plate containing 50  $\mu$ g/ml ampicillin and 1.6  $\mu$ g of X-Gal. The plate was left at room temperature for 30 min to allow the diffusion of ampicillin and X-Gal into the LB, and then incubated at 37°C for overnight. The partial restriction map and multiple cloning sites of pT-Adv vector are shown in Figure 2.7.

Chloroform extraction method (Ohyama, 1997) was used to screen the recombinant clones. About 10 white or pale blue clones were picked with sterile toothpicks from each plate and inoculated into 3 ml LB medium with 50  $\mu$ g/ml ampicillin. The bacterial culture was then incubated at 37°C for overnight with shaking at 225 rpm in a rotary shaking incubator (Lab-Line, USA). In the next morning, 20  $\mu$ l of phenol: chloroform: isoamyl alcohol (25:24:1, pH 4.7) was mixed with equal volume of bacterial culture by vortex. The mixture was then centrifuged at 12,000 g for 1 min. Ten microliters of supernatant was separated on a 1% agarose, 0.5x TBE gel to screen the recombinant clones.

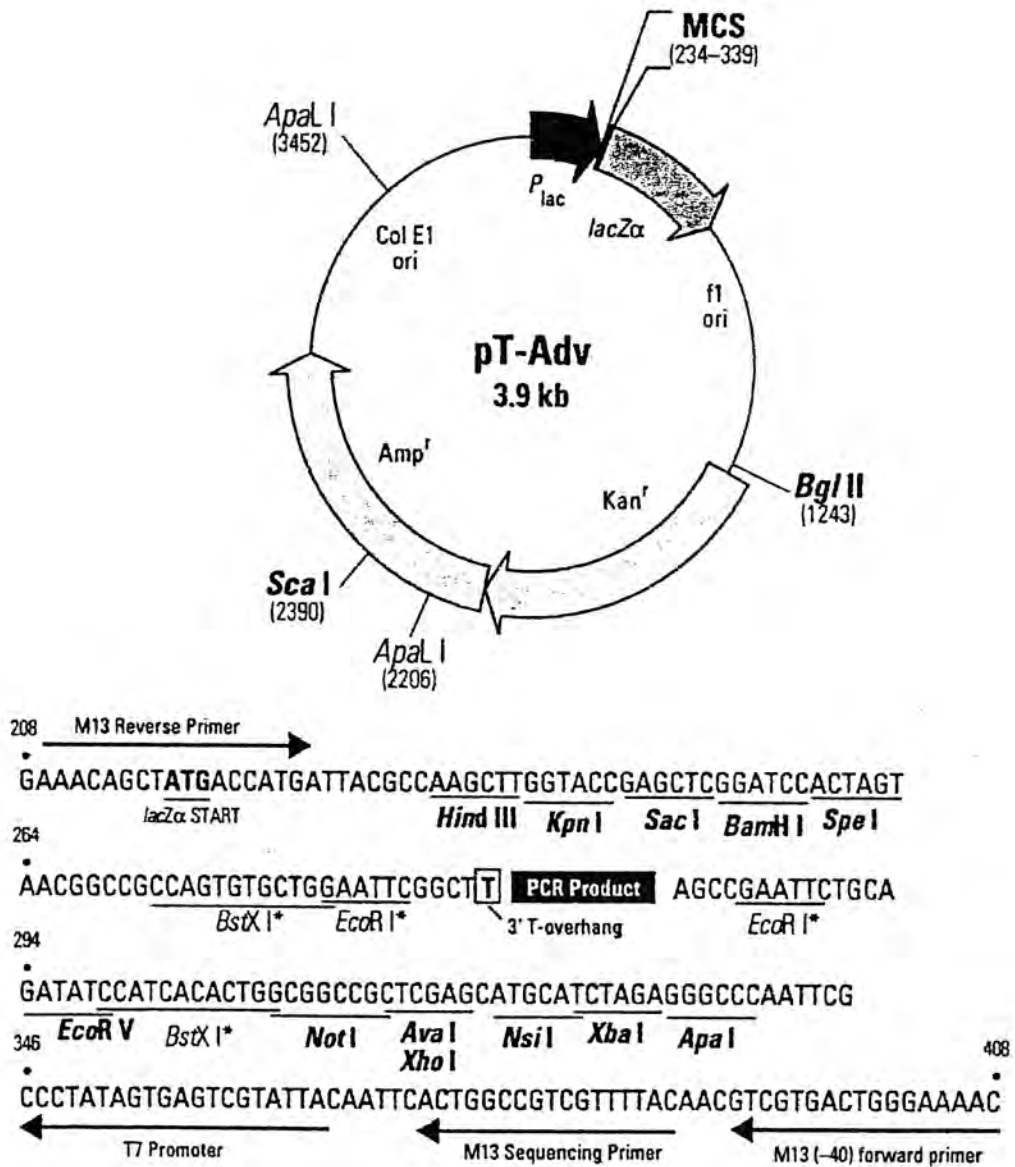


Figure 2.7. Restriction map and multiple cloning site of the pT-Adv vector (Adapted from the manual of AdvanTAge™ PCR cloning system, CLONTECH).

## **2.11 Purification of plasmid DNA from recombinant clone**

### **2.11.1 Materials**

Bacto-typtone and yeast extract were obtained from Becton Dickinson Company (USA). QIAprep Spin Miniprep kit was obtained from QIAgen Company (USA).

### **2.11.2 Methods**

The QIAprep Spin Miniprep kit was used to isolate plasmid DNA from recombinant clones for sequencing. Clones with interests were picked and inoculated into 5 ml LB with 50 µg/ml ampicillin. The bacterial culture was incubated at 37°C for overnight with shaking at 225 rpm in a rotary shaking incubator (Lab-Line, USA). In the next morning, the bacteria culture was centrifuged at 4°C at 2,500 g for 10 min. The supernatant was discarded and the cell pellet was resuspended in 250 µl of Buffer P1 by inverting of the tube. Two hundred and fifty microliters of Buffer P2 was then added into the cell resuspension to allow the lysis of cells. In the following step, 350 µl of Buffer P3 was added into the cell lysate and mixed well. The mixture was then centrifuged at 14,000 rpm for 10 min. The supernatant was applied to the QIAprep column and centrifuged at 14,000 rpm for 1 min. The column was then washed with 0.75 ml of Buffer PE with centrifugation at 14,000 rpm for 1 min. After the flow-through was discarded, the column was centrifuged at 14,000 rpm for additional 1 min to remove remain ethanol. Fifty microliters of Buffer EB (10mM Tris-Cl, pH 8.5) was applied in the column to elute the DNA by centrifugation at 14,000 rpm for 1 min twice. The concentration of the purified plasmid DNA was determined from the absorbance at 260 nm.

## 2.12 DNA sequencing of differentially expressed cDNA fragments

The CEQ 2000 Dye Terminator Cycle Sequencing system (Beckman, USA) was used for DNA sequencing of the FDD fragments with interests. M13 reverse primer (5' AAACAGCTATGACCATG 3') and M13 sequencing primer (5' GTAAAACGACGGCCAGT 3') were used respectively in two separate sequencing reactions starting from different direction (5' or 3').

### 2.12.1 Materials

CEQ 2000 terminator cycle sequencing kit was purchased from Beckman Company (USA). Formamide, 100 mM Na<sub>2</sub>EDTA and 3 M sodium acetate were obtained from Sigma Chemical Company (USA). Ethanol was obtained from Merck Company (USA). M13 reverse primer, M13 sequencing primer and dNTP mix (1:1:1:1) were obtained from Genomyx Company (USA).

### 2.12.2 Methods

The mixture for sequencing reaction contained 125 fmol of purified plasmid DNA template, 1x sequencing reaction buffer, 2 µl of dNTP mix, 2 µl of ddUTP dye terminator, 2 µl of ddGTP dye terminator, 2 µl of ddCTP dye terminator, 2 µl of ddATP dye terminator, 1 unit of Polymerase enzyme and 3.2 pmol of sequencing primer (M13 reverse or M13 sequencing).

The sequencing reaction was performed in a thermal cycler (GenAmp<sup>®</sup> PCR System 9700). The thermal cycle profile was as follows: 30 cycles at 96°C for 20 sec, 50°C for 20 sec, and 60°C for 4 min and hold at 4°C. After the sequencing reactions were



completed, 4  $\mu$ l of stop solution (1.5 M sodium acetate and 50 mM EDTA) and 20  $\mu$ g of glycogen (from the sequencing kit) were added to stop the reaction. For precipitation, 60  $\mu$ l of ice-cold 95% ethanol was added and the mixture was then centrifuged at 14,000 rpm at 4°C for 15 min. The supernatant was discarded and the pellet was rinsed twice with 200  $\mu$ l of ice-cold 70% ethanol by centrifugation at 14,000 rpm at 4°C for 15 min. After rinsing, the pellet was then vacuum-dried for 40 min and resuspended in 40  $\mu$ l of sample loading buffer (from the sequencing kit). The resuspended sample was transferred to the appropriate wells of the CEQ polypropylene sample plate from Beckman (USA). Each of the resuspended samples was covered with one drop of light mineral oil (Beckman Company, USA) on the top. The CEQ sample plate was then loaded into the CEQ capillary automatic sequencer (Beckman, USA) for automated sequencing.

### 2.12.3 BLAST search against the GenBank DNA databases

The Basic Local Alignment Search Tool (BLAST) was used for homology search of the sequence obtained from CEQ against the GenBank DNA databases (<http://www.ncbi.nlm.nih.gov/cgi-bin/BLAST/nph-newblast>).

## 2.13 Northern blot analysis of differentially expressed cDNA fragments

Norther blot analysis was applied to confirm the expression pattern of the FDD fragments with interests. The transcript size was estimated by DIG-labeled RNA molecular marker I.

### 2.13.1 Formaldehyde gel electrophoresis of total RNA



### 2.13.1.1 Materials

Formaldehyde, formamide, MOPS, ethidium bromide, sodium chloride and sodium citrate were obtained from Sigma Chemical Company (USA). Agarose was obtained from Life Technologies (USA). DIG-labeled RNA molecular marker I was obtained from Boehringer Mannheim Company (Germany). Hybond N<sup>+</sup> nylon membrane was obtained from Amersham Company (USA).

### 2.13.1.2 Methods

Fifteen micrograms of total RNA samples from different treatment groups were mixed with 17  $\mu$ l of loading buffer (10  $\mu$ l of formamide, 2.2 M formaldehyde, 1x MOPS, 2  $\mu$ l of loading dye and 0.1  $\mu$ l of ethidium bromide). RNA mixture was denatured by heating at 65°C for 10 min and quick-chilled on ice. The DIG-labeled RNA molecular weight marker I was prepared in the same manner simultaneously. The denatured RNA samples and DIG-labeled RNA molecular marker I were then separated on a 1% agarose gel containing 1x MOPS buffer by horizontal gel electrophoresis at 100V for about 2 hours. After electrophoresis, the RNA was transferred to a positively charged nylon membrane in 10x SSC buffer by capillary transfer method for overnight. The membrane was baked at 80°C for 2 hours to fix the RNA on the membrane.

## 2.13.2 Preparation of cDNA probes for hybridization

### 2.13.2.1 EcoRI digestion of cDNA inserts from plasmid DNA

#### 2.13.2.1.1 Materials

EcoRI buffer and EcoRI enzyme were obtained from New England Biolabs (UK). Nuclease-free water was obtained from Promega Company (USA). Sterile scalpel blades were obtained from Hecos (Shanghai, China).

#### 2.13.2.1.2 Methods

Twenty micrograms of plasmid DNA was mixed with 15  $\mu$ l of EcoRI buffer and 5  $\mu$ l of EcoRI enzyme. Appropriate amount of nuclease-free water was added to get a total volume of 150  $\mu$ l. The mixture was then incubated at 37°C for overnight. In the next morning, the reaction digest was electrophoresed on a 1% agarose gel at 50 V for 1 hr. The insert was excised from the gel by a sterile scalpel blade under UV light and prepared for later purification.

#### 2.13.2.2 Purification of DNA from agarose gel

##### 2.13.2.2.1 Materials

QIAquick gel extraction kit was obtained from QIAgen Company (USA). Nuclease-free water was obtained from Promega Company (USA).

##### 2.13.2.2.2 Methods

QIAquick Gel Extraction Kit (QIAgen, USA) was used to purify the DNA from agarose gel. After the band was cut from the gel, 3 gel vol. (1 gel vol. means the volume equal to the weight of gel slice looking 1 g as 1 ml) of Buffer QG was added to 1 gel vol. of gel slice and the gel mixture was incubated at 50°C for 10 min. One gel vol. of isopropanol was then added and vortexed vigorously. The gel mixture was applied into QIAquick spin

column and centrifuged at 14,000 rpm for 1 min. The column was washed with 0.75 ml of PE solution and centrifuged at 14,000 rpm for 1 min. After the flow-through was discarded, the column was centrifuged at 1,4000 rpm for additional 1 min to remove remain ethanol. For elution of DNA, 50  $\mu$ l of Buffer EB (10 mM Tris-Cl, pH 8.5) was added into the middle of the column and DNA was eluted by centrifugation at 14,000 rpm for 1 min twice. To precipitate DNA, 10  $\mu$ l of 3 M NaAc, 1  $\mu$ l of glycogen, and 250  $\mu$ l of 95% ethanol was added into the elution and incubated at -20°C for overnight. The mixture was then centrifuged at 14,000 rpm for 20 min and washed by 1 ml of 75% ethanol. Finally the pellet was air-dried for 10 min and then dissolved in 10  $\mu$ l of nuclease-free water.

#### 2.13.2.3 DIG labeling of cDNA

DIG labeling system was used for labeling the plasmid DNA from pT-Adv vectors.

##### 2.13.2.3.1 Materials

Random Prime DNA DIG Labeling kit and glycogen were obtained from Boehringer Mannheim Company (Germany). EcoRI buffer and EcoRI enzyme were obtained from New England Biolabs (UK). Lithium chloride (LiCl) was obtained from Sigma Chemical Company (USA). EDTA was obtained from Riedel-del Haën Company (Germany). Ethanol was obtained from Merck Company (USA).

##### 2.13.2.3.2 Methods

The DNA insert was isolated from the pT-Adv vector by EcoRI restriction enzyme digestion and purified with QIAquick gel extraction kit (refer to 2.13.2.1 and 2.13.2.2).

Ten microliters of DNA template (about 300 ng) was denatured at 100°C for 10 min and quick-chilled on ice. Two microliters of hexanucleotide mix (vial 5), 2 µl of dNTP mix (vial 6) and 1 µl of Klenow enzyme (vial 7) were then mixed with denatured DNA and incubated at 37°C for overnight labeling. In the next morning, 2 µl of 0.2 M EDTA (pH 8.0) and 1 µl of glycogen were added to stop the reaction. After precipitation of the labeled DNA by adding 2.5 µl of 4 M lithium chloride (LiCl) and 75 µl of prechilled (-20°C) ethanol at -70°C for 30 min, the mixture was centrifuged at 12,000 g for 15 min. The pellet was then washed with 50 µl of 70% ice-cold ethanol and the mixture was centrifuged at 12,000 g for 15 min once more. Finally the DNA was air-dried briefly and dissolved in 50 µl of TE-buffer (10 mM Tris-HCl, 1 mM EDTA, pH 8.0). About 25 ng of DIG-labeled DNA was used per 1 ml of DIG Easy Hyb solution for hybridization. Before hybridization, the DIG-labeled DNA was denatured at 100°C for 10 min.

### 2.13.3 Hybridization

#### 2.13.3.1 Materials

DIG Easy Hyb solution, blocking reagent powder, polyclonal antibody against digoxigenin (Anti-AP), nitroblue tetrazolium chloride (NBT) and 5-bromo-4-chloro-3-indolyl-phosphate (BCIP) were obtained from Boehringer Mannheim Company (Germany). Maleic acid, sodium chloride, sodium citrate, trizma base, tween 20 and magnesium chloride were obtained from Sigma Chemical Company (USA). Dimethylformamide was obtained from Fluka Company (USA).

#### 2.13.3.2 Methods

The nylon membrane was pre-hybridized at 42°C for 2 hr in 20 ml of DIG Easy Hyb solution. The DIG-labeled DNA probe was then added into the pre-hybridization buffer and hybridized with the RNA fixed on the membrane at 42°C for overnight. In the next morning, the washing steps were performed as follows: 2x SSC/0.1% SDS at room temperature for 15 min twice; 0.1x SSC/0.1% SDS at 60°C for 15 min twice. The membrane was then rinsed briefly with washing buffer [0.1 M maleic acid (pH 7.5), 0.15 M NaCl and 0.3% Tween 20) and blocked with blocking buffer [1% blocking reagent, 0.1 M maleic acid (pH 7.5), 0.15 M NaCl] for 45 min at room temperature. Following blocking, the membrane was incubated with blocking buffer containing polyclonal antibody against digoxigenin (diluted 1: 100000) for 45 min. After the membrane was washed with washing buffer for 15 min twice, it was then rinsed with detection buffer (0.1 M Tris-HCl, 0.1 M NaCl, pH 9.5) for 5 min and immersed in 40 ml of staining solution [0.1 M Tris-HCl, 0.1 M NaCl, 50 mM MgCl<sub>2</sub>, 200 µl of NBT and 150 µl of BCIP solutions (pH 9.5)] for color development in dark. The purple color signal appeared on the membrane was scanned for record.



## CHAPTER 3: RESULTS

### 3.1 Liver morphology

It was found that livers of CCl<sub>4</sub>-treated *cyp2e1*<sup>+/+</sup> mice for 12, 24 and 48 hr were more pale-orange than CCl<sub>4</sub>-treated *cyp2e1*<sup>-/-</sup> mice and the controls. No such color change was observed in livers of CCl<sub>4</sub>-treated *cyp2e1*<sup>+/+</sup> mice for 2 and 6 hr (Figure 3.1). The data of 24 hr CCl<sub>4</sub> treatment were in agreement with our previous results (Wong *et. al.*, 1998) in which it was found that the liver color in CCl<sub>4</sub>-treated *cyp2e1*<sup>+/+</sup> mice was more pale-orange than that observed in CCl<sub>4</sub>-treated *cyp2e1*<sup>-/-</sup> mice and the controls. In addition, more dramatic color change was observed in livers from 24 hr CCl<sub>4</sub> treatment in comparison to those from 12 and 48 hr suggesting that CCl<sub>4</sub>-induced liver injury reached the maximum at 24 hr and then started to recover at 48 hr.

### 3.2 Serum ALT and AST activities

Significant elevations of serum alanine aminotransferase (ALT) and aspartate aminotransferase (AST) activities were observed in 24 hr CCl<sub>4</sub>-treated *cyp2e1*<sup>+/+</sup> mice (ALT, 495-fold; AST, 120-fold). In contrast, no significant elevations of ALT and AST activities were observed in 24 hr CCl<sub>4</sub>-treated *cyp2e1*<sup>-/-</sup> mice (Figure 3.2, Table 3.1). These data were in well agreement with our previous results (Wong *et. al.*, 1998) in which the fold increases of ALT and AST activities in 24 hr CCl<sub>4</sub>-treated *cyp2e1*<sup>+/+</sup> mice are 422- and 125-fold respectively. In the time course study, ALT and AST activities increased from 6 to 48 hr, reached a maximum at 24 hr, and then declined at 48 hr after CCl<sub>4</sub> treatment in *cyp2e1*<sup>+/+</sup> mice when compared to their corresponding controls. The fold

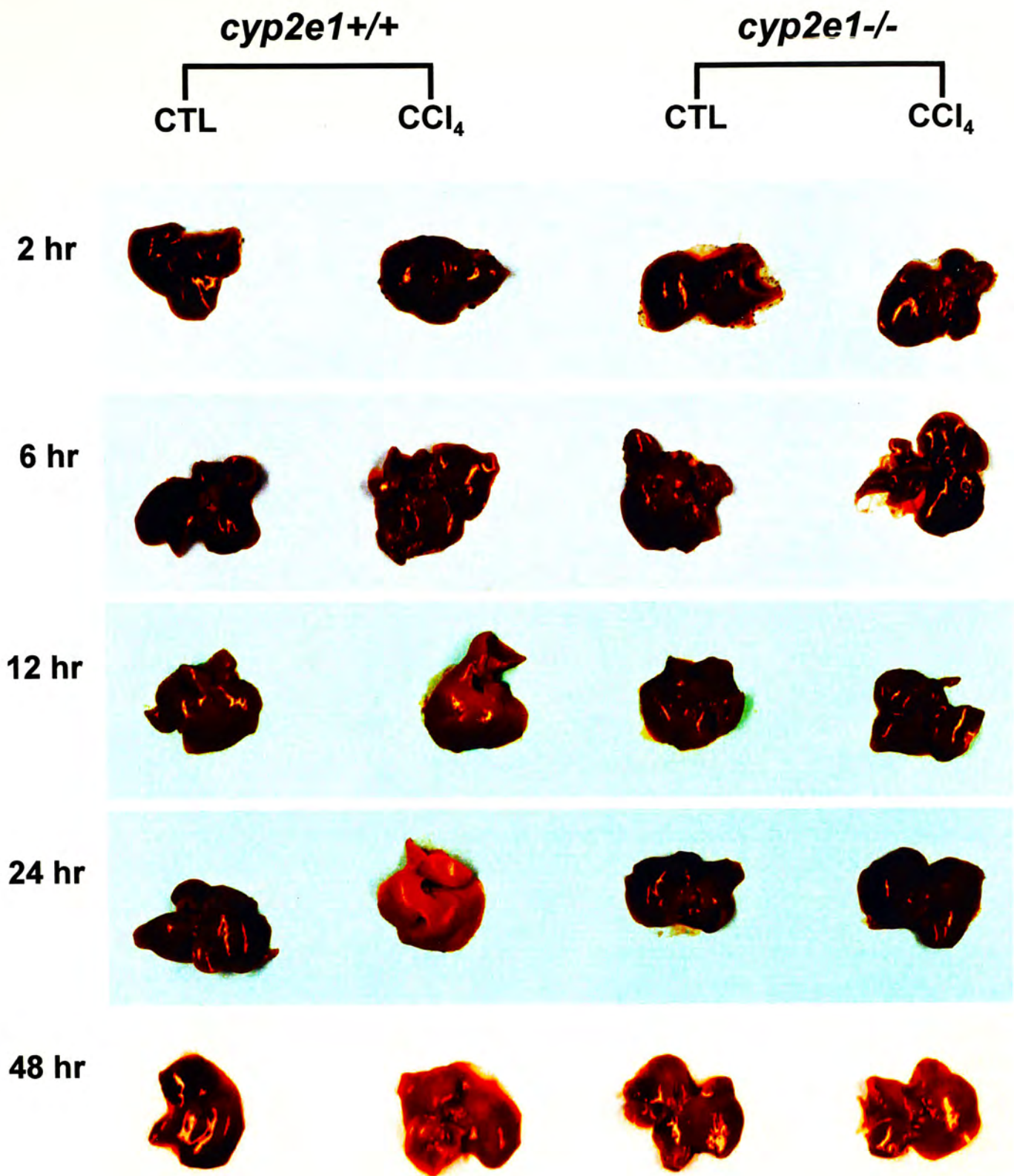


Figure 3.1. Liver morphology of *cyp2e1*<sup>+/+</sup> and *cyp2e1*<sup>-/-</sup> mice treated with corn oil (CTL) or CCl<sub>4</sub> for 2, 6, 12, 24 and 48 hr. Obvious color change was observed in livers of *cyp2e1*<sup>+/+</sup> mice treated with CCl<sub>4</sub> for 12, 24 and 48 hr as compared to their corresponding controls. No obvious color change was observed in livers of *cyp2e1*<sup>+/+</sup> mice treated with CCl<sub>4</sub> for 2 and 6 hr as compared to their corresponding controls.



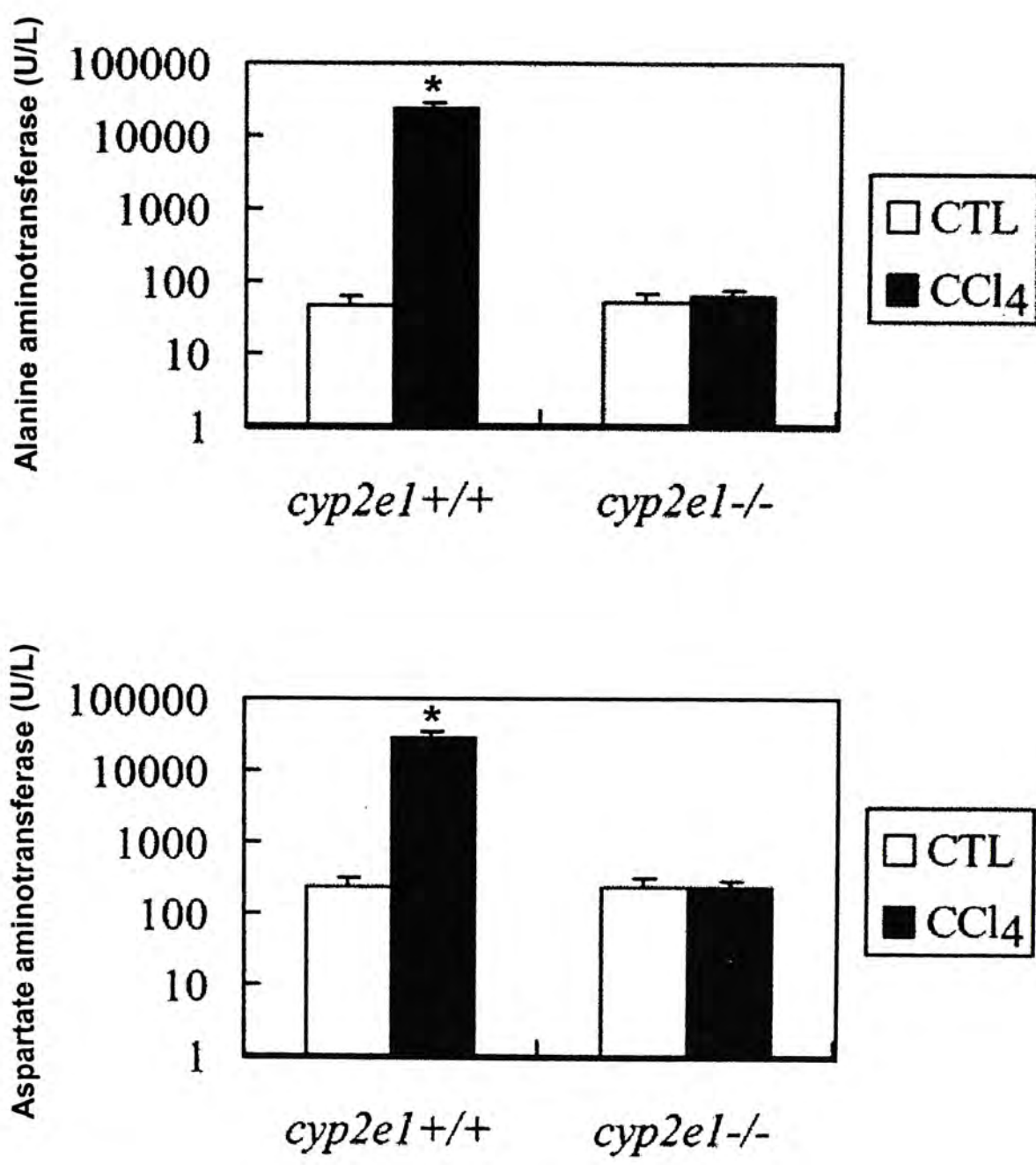


Figure 3.2. Serum ALT and AST activities in *cyp2e1*<sup>+/+</sup> and *cyp2e1*<sup>-/-</sup> mice after 24 hr exposure to 1 ml/kg CCl<sub>4</sub> i.p. injection. Controls were treated with corn oil (CTL) at the same dose. Data were based on comparisons of mean  $\pm$  SD values (n=6). Independent *t* tests were calculated to assess the statistical significance between control- and CCl<sub>4</sub>-treated groups within a mouse strain ( $p < 0.05$ ). \* represents significant difference between the two treatment groups within a mouse strain. CTL, control-treated group(s); CCl<sub>4</sub>, CCl<sub>4</sub>-treated group(s).

Table 3.1 Serum ALT and AST activities in *cyp2e1*<sup>+/+</sup> and *cyp2e1*<sup>-/-</sup> mice after exposure to 1 ml/kg CCl<sub>4</sub> i.p. injection.

Time of treatment	ALT activity				AST activity			
	<i>cyp2e1</i> <sup>+/+</sup>		<i>cyp2e1</i> <sup>-/-</sup>		<i>cyp2e1</i> <sup>+/+</sup>		<i>cyp2e1</i> <sup>-/-</sup>	
	CTL	CCl <sub>4</sub>	CTL	CCl <sub>4</sub>	CTL	CCl <sub>4</sub>	CTL	CCl <sub>4</sub>
24 hr (for FDD analysis)	30	18462	29	33	273	20641	244	271
	±	±	±	±	±	±	±	±
	6	5695	3	9	103	3703	73	36
2 hr	56	72	55	46	184	276	197	215
	±	±	±	±	±	±	±	±
	11	10	6	6	68	67	105	39
6 hr	34	201	34	50	147	353	197	249
	±	±	±	±	±	±	±	±
	8	60	9	13	55	41	61	121
12 hr	50	1297	34	45	118	2126	114	116
	±	±	±	±	±	±	±	±
	1	134	4	16	12	279	3	17
24 hr	48	13903	52	60	230	27437	241	241
	±	±	±	±	±	±	±	±
	17	5803	13	13	74	6960	83	47
48 hr	38	3678	30	34	107	3555	109	132
	±	±	±	±	±	±	±	±
	11	500	7	8	25	37	11	26

Data were based on comparisons of mean ± SD values (n=3-6). CTL, control-treated group(s); CCl<sub>4</sub>, CCl<sub>4</sub>-treated group(s).

increases of ALT activity after 2, 6, 12, 24 and 48 hr CCl<sub>4</sub> treatment were 1.3, 6, 26, 615 and 96 respectively, while the fold increases of AST activity after 2, 6, 12, 24 and 48 hr CCl<sub>4</sub> treatment were 1.5, 2.4, 18, 75 and 33 respectively (Figure 3.3). No such significant changes in ALT and AST activities were observed in all time points tested in *cyp2e1*<sup>-/-</sup> mice when compared to their corresponding controls (Figure 3.3).

### **3.3 Tail-genotyping by PCR**

Since there was no external phenotypic difference between *cyp2e1*<sup>+/+</sup> and *cyp2e1*<sup>-/-</sup> mice, tail-genotyping by PCR was used to confirm the genotypes of all the mice used in our experiments. The PCR product obtained from *cyp2e1*<sup>+/+</sup> and *cyp2e1*<sup>-/-</sup> mice was 957 bp and 1.6 kb respectively (Figure 3.4). This was in agreement with the expected size for those genotypes.

### **3.4 DNase I treatment**

Liver RNAs from *cyp2e1*<sup>+/+</sup> and *cyp2e1*<sup>-/-</sup> mice treated with CCl<sub>4</sub> or corn oil for 24 hr were used for FDD RT-PCR analysis. Trace amounts of DNA contamination in RNA samples can be amplified and contribute false positives to FDD banding patterns. As shown in Figure 3.5, no observable genomic DNA contamination was observed in RNA samples after DNase I treatment. These liver RNA samples were then subjected to the FDD RT-PCR analysis.

### **3.5 FDD RT-PCR and excision of differentially expressed cDNA fragments**



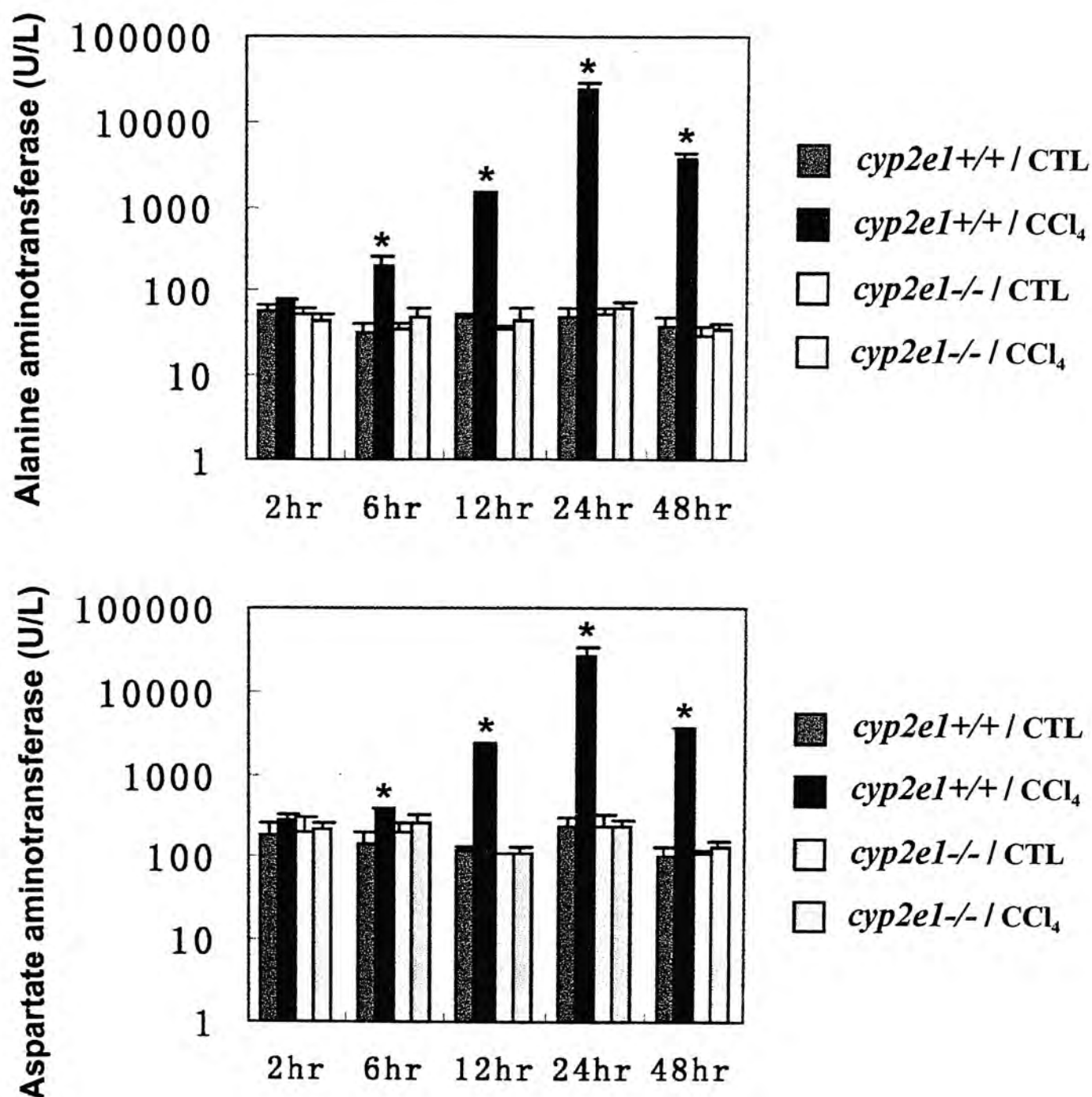


Figure 3.3. Serum ALT and AST activities in *cyp2e1*<sup>+/+</sup> and *cyp2e1*<sup>-/-</sup> mice after 2, 6, 12, 24 and 48 hr exposure to 1 ml/kg CCl<sub>4</sub> i.p. injection. Controls were treated with corn oil (CTL) at the same dose. Data were based on comparisons of mean  $\pm$  SD values (n=3-6). Independent *t* tests were calculated to assess the statistical significance between control- and CCl<sub>4</sub>-treated groups within a mouse strain ( $p < 0.05$ ). \* represents significant difference between the two treatment groups within a mouse strain. CTL, control-treated group(s); CCl<sub>4</sub>, CCl<sub>4</sub>-treated group(s).

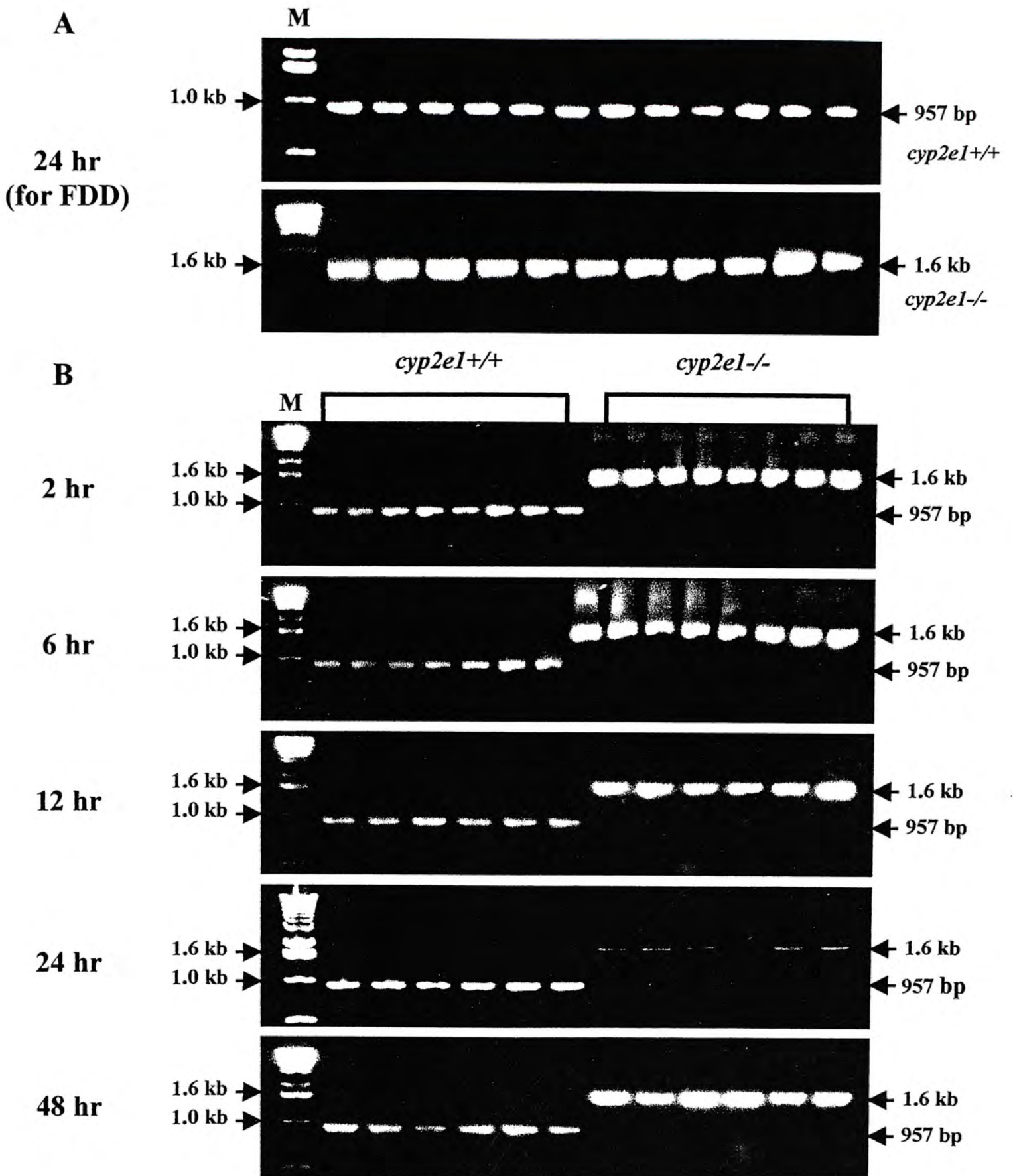


Figure 3.4. Tail-genotyping of *cyp2e1+/+* and *cyp2e1-/-* mice used for FDD RT-PCR analysis (A) and time course study (B). The PCR products were loaded on 1.5% agarose, 0.5x TBE gels with ethidium bromide staining. M, 1 kb DNA marker.

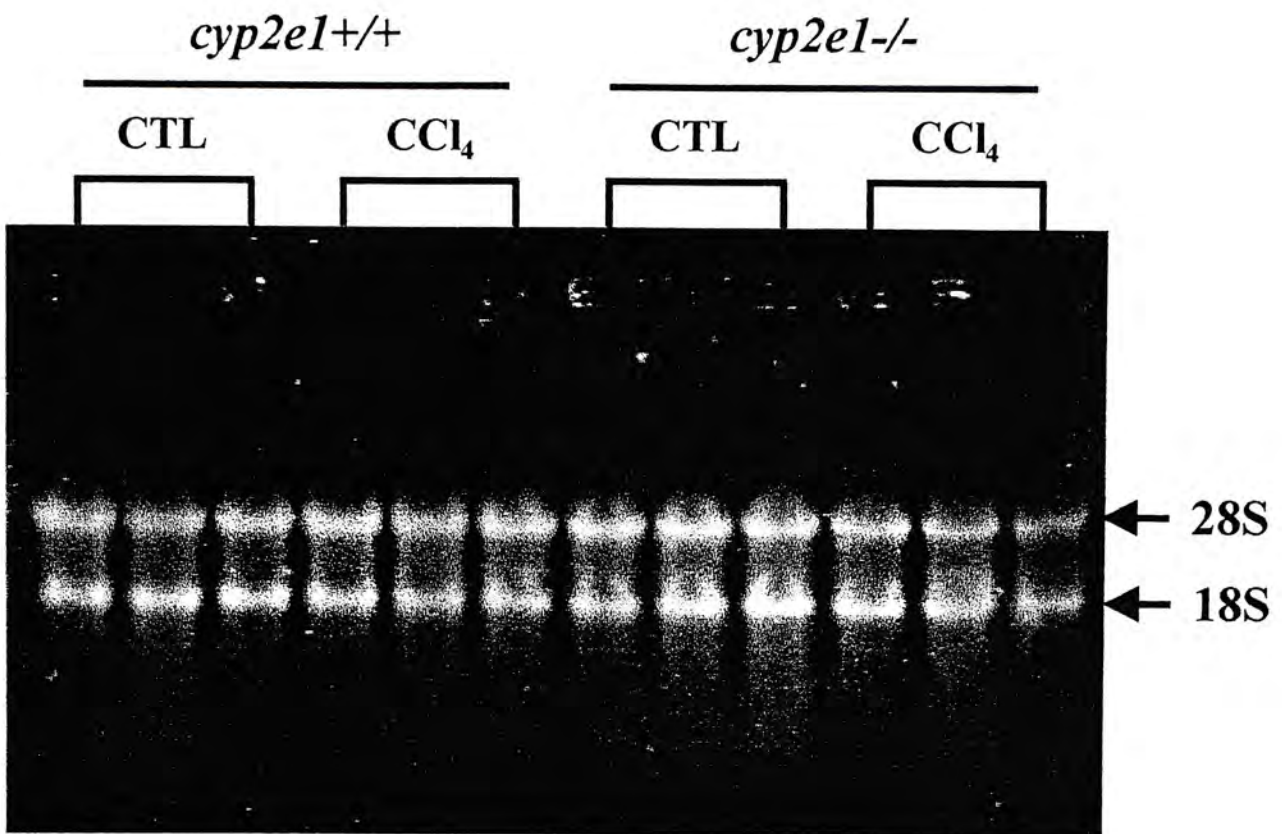


Figure 3.5. Electrophoretic separation of total liver RNAs after DNase I treatment on a 1% agarose gel containing 1x MOPS and 2.2 M formaldehyde with ethidium bromide staining. For each lane, 10  $\mu$ g of RNA was loaded.

Fluorescent differential display (FDD) method was applied to search for CYP2E1-dependent genes involved in CCl<sub>4</sub>-induced hepatotoxicity. Three fluoroDD gels were run by using different pairs of AP and ARP primer combinations (AP 5 & ARP 2, AP 5 & ARP 4, AP 5 & ARP 7). Thirty-four cDNA fragments showing differential expression patterns in *cyp2e1*<sup>+/+</sup> but not in *cyp2e1*<sup>-/-</sup> mice were obtained from these gels.

The TMR-labeled FDD PCR products from AP 5 & ARP 2 (Gel A) were illustrated in Figure 3.6. Five CYP2E1-dependent and CCl<sub>4</sub> responsive cDNA fragments (A1-A5) were excised from this Gel A (Table 3.2). Among them, three cDNA fragments (A2, A3 and A4) were up-regulated while two cDNA fragments (A1 and A5) were down-regulated in *cyp2e1*<sup>+/+</sup> mice after 24 hr CCl<sub>4</sub> treatment. In contrast, the expression levels of these five cDNA fragments were not altered in *cyp2e1*<sup>-/-</sup> mice after 24 hr CCl<sub>4</sub> treatment when compared to their corresponding controls indicating that the differential expression of these cDNA fragments is CYP2E1-dependent.

The TMR-labeled FDD PCR products from AP 5 & ARP 4 (Gel B) were illustrated in Figure 3.7. Thirteen CYP2E1-dependent and CCl<sub>4</sub> responsive cDNA fragments (B1-B13) were excised from this Gel B (Table 3.3). Among them, eight cDNA fragments (B1, B2, B3, B4, B7, B8, B12 and B13) were up-regulated while five cDNA fragments (B5, B6, B9, B10 and B11) were down-regulated in *cyp2e1*<sup>+/+</sup> mice after 24 hr CCl<sub>4</sub> treatment. In contrast, the expression levels of these thirteen cDNA fragments were not altered in *cyp2e1*<sup>-/-</sup> mice after 24 hr CCl<sub>4</sub> treatment when compared to their corresponding controls indicating that the differential expression of these cDNA fragments is CYP2E1-dependent.

The TMR-labeled FDD PCR products from AP 5 & ARP 7 (Gel C) were illustrated in Figure 3.8. Sixteen CYP2E1-dependent and CCl<sub>4</sub> responsive cDNA fragments (C1-C16)



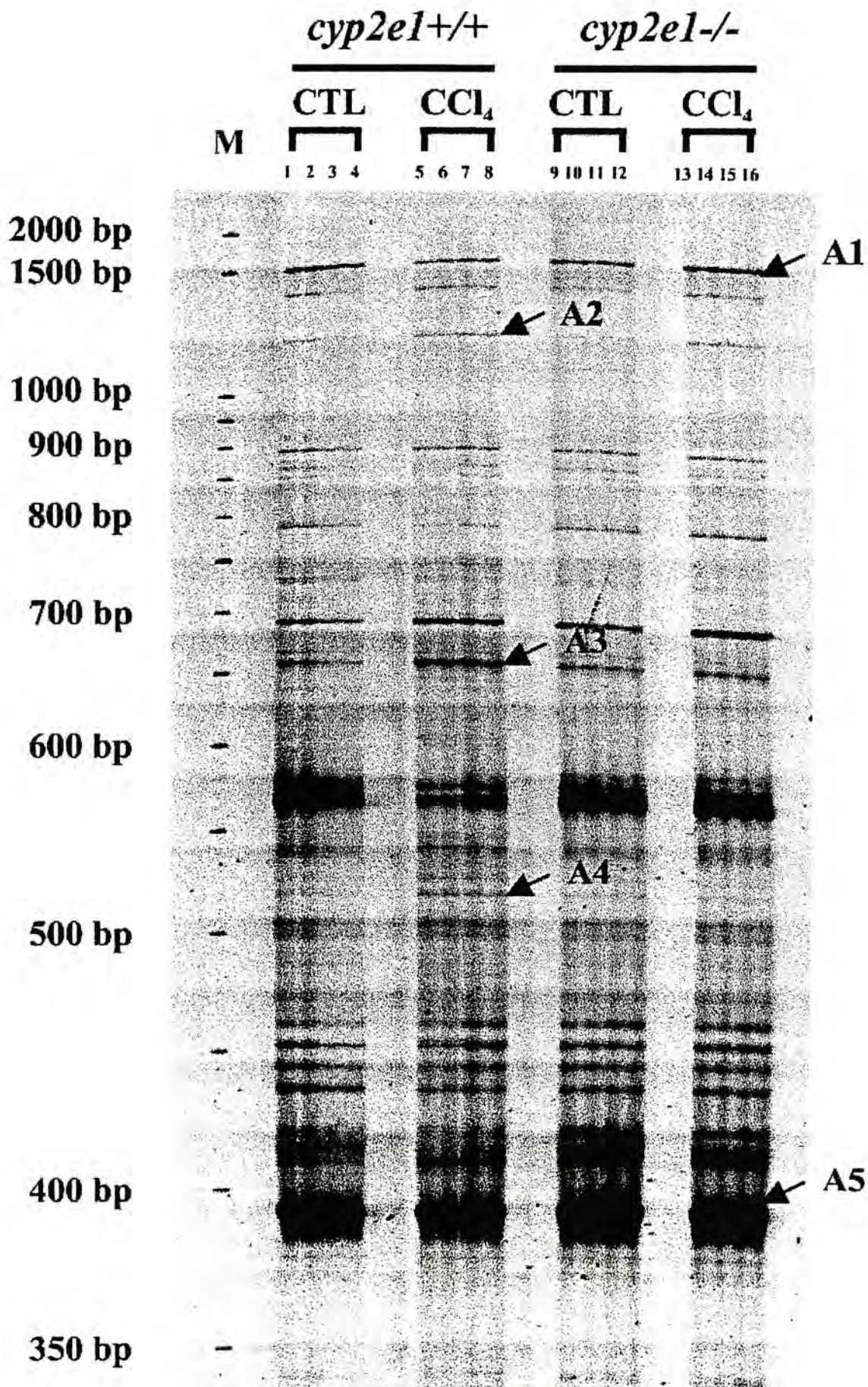


Figure 3.6. Gel A: Fluorescent differential display of liver RNAs from *cyp2e1*<sup>+/+</sup> and *cyp2e1*<sup>-/-</sup> mice treated with corn oil (CTL) or CCl<sub>4</sub> for 24 hr. Total RNA was reverse transcribed using the AP 5 primer. PCR reactions were performed in duplicate for each mouse in the presence of 3'-TMR-labeled AP 5 and 5'-ARP 2 primers. The TMR-labeled fluorescent PCR products were run on a 5.6% denaturing polyacrylamide gel. Each lane represents one PCR reaction. Two mice (i.e. four PCR reactions) were used for each treatment group. M, TMR-labeled molecular weight DNA marker.



Table 3.2 CYP2E1-dependent cDNA fragments excised from Gel A.

Primers Used	Fragment No.	FDD Size (bp)	FDD Expression Pattern						Up- or Down- Regulated
			<i>cyp2e1+/+</i>			<i>cyp2e1-/-</i>			
			CTL	CCl <sub>4</sub>	CTL	CTL	CCl <sub>4</sub>	CCl <sub>4</sub>	
AP 5 & ARP 2	A1	1500	+++	+	+++	+++	+++	+++	Down
AP 5 & ARP 2	A2	1200	+	+++	+	+	+	+	Up
AP 5 & ARP 2	A3	660	+	+++	+	+	+	+	Up
AP 5 & ARP 2	A4	520	+	+++	+	+	+	+	Up
AP 5 & ARP 2	A5	390	+++	+	+++	+++	+++	+++	Down

FDD RT-PCR reactions were performed in the presence of AP 5 & ARP 2. + indicated the intensity of expressed FDD bands by visual inspection, while - indicated that no FDD band was observed.

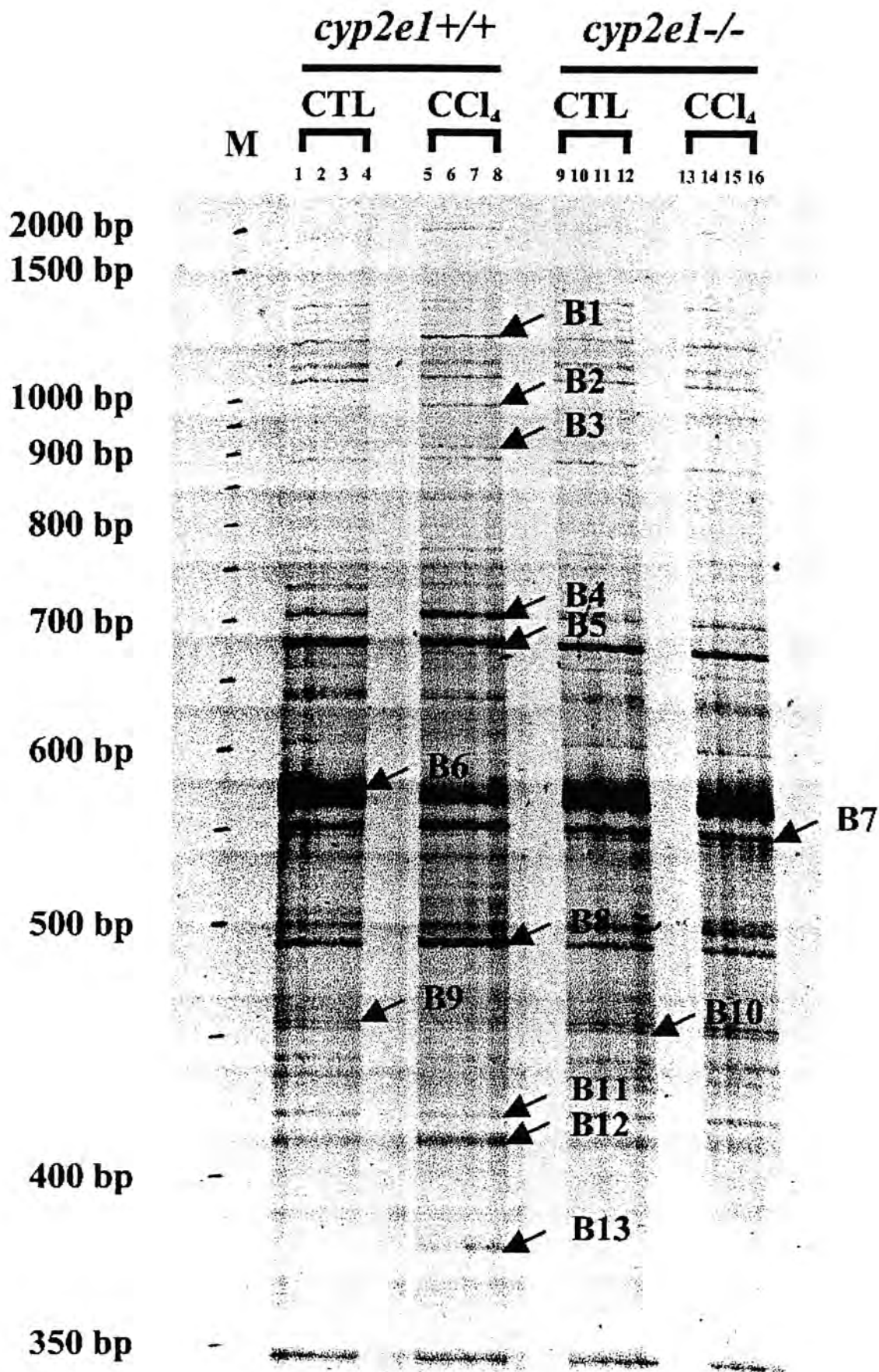


Figure 3.7. Gel B: Fluorescent differential display of liver RNAs from *cyp2e1*<sup>+/+</sup> and *cyp2e1*<sup>-/-</sup> mice treated with corn oil (CTL) or CCl<sub>4</sub> for 24 hr. Total RNA was reverse transcribed using the AP 5 primer. PCR reactions were performed in duplicate for each mouse in the presence of 3'-TMR-labeled AP 5 and 5'-ARP 4 primers. The TMR-labeled fluorescent PCR products were run on a 5.6% denaturing polyacrylamide gel. Each lane represents one PCR reaction. Two mice (i.e. four PCR reactions) were used for each treatment group. M, TMR-labeled molecular weight DNA marker.

Table 3.3 CYP2E1-dependent cDNA fragments excised from Gel B.

Primers Used	Fragment No.	FDD Size (bp)	FDD Expression Pattern						Up- or Down-Regulated
			<i>cyp2e1+/+</i>			<i>cyp2e1-/-</i>			
			CTL	CCl <sub>4</sub>	CTL	CTL	CCl <sub>4</sub>	CCl <sub>4</sub>	
AP 5 & ARP 4	B1	1200	+	+++	+	+	+	+	Up
AP 5 & ARP 4	B2	990	+	+++	+	+	+	+	Up
AP 5 & ARP 4	B3	900	-	+	-	-	-	-	Up
AP 5 & ARP 4	B4	710	+	+++	+	+	+	+	Up
AP 5 & ARP 4	B5	680	+++	++	+++	+++	+++	+++	Down
AP 5 & ARP 4	B6	570	+++	+	+++	+++	+++	+++	Down
AP 5 & ARP 4	B7	550	+	+++	+	+	+	+	Up
AP 5 & ARP 4	B8	490	+	+++	+	+	+	+	Up
AP 5 & ARP 4	B9	460	++	+	++	++	++	++	Down
AP 5 & ARP 4	B10	450	++	+	++	++	++	++	Down
AP 5 & ARP 4	B11	420	+++	+	+++	+++	+++	+++	Down
AP 5 & ARP 4	B12	410	+	+++	+	+	+	+	Up
AP 5 & ARP 4	B13	375	-	+	-	-	-	-	Up

FDD RT-PCR reactions were performed in the presence of AP 5 & ARP 4. + indicated the intensity of expressed FDD bands by visual inspection, while - indicated that no FDD band was observed.



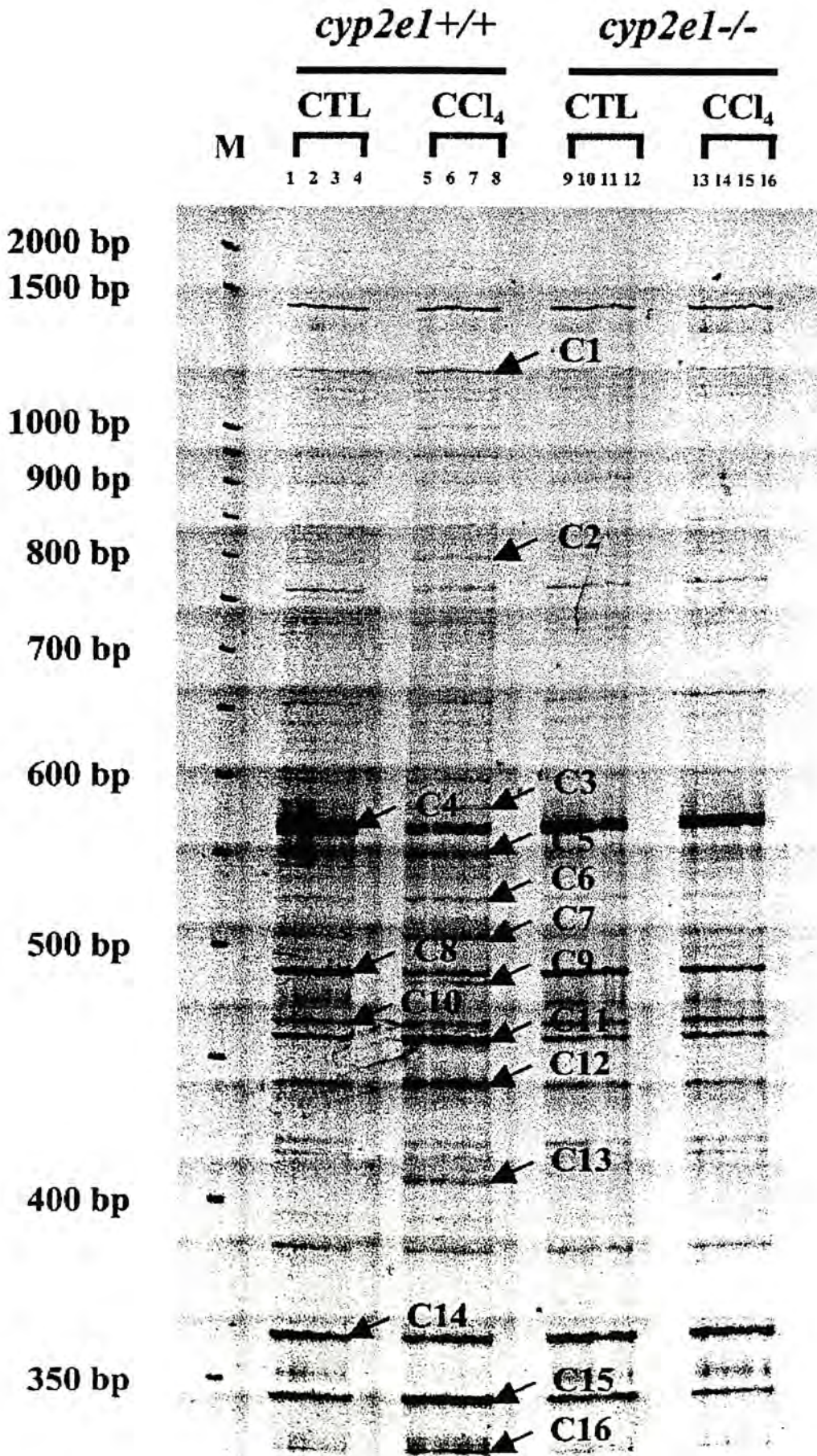


Figure 3.8. Gel C: Fluorescent differential display of liver RNAs from *cyp2e1*<sup>+/+</sup> and *cyp2e1*<sup>-/-</sup> mice treated with corn oil (CTL) or CCl<sub>4</sub> for 24 hr. Total RNA was reverse transcribed using the AP 5 primer. PCR reactions were performed in duplicate for each mouse in the presence of 3'-TMR-labeled AP 5 and 5'-ARP 7 primers. The TMR-labeled fluorescent PCR products were run on a 5.6% denaturing polyacrylamide gel. Each lane represents one PCR reaction. Two mice (i.e. four PCR reactions) were used for each treatment group. M, TMR-labeled molecular weight DNA marker.

were excised from this Gel C (Table 3.4). Among them, twelve cDNA fragments (C1, C2, C3, C5, C6, C7, C9, C11, C12, C13, C15 and C16) were up-regulated while four cDNA fragments (C4, C8, C10 and C14) were down-regulated in *cyp2e1*<sup>+/+</sup> mice after 24 hr CCl<sub>4</sub> treatment. In contrast, the expression levels of these sixteen cDNA fragments were not altered in *cyp2e1*<sup>-/-</sup> mice after 24 hr CCl<sub>4</sub> treatment when compared to their corresponding controls indicating that the differential expression of these cDNA fragments is CYP2E1-dependent.

### **3.6 Reamplification of excised cDNA fragments**

All of the thirty-four CYP2E1-dependent cDNA fragments excised from the three FDD gels were tried for PCR reamplification with M13 reverse (-48) and T7 promoter primers. Among the thirty-four cDNA fragments, thirty cDNA fragments (Figures 3.9 and 3.10) were successfully reamplified (88%) with the expected fragment size (Tables 3.5-3.7). Fragments B1 and B3 were reamplified with wrong fragment size. Fragments A3 and C1 could not be successfully reamplified. It may be due to the big fragment size or inadequate amount of cDNA eluted from the excised gel slices for PCR reamplification.

### **3.7 Subcloning of reamplified cDNA fragments**

AdvaTAge cloning system was used to subclone the reamplified cDNA fragments. After subcloning, high quality plasmid DNA from each recombinant colony was prepared using QIAprep<sup>®</sup> Spin Miniprep kits. The size of DNA inserts from each recombinant colony was then checked by EcoRI restriction enzyme digestion. The EcoRI digested DNA fragments from all recombinant clones were illustrated in Figure 3.11 (Clones A2, A5, B7,



Table 3.4 CYP2E1-dependent cDNA fragments excised from Gel C.

Primers Used	Fragment No.	FDD Size (bp)	FDD Expression Pattern						Up- or Down- Regulated
			<i>cyp2e1</i> +/+			<i>Cyp2e1</i> -/-			
			CTL	CCl <sub>4</sub>	CTL	CTL	CCl <sub>4</sub>	CCl <sub>4</sub>	
AP 5 & ARP 7	C1	1200	+	+++	+	+	+	+	Up
AP 5 & ARP 7	C2	800	-	+	-	-	-	-	Up
AP 5 & ARP 7	C3	575	-	+	-	-	-	-	Up
AP 5 & ARP 7	C4	560	+++	+	+++	+++	+++	+++	Down
AP 5 & ARP 7	C5	550	+	+++	+	+	+	+	Up
AP 5 & ARP 7	C6	525	+	+++	+	+	+	+	Up
AP 5 & ARP 7	C7	505	+	+++	+	+	+	+	Up
AP 5 & ARP 7	C8	490	+++	+	+++	+++	+++	+++	Down
AP 5 & ARP 7	C9	485	-	+	-	-	-	-	Up
AP 5 & ARP 7	C10	470	+++	+	+++	+++	+++	+++	Down
AP 5 & ARP 7	C11	460	+	+++	+	+	+	+	Up
AP 5 & ARP 7	C12	440	+	+++	+	+	+	+	Up
AP 5 & ARP 7	C13	410	-	+	-	-	-	-	Up
AP 5 & ARP 7	C14	360	+++	+	+++	+++	+++	+++	Down
AP 5 & ARP 7	C15	345	+	+++	+	+	+	+	Up
AP 5 & ARP 7	C16	320	+	+++	+	+	+	+	Up

FDD RT-PCR reactions were performed in the presence of AP 5 & ARP 7. + indicated the intensity of expressed FDD bands by visual inspection, while - indicated that no FDD band was observed.

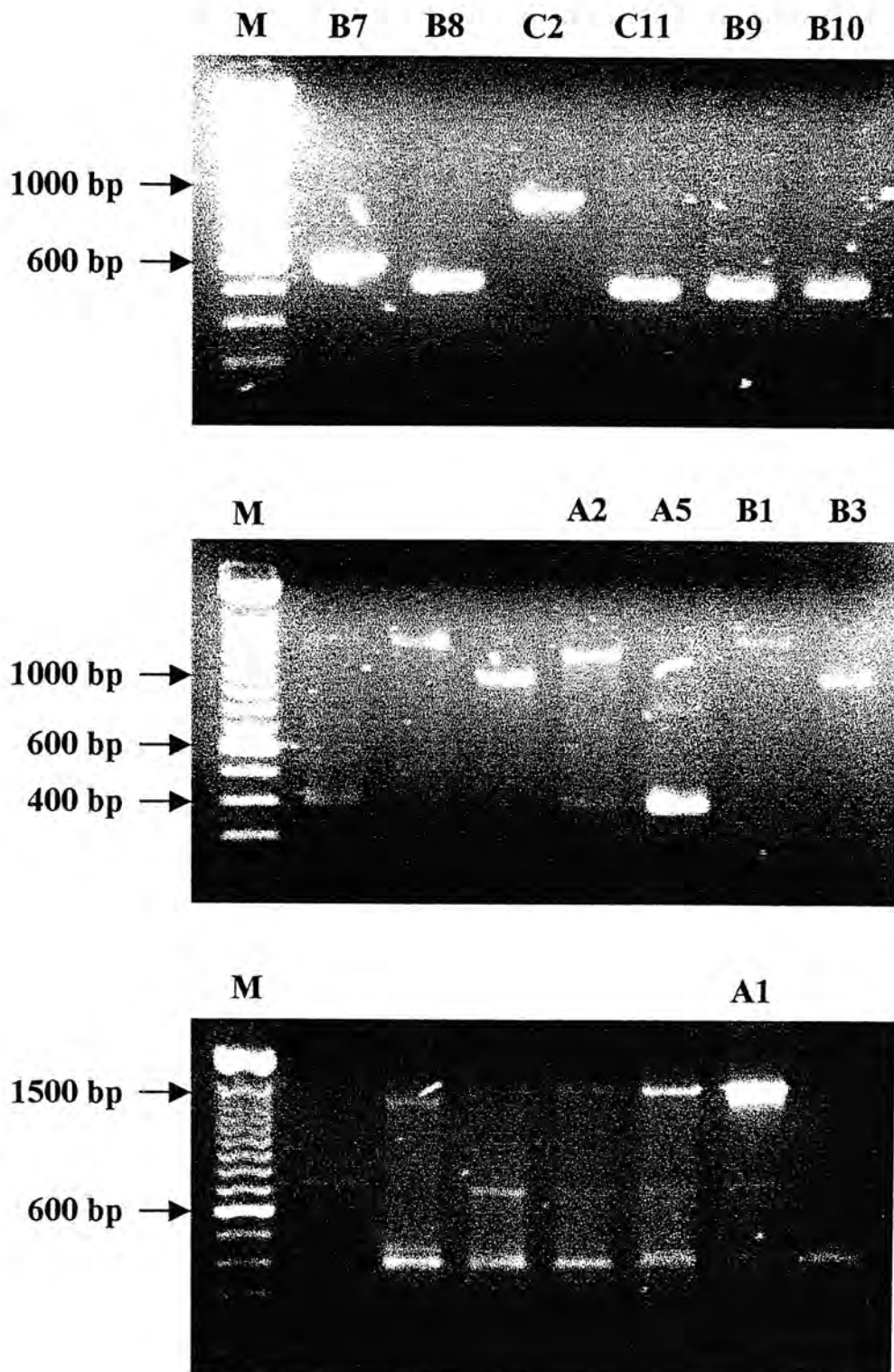


Figure 3.9. Reamplification of cDNA fragments excised from FDD gels A, B and C (Part A). The excised cDNA fragments were eluted in TE buffer and amplified by PCR using M13 reverse (-48) and T7 promoter primers. The PCR products were loaded on 1.5% agarose, 0.5x TBE gels with ethidium bromide staining. M, 100 bp DNA marker.

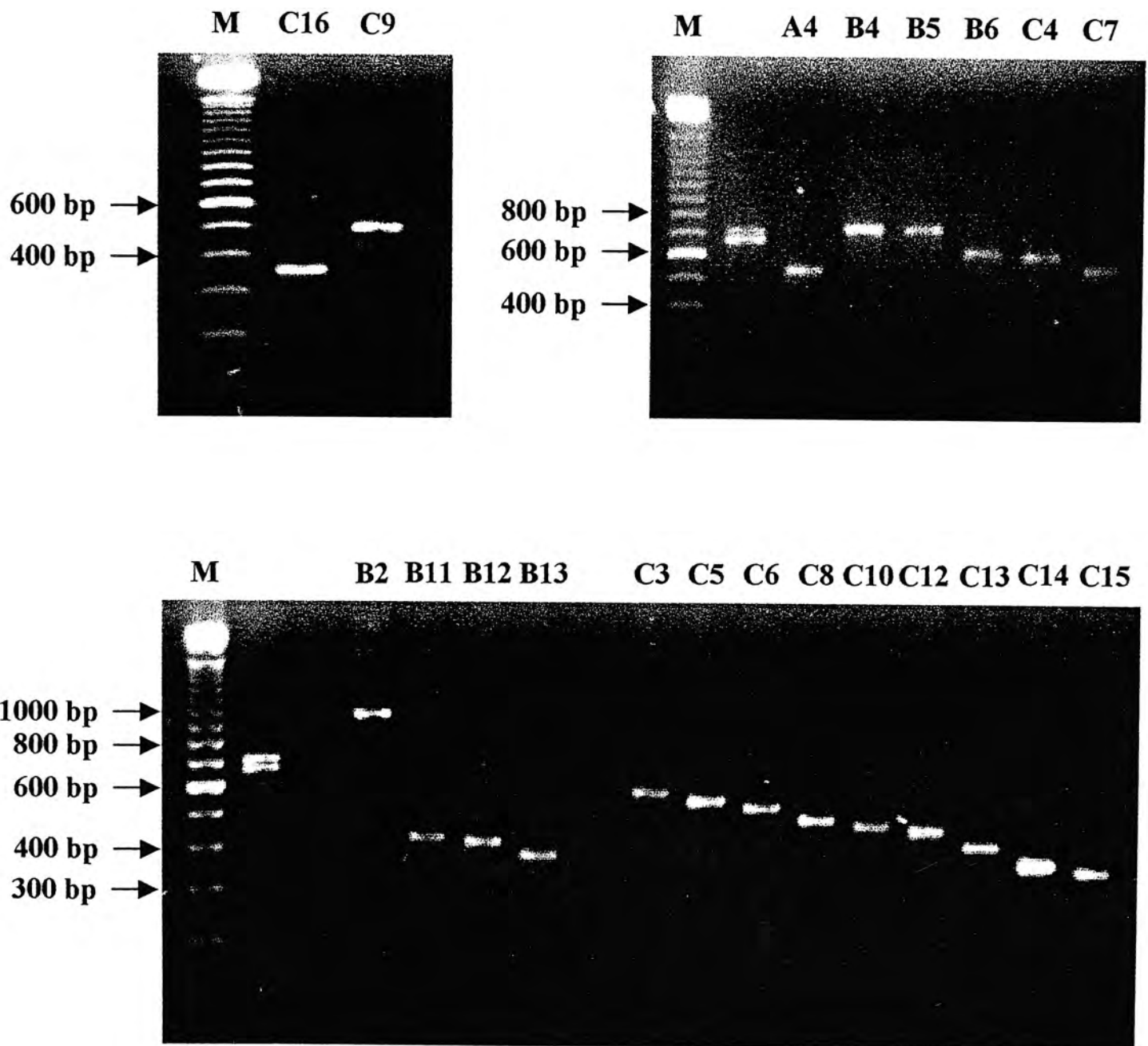


Figure 3.10. Reamplification of cDNA fragments excised from FDD gels A, B and C (Part B). The excised cDNA fragments were eluted in TE buffer and amplified by PCR using M13 reverse (-48) and T7 promoter primers. The PCR products were loaded on 1.5% agarose, 0.5x TBE gels with ethidium bromide staining. M, 100 bp DNA marker.

Table 3.5 Summary of cDNA fragments reamplified from Gel A.

Primers Used	Fragment No.	FDD Size (bp)	FDD Expression Pattern				Reamplification	
			<i>cyp2e1</i> +/+		<i>cyp2e1</i> -/-		PCR Product Size (bp)	Successful/Failed (√/×)
			CTL	CCl <sub>4</sub>	CTL	CCl <sub>4</sub>		
AP 5 & ARP 2	A1	1500	+++	+	+++	+++	1500	√
AP 5 & ARP 2	A2	1200	+	+++	+	+	1200	√
AP 5 & ARP 2	A3	660	+	+++	+	+	660	× (No PCR product)
AP 5 & ARP 2	A4	520	+	+++	+	+	520	√
AP 5 & ARP 2	A5	390	+++	+	+++	+++	400	√

+ indicated the intensity of expressed FDD bands by visual inspection, while - indicated that no FDD band was observed. √ means successful reamplification while × means failed reamplification (either no PCR products or PCR products with wrong size).

Table 3.6 Summary of cDNA fragments reamplified from Gel B.

Primers Used	Fragment No.	FDD Size (bp)	FDD Expression Pattern				Reamplification	
			<i>cyp2e1</i> +/+		<i>cyp2e1</i> -/-		PCR Product Size (bp)	Successful/Failed (√/×)
			CTL	CCl <sub>4</sub>	CTL	CCl <sub>4</sub>		
AP 5 & ARP 4	B1	1200	+	+++	+	+	1300	× (Wrong size)
AP 5 & ARP 4	B2	990	+	+++	+	+	1000	√
AP 5 & ARP 4	B3	900	-	+	-	-	1000	× (Wrong size)
AP 5 & ARP 4	B4	710	+	+++	+	+	720	√
AP 5 & ARP 4	B5	680	+++	++	+++	+++	710	√
AP 5 & ARP 4	B6	570	+++	+	+++	+++	590	√
AP 5 & ARP 4	B7	550	+	+++	+	+	570	√
AP 5 & ARP 4	B8	490	+	+++	+	+	500	√
AP 5 & ARP 4	B9	460	++	+	++	++	480	√
AP 5 & ARP 4	B10	450	++	+	++	++	480	√
AP 5 & ARP 4	B11	420	+++	+	+++	+++	420	√
AP 5 & ARP 4	B12	410	+	+++	+	+	410	√
AP 5 & ARP 4	B13	375	-	+	-	-	390	√

+ indicated the intensity of expressed FDD bands by visual inspection, while - indicated that no FDD band was observed. √ means successful reamplification while × means failed reamplification (either no PCR products or PCR products with wrong size).



Table 3.7 Summary of cDNA fragments reamplified from Gel C.

Primers Used	Fragment No.	FDD Size (bp)	FDD Expression Pattern				Reamplification	
			<i>cyp2e1</i> +/+	<i>cyp2e1</i> -/-	PCR Product Size (bp)	Successful/Failed (√/×)		
			CTL	CTL	CCl <sub>4</sub>	CCl <sub>4</sub>		
AP 5 & ARP 7	C1	1200	+	+	+++	+	1200 × (No PCR product)	
AP 5 & ARP 7	C2	800	-	-	+	-	820 √	
AP 5 & ARP 7	C3	575	-	-	+	-	590 √	
AP 5 & ARP 7	C4	560	+++	+++	+	+++	590 √	
AP 5 & ARP 7	C5	550	+	+	+++	+	570 √	
AP 5 & ARP 7	C6	525	+	+	+++	+	540 √	
AP 5 & ARP 7	C7	505	+	+	+++	+	520 √	
AP 5 & ARP 7	C8	490	+++	+++	+	+++	500 √	
AP 5 & ARP 7	C9	485	-	-	+	-	500 √	
AP 5 & ARP 7	C10	470	+++	+++	+	+++	480 √	
AP 5 & ARP 7	C11	460	+	+	+++	+	470 √	
AP 5 & ARP 7	C12	440	+	+	+++	+	440 √	
AP 5 & ARP 7	C13	410	-	-	+	-	410 √	
AP 5 & ARP 7	C14	360	+++	+++	+	+++	380 √	
AP 5 & ARP 7	C15	345	+	+	+++	+	360 √	
AP 5 & ARP 7	C16	320	+	+	+++	+	360 √	

+ indicated the intensity of expressed FDD bands by visual inspection, while - indicated that no FDD band was observed. √ means successful reamplification while × means failed reamplification (either no PCR products or PCR products with wrong size).

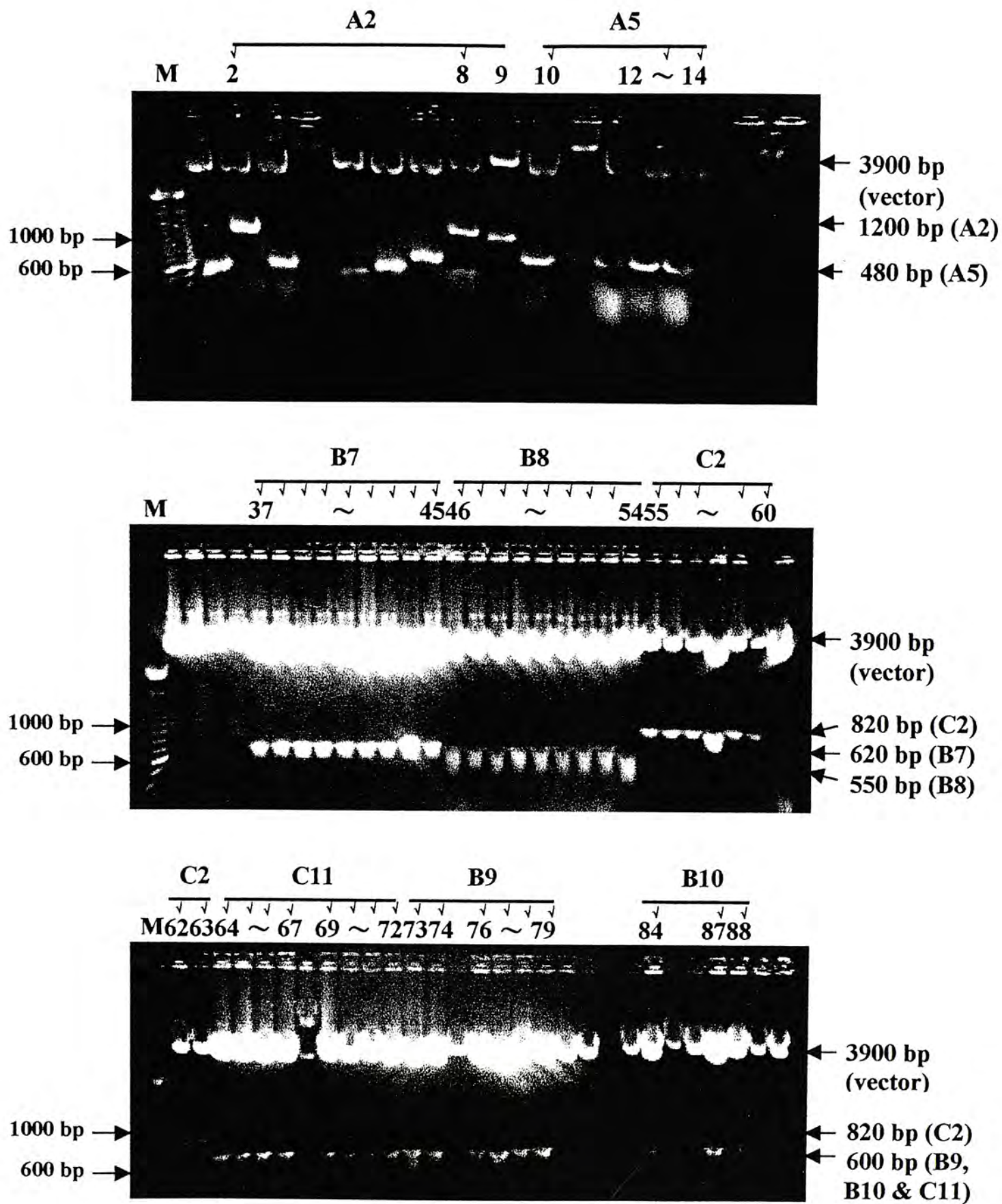


Figure 3.11. EcoRI restriction enzyme digestion of recombinant clones containing inserts A2, A5, B7, B8, C2, C11, B9 and B10. The digested products were resolved on 1.2% agarose, 0.5x TBE gels with ethidium bromide staining. √ represented the recombinant colony containing the insert with correct size. M, 100 bp DNA marker.

B8, C2, C11, B9 and B10), Figure 3.12 (Clones A1, A4 and B4), Figure 3.13 (Clones B4, B5, B6, C4 and C7), Figure 3.14 (Clones B2, B11, B12, B13, C3, C5, C6 and C8) and Figure 3.15 (Clones C12, C8, C10, C13, C14, C15, C16 and C9). In summary, all of the thirty reamplified cDNA fragments were successfully subcloned (Tables 3.8-3.10). The insert size of most clones was more or less in agreement with the size of their corresponding reamplified cDNA fragments while the insert size of clones B9, B10 and C11 was not in agreement with the size of their corresponding reamplified cDNA fragments. After purification, the high quality plasmid DNAs from the thirty recombinant clones were then used for DNA sequencing and as probes for Northern blot analysis.

### **3.8 DNA sequencing of subcloned cDNA fragments**

Among the thirty cDNA fragments subcloned, twenty-eight of them were successfully sequenced by using either M13 sequencing or M13 reverse primers (Figures 3.16-3.43, data from M13 reverse primer are not shown) and two of them (A2 and C8) were failed (Table 3.11). Twenty-five cDNA fragments were identified as known genes including *Mus musculus* hemopexin (A1), *Mus musculus* t-complex protein 1 (A4, C15 and C16), mouse major urinary protein (A5), *Mus musculus* guanine nucleotide binding protein, beta-2 (B2), mouse adipose differentiation-related protein (B4), his-tagged-multidrug resistance glycoprotein (B5), rat GAP-associated protein (B6), *Mus musculus* integrin linked kinase (B7), ribosomal protein S10 (B8), fatty acid binding protein, intestine (B9), *Mus musculus* clusterin (B10), *Rattus norvegicus* phospholipase C, gamma 1 (B11), mouse cytoplasmic gamma-actin (B13 and C9), *Rattus norvegicus* mRNA for acyl-CoA synthetase 5 (C2), *Mus musculus* cullin 1 (C4), mouse DNA for virus-like (VL30)

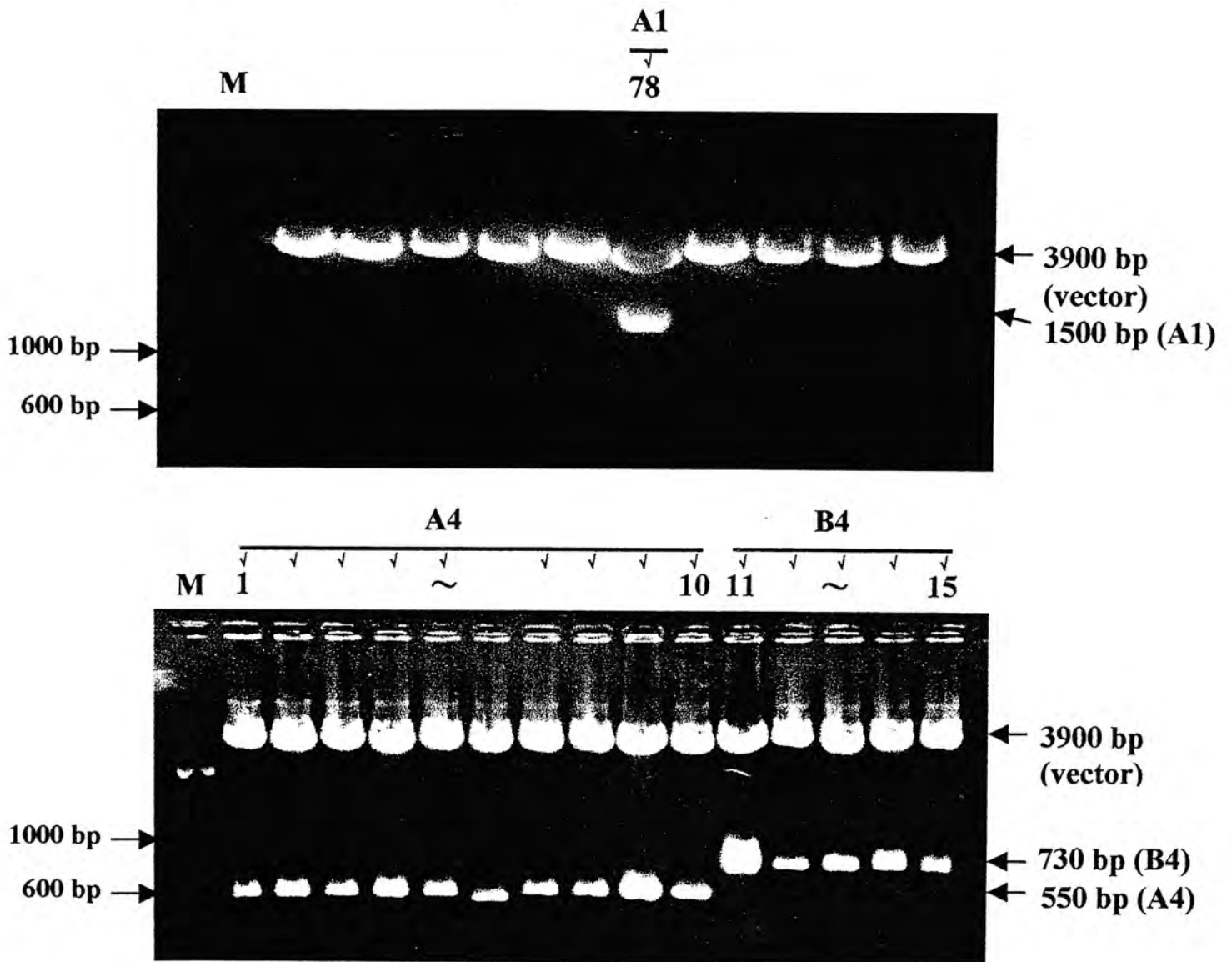


Figure 3.12. *Eco*RI restriction enzyme digestion of recombinant clones containing inserts A1, A4 and B4. The digested products were resolved on 1.2% agarose, 0.5x TBE gels with ethidium bromide staining. ✓ represented the recombinant colony containing the insert with correct size. M, 100 bp DNA marker.



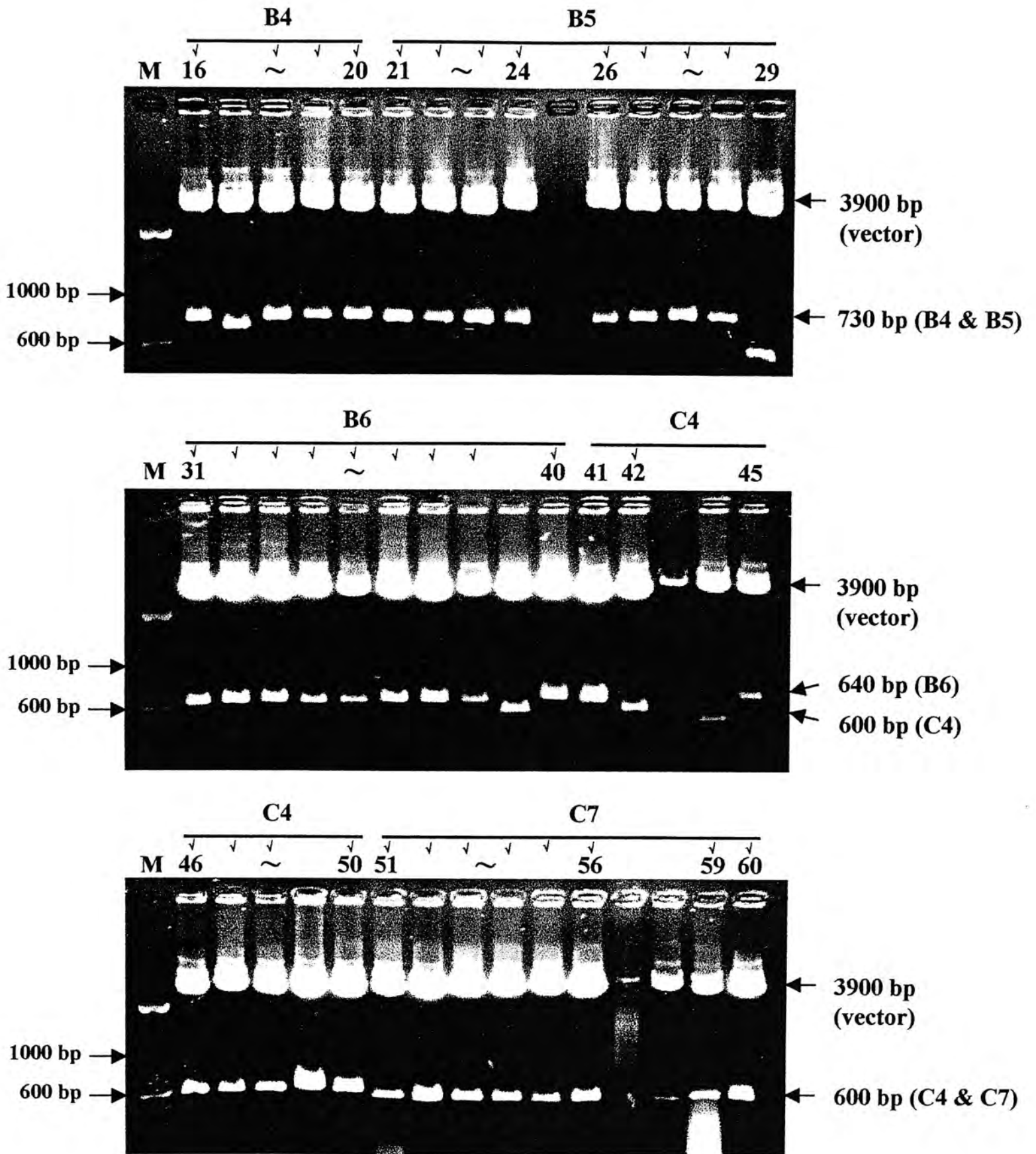


Figure 3.13. EcoRI restriction enzyme digestion of recombinant clones containing inserts B4, B5, B6, C4 and C7. The digested products were resolved on 1.2% agarose, 0.5x TBE gels with ethidium bromide staining. ✓ represented the recombinant colony containing the insert with correct size. M, 100 bp DNA marker.

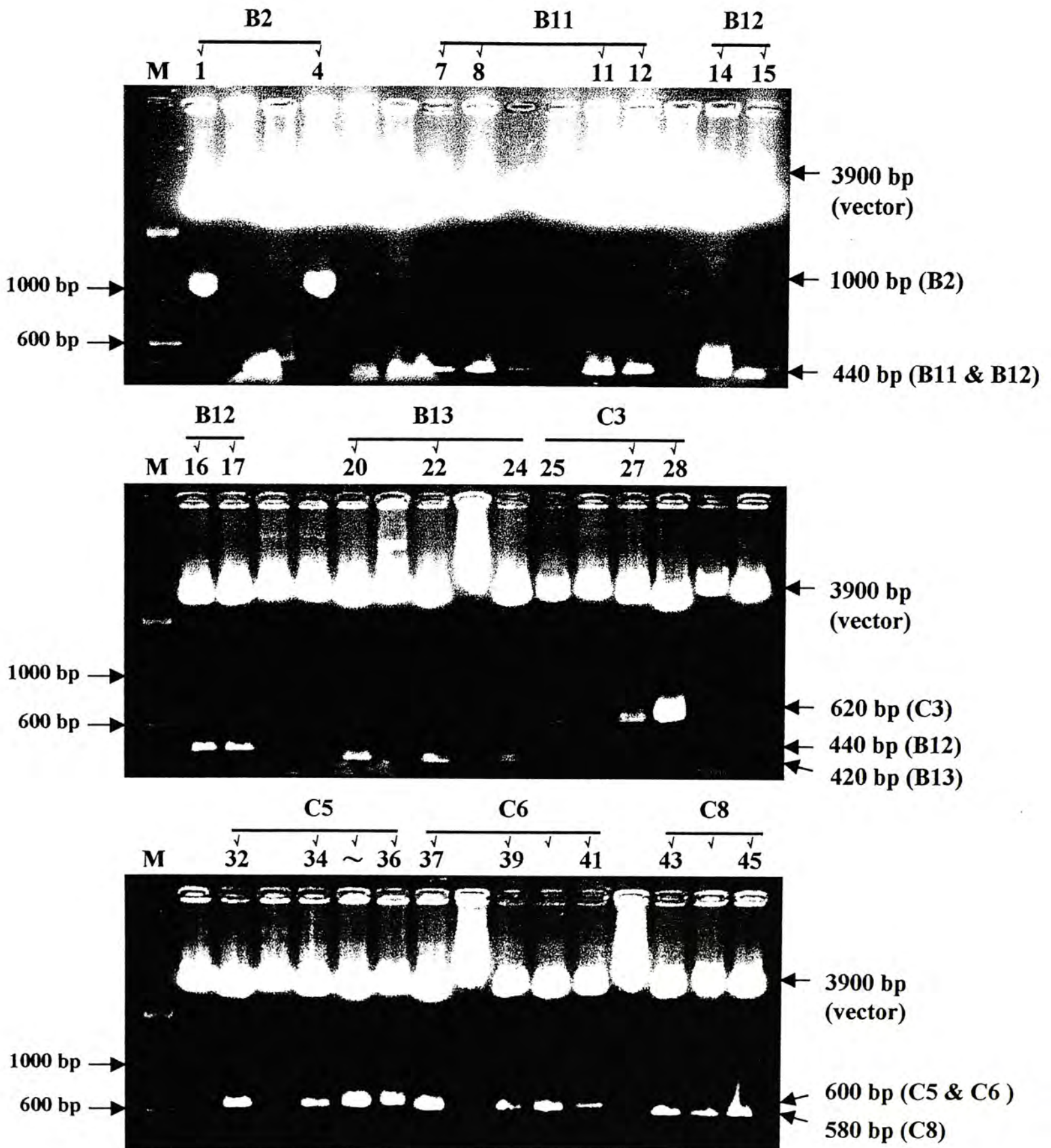


Figure 3.14. EcoRI restriction enzyme digestion of recombinant clones containing inserts B2, B11, B12, B13, C3, C5, C6 and C8. The digested products were resolved on 1.2% agarose, 0.5x TBE gels with ethidium bromide staining.  $\checkmark$  represented the recombinant colony containing the insert with correct size. M, 100 bp DNA marker.

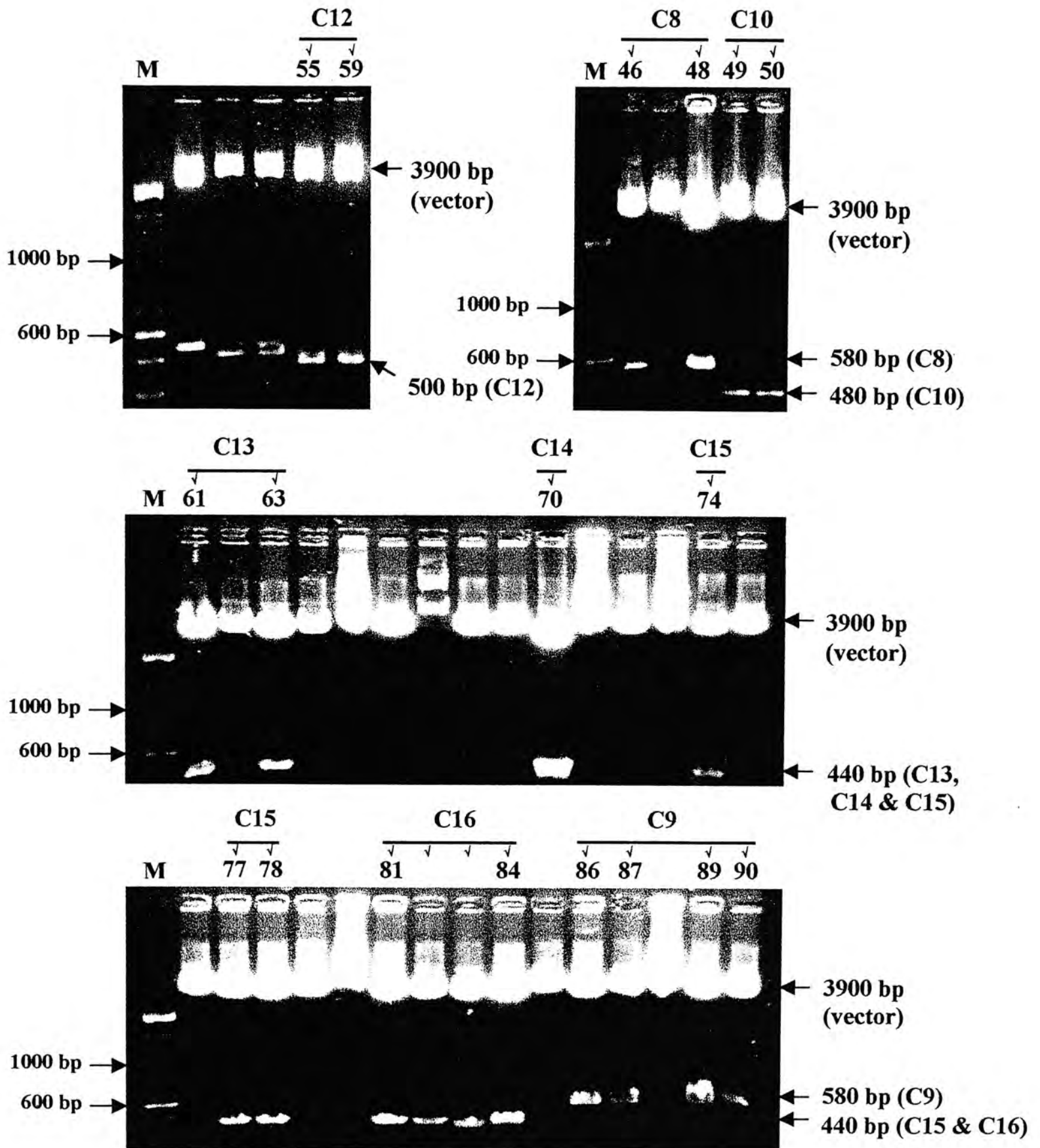


Figure 3.15. EcoRI restriction enzyme digestion of recombinant clones containing inserts C12, C8, C10, C13, C14, C15, C16 and C9. The digested products were resolved on 1.2% agarose, 0.5x TBE gels with ethidium bromide staining. √ represented the recombinant colony containing the insert with correct size. M, 100 bp DNA marker.

Table 3.8 Summary of subcloning of cDNA fragments reamplified from Gel A.

Primers Used	Fragment No.	FDD Size (bp)	FDD Expression Pattern				Reamplification		Subcloning
			<i>cyp2e1</i> +/+		<i>Cyp2e1</i> -/-		PCR Product Size (bp)	EcoRI Digested Fragment Size (bp)	
			CTL	CCl <sub>4</sub>	CTL	CCl <sub>4</sub>			
AP 5 & ARP 2	A1	1500	+++	+	+++	+++	1500	1500	
AP 5 & ARP 2	A2	1200	+	+++	+	+	1200	1200	
AP 5 & ARP 2	A4	520	+	+++	+	+	520	550	
AP 5 & ARP 2	A5	390	+++	+	+++	+++	400	480	

+ indicated the intensity of expressed FDD bands by visual inspection, while - indicated that no FDD band was observed.



Table 3.9 Summary of subcloning of cDNA fragments reamplified from Gel B.

Primers Used	Fragment No.	FDD Size (bp)	FDD Expression Pattern				Reamplification PCR Product Size (bp)	Subcloning EcoRI Digested Fragment Size (bp)
			<i>cyp2e1</i> +/+		<i>Cyp2e1</i> -/-			
			CTL	CCl <sub>4</sub>	CTL	CCl <sub>4</sub>		
AP 5 & ARP 4	B2	990	+	+++	+	+	1000	1000
AP 5 & ARP 4	B4	710	+	+++	+	+	720	730
AP 5 & ARP 4	B5	680	+++	++	+++	+++	710	730
AP 5 & ARP 4	B6	570	+++	+	+++	+++	590	640
AP 5 & ARP 4	B7	550	+	+++	+	+	570	620
AP 5 & ARP 4	B8	490	+	+++	+	+	500	550
AP 5 & ARP 4	B9	460	++	+	++	++	480	600 *
AP 5 & ARP 4	B10	450	++	+	++	++	480	600 *
AP 5 & ARP 4	B11	420	+++	+	+++	+++	420	440
AP 5 & ARP 4	B12	410	+	+++	+	+	410	440
AP 5 & ARP 4	B13	375	-	+	-	-	390	420

+ indicates the intensity of expressed FDD bands by visual inspection, while - indicated that no FDD band was observed.

\* means the sizes of EcoRI digested cDNA fragments were not in agreement with the sizes of their corresponding reamplified cDNA fragments.

Table 3.10 Summary of subcloning of cDNA fragments reamplified from Gel C.

Primers Used	Fragment No.	FDD Size (bp)	FDD Expression Pattern			Reamplification		Subcloning
			<i>cyp2e1</i> +/+	<i>Cyp2e1</i> -/-	PCR Product Size (bp)	EcoRI Digested Fragment Size (bp)		
			CTL	CTL	CCl <sub>4</sub>			
AP 5 & ARP 7	C2	800	-	-	-	820	820	
AP 5 & ARP 7	C3	575	-	-	-	590	620	
AP 5 & ARP 7	C4	560	+++	+++	+++	590	600	
AP 5 & ARP 7	C5	550	+	+	+	570	600	
AP 5 & ARP 7	C6	525	+	+	+	540	600	
AP 5 & ARP 7	C7	505	+	+	+	520	600	
AP 5 & ARP 7	C8	490	+++	+++	+++	500	580	
AP 5 & ARP 7	C9	485	-	-	-	500	580	
AP 5 & ARP 7	C10	470	+++	+++	+++	480	480	
AP 5 & ARP 7	C11	460	+	+	+	470	600 *	
AP 5 & ARP 7	C12	440	+	+	+	440	500	
AP 5 & ARP 7	C13	410	-	-	-	410	440	
AP 5 & ARP 7	C14	360	+++	+++	+++	380	440	
AP 5 & ARP 7	C15	345	+	+	+	360	440	
AP 5 & ARP 7	C16	320	+	+	+	360	440	

+ indicates the intensity of expressed FDD bands by visual inspection, while - indicated that no FDD band was observed.

\* means the sizes of EcoRI digested cDNA fragments were not in agreement with the sizes of their corresponding reamplified cDNA fragments.

Fragment No. & size	Sequence homology	Transcript size (bp)	E-value	Identities
A1 (1500 bp)	<i>Mus musculus</i> hemopexin	1430	0.0	499/527 (94%)

Query: 111 catgtgaagaaacccatctggctttattaggatgaaaatggagaggtgggctgggcatat 170  
 |||||||||||||||||||||||||||||||||||||||||||||||||||||||||||  
 Sbjct: 1430 catgtgaagaaacccatctggctttattaggatgaaaatggagaggtgggctgggc-atat 1372

Query: 171 cagggcctctttattgactgcagccaaggatgctgttcaccttctgaggctgaggcagac 230  
 ||||| ||||| ||||||||||||||||||| |||||||||||||||||||  
 Sbjct: 1371 cagggc-tctttactgactgcagccaaggatgct---caccttctgaggctgaggcagac 1316

Query: 231 tcttggctgcattcagtttgctatactgctatagcagtacaaattgggcccattggataa 290  
 ||||||||||||| ||||||||||||||||||| |||||||||||||||||||  
 Sbjct: 1315 tcttggctgcattgagtttgctatactgctatagcagtacaaattgggcccattggataa 1256

Query: 291 agtacaagctggaaccattggaagaacatgtggttggtttgccaagagacttgtccaac 350  
 ||||||||||||||||||| ||||||||||||||||||| | |||||||||||||||||||  
 Sbjct: 1255 agtacaagctggaaccattggaagaacatgtggttggg---gccaagagacttgtccaac 1199

Query: 351 acagggcccatcaactttcctcatggggccaggaaacctctgtccatggtgcctgggct 410  
 ||||||||||||||||||| ||||||||||||||||||| |||||||||||||||||||  
 Sbjct: 1198 acagggcccatcaacttt-ctcatggggccaggaaacctctgtccatggtgcctgggct 1140

Query: 411 ccctgacttcaggtccagccaccaaagccgctcctgatgagacatagagcctggaag- 469  
 ||||||||||||||||||| ||||||||||||||||||| |||||||||||||||||||  
 Sbjct: 1139 -cctgacttcaggtccagccaccaaagccgctcctgatgagacatagagcctggaaga 1081

Query: 470 accgggagcagaaaaagctgcatctatggtctcaggctgatcccaggacggctccaag 529  
 ||| ||||||||||||| ||||||||||||||||||| |||||||||||||||||||  
 Sbjct: 1080 accgggagcagaaaaagctgcatctatggtctcaggctgatcccaggagggctccaag 1021

Query: 530 ttccttctcc-gccgcttgggataaccactcactagggttatgcctccctttgtaggaa 588  
 ||||||||| ||||||| ||||| ||||| ||||||||||| ||||||||||| |||||  
 Sbjct: 1020 ttccttctccagccgcttgggataaccacttactagggttattgcctccctttgtaggaa 961

Query: 589 gacatacacctgaagtgcctgaatcagatagacttcatcatcccag 635  
 ||||||||| || ||||||||| ||||||||||||| |||||||||||||  
 Sbjct: 960 gacatacacttg-agtgcctggatcagatagactttatcatcccag 915

Figure 3.16. Sequencing comparison between cDNA fragment A1 and *Mus musculus* hemopexin. The insert was sequenced using CEQ 2000 dye terminator cycle sequencing system in the presence of M13 sequencing primer. The sequence of cDNA fragment A1 was compared to entire non-redundant sequence database at the National Library of Medicine using BLAST.

Fragment No. & size	Sequence homology	Transcript size (bp)	E-value	Identities
A4 (520 bp)	<i>Mus musculus</i> t-complex protein 1 (TCP1)	1812	0.0	455/468 (97%)

```

Query: 108 cagcttgctgtactttaatgtgagacaccaaggctacggcattgcacctgacactgta 167
          |||
Sbjct: 1803 cagcttgctgtactttaatgtgagacaccaaggctacggcattgcacctgacactgta 1744

Query: 168 taaataagagggaaaccaatcagtcacatcaagggctccagagtgaacagcattttcataa 227
          |||
Sbjct: 1743 taaataacagggaaatccaatcagtcacatcaagggctccagagtgaacagcattttcataa 1684

Query: 228 cttccggtggttatcgtctttgctttctgggtgtaattttatcagatcatcaatccgaagg 287
          |||
Sbjct: 1683 cttccggtggttatcgtctttgcattctgggtgtaattttatcagatcatcaatccgaagg 1624

Query: 288 atggtgattgcagcctctggtggaacttcaggctcttcactttaactatggttggttca 347
          |||
Sbjct: 1623 atggtgattgcagcctctggtggaacttcaggctcttcactttaactatggttggttca 1564

Query: 348 aacaccctgcttgcttggtgtctcgtgggttcccatggaccaaatcaagaccaatccac 407
          ||
Sbjct: 1563 aagaccctgcttgcttggtgtctcgtgggttcccatggaccaaatcaagaccaatccac 1504

Query: 408 tttagatTTTTACGTCCCGGGGTTCACTTGAGCCTCATTGTGAAAAGCTCTTAAGTGGC 467
          |||
Sbjct: 1503 tttagatTTTTACGTTCCG-GGTTCACTTGAGCCTCATTGTGAAAAGCTCTTAAGTGGC 1445

Query: 468 aaacagggtccgtggagtcctgggcagcattcactg-cagtgtattaggaatcacaagcag 526
          ||
Sbjct: 1444 aaccagggtccgtggagtcctgggcagcattcactgccagtgtattaggaatcacaagcag 1385

Query: 527 agatctgccaaactctgcaatagcaagctgtccccgagatcccatgct 574
          |||
Sbjct: 1384 agatcttgcaaaactctgcaatagcaagctgtccccgagatcccatgct 1337

```

Figure 3.17. Sequencing comparison between cDNA fragment A4 and *Mus musculus* t-complex protein 1 (TCP1). The insert was sequenced using CEQ 2000 dye terminator cycle sequencing system in the presence of M13 sequencing primer. The sequence of cDNA fragment A4 was compared to entire non-redundant sequence database at the National Library of Medicine using BLAST.



Fragment No. & size	Sequence homology	Transcript size (bp)	E-value	Identities
A5 (390 bp)	Mouse major urinary protein (MUP)	872	e-165	333/340 (97%)

Query: 105 agcatggaatccttagagaaaatatcattgacctatccaatgccaatcgctgcctccagg 164  
 |||  
 Sbjct: 531 agcatggaatccttagagaaaatatcattgacctatccaatgccaatcgctgcctccagg 590

Query: 165 cccgagaatgaagaatggcctgagcctccagtgttgagtggagacttctcaccaggactc 224  
 |||  
 Sbjct: 591 cccgagaatgaagaatggcctgagcctccagtgttgagtggagacttctcaccaggactc 650

Query: 225 caccatcatcccttctctatccatacagcatccccagataaaattctgtgatctgcattcc 284  
 |||  
 Sbjct: 651 caccatcatcccttctctatccatacagcatccccagataaaattctgtgatctgcattcc 710

Query: 285 atcctgtctcactgagaagtccaattcccagctctatccacatggttacctaggatacctca 344  
 |||  
 Sbjct: 711 atcctgtctcactgagaagtccaatt-ccagctctatccacatggttacctaggatacctca 769

Query: 345 tccaagaatcaaagacttctttaaatttctctttgatacaccatga-aaattttcatg 403  
 | |||  
 Sbjct: 770 t-caagaatcaaagacttctttaaattt-ttctttgatataccatgacaatttttcatg 827

Query: 404 aatttcttctcttctctgttcaataaatgattacccttgc 443  
 |||  
 Sbjct: 828 aatttcttctcttctctgttcaataaatgattacccttgc 867

Figure 3.18. Sequencing comparison between cDNA fragment A5 and mouse major urinary protein (MUP). The insert was sequenced using CEQ 2000 dye terminator cycle sequencing system in the presence of M13 sequencing primer. The sequence of cDNA fragment A5 was compared to entire non-redundant sequence database at the National Library of Medicine using BLAST.

Fragment No. & size	Sequence homology	Transcript size (bp)	E-value	Identities
B2 (990 bp)	<i>Mus musculus</i> guanine nucleotide binding protein, beta-2	1101	0.0	449/456 (98%)

Query: 117 accgcagttcccggacatgatcctgtctgctgctcgcgagacaagaccatcatcatgtggaa 176  
 |||  
 Sbjct: 176 accgcagttcccggacatgatcctgtctgctgctcgcgagacaagaccatcatcatgtggaa 235

Query: 177 gctgaccagagatgagaccaactatggcataccacagcgtgctctgagaggtcactccca 236  
 |||  
 Sbjct: 236 gctgaccagagatgagaccaactatggcataccacagcgtgctctgagaggtcactccca 295

Query: 237 cttcgtagtgatggtgttatctcctctgatggcagtttgcctctcgggctcctggga 296  
 |||  
 Sbjct: 296 cttcgtagtgatggtgttatctcctctgatggcagtttgcgctctcgggctcctggga 355

Query: 297 cggaacgctgcgctctgggatctcacaacgggcaccaccacaatgcgatttgtcggcca 356  
 |||  
 Sbjct: 356 cggaacgctgcgctctgggatctcacaacgggcaccaccacaaggcgatttgtcggcca 415

Query: 357 caccaacgatgtgttgagcgtggccttctcctctgacaaccggcagattgtctctgggtc 416  
 |||  
 Sbjct: 416 caccaaggatgtgttgagcgtggccttctcctctgacaaccggcagattgtctctgggtc 475

Query: 417 ccgagacaagaccataaagtgatggaatactctgggtgtctgcaagtacacgggtccaaga 476  
 |||  
 Sbjct: 476 ccgagacaagaccataaagttatggaatactctgggtgtctgcaagtacacgggtccagga 535

Query: 477 tgagagtcattcagaatgggtgtcttgtgtccgcttctccccgaacagcagccaccctat 536  
 |||  
 Sbjct: 536 tgagagtcattcagaatgggtgtcttgtgtccgcttctccccgaacagcagcaaccctat 595

Query: 537 catcgtcacctgcggatgggacaagctggtcaaggt 572  
 |||  
 Sbjct: 596 catcgtctcctgcggatgggacaagctggtcaaggt 631

Figure 3.19. Sequencing comparison between cDNA fragment B2 and *Mus musculus* guanine nucleotide binding protein, beta-2. The insert was sequenced using CEQ 2000 dye terminator cycle sequencing system in the presence of M13 sequencing primer. The sequence of cDNA fragment B2 was compared to entire non-redundant sequence database at the National Library of Medicine using BLAST.

Fragment No. & size	Sequence homology	Transcript size (bp)	E-value	Identities
B4 (710 bp)	Mouse adipose differentiation-related protein (ADRP)	1680	0.0	487/499 (97%)

```

Query: 121 tgaatctttattcgggtccagaacagacggtttacagccaataacaatacaaaggccacaga 180
          |||
Sbjct: 1675 tgaatctttattcgggtccaga-cagacggtttacagccaataacaatacaaaggccacaga 1617

Query: 181 caagactgtaagtgcacatctgagcttttaggttcctccaggtcctcacaagactaacacag 240
          |||
Sbjct: 1616 caagactgtaagtgcacatctgagcttttaggttcctccaggtcctcacaagactaacacag 1557

Query: 241 gccactcaccagccaggtaagagaactcctgtgccagggccagctggggcaagaccataa 300
          |||
Sbjct: 1556 gccactcaccagccaggtaagagaactcctgtgccagggccagctggggcaagaccataa 1497

Query: 301 ctgggctgtgagtgaccataatgaggcccttggttctaagaagctgcttttctaagctaa 360
          |||
Sbjct: 1496 ctgagctgtgagtgaccataatgaggcccttggttctaagaagctgcttttctaagctaa 1437

Query: 361 agccatctaccaagttaatttcaatacagcaaaaggggtcatctggccagcaacatcatg 420
          |||
Sbjct: 1436 agccatctaccaagttaatttcaatacagcaaaaggggtcatctggccagcaacatcatg 1377

Query: 421 ctctggtgacaaggaggggtttactgagctttgacctcagactgctggaccttcaggctg 480
          |||
Sbjct: 1376 ctctggtgacaaggaggggtttactgagctttgacctcagactgctggaccttcaggctg 1317

Query: 481 gcctgtttcaccacggtagactgaggataaaggggaccta-cagccagttgagaggcgtg 539
          |||
Sbjct: 1316 gccttgttcacctcggtagactgaggataaaggggacctaccagccagttgagaggcgtg 1257

Query: 540 ttgtaacaaaagtattccataacttcatctaaagattcc-tcattttctgcagctgcccc 598
          |||
Sbjct: 1256 ttgtaacaaaagtaatccataacttcatctaaagattccttcattttctgcagctgcccc 1197

Query: 599 -tgctagatgtgaggacgc 616
          |||
Sbjct: 1196 ttgctagatgtgaggacgc 1178

```

Figure 3.20. Sequencing comparison between cDNA fragment B4 and mouse adipose differentiation-related protein (ADRP). The insert was sequenced using CEQ 2000 dye terminator cycle sequencing system in the presence of M13 sequencing primer. The sequence of cDNA fragment B4 was compared to entire non-redundant sequence database at the National Library of Medicine using BLAST.

Fragment No. & size	Sequence homology	Transcript size (bp)	E-value	Identities
B5 (680 bp)	His-tagged-multidrug resistance glycoprotein	4045	2e-23	72/74 (97%)

```

Query: 1  gggcgaattgggccctcttagatgcatgctcgagcggcccgccagttgtgatggatatctg 60
          |||
Sbjct: 14 gggcgaattgggccctct-agatgcatgctcgagcggcccgccagt-gtgatggatatctg 71

```

```

Query: 61  cagaattcgcctt 74
          |||
Sbjct: 72  cagaattcgcctt 85

```

Figure 3.21. Sequencing comparison between cDNA fragment B5 and his-tagged-multidrug resistance glycoprotein. The insert was sequenced using CEQ 2000 dye terminator cycle sequencing system in the presence of M13 sequencing primer. The sequence of cDNA fragment B5 was compared to entire non-redundant sequence database at the National Library of Medicine using BLAST.





Fragment No. & size	Sequence homology	Transcript size (bp)	E-value	Identities
B8 (490 bp)	Ribosomal protein S10	588	0.0	425/440 (96%)

```

Query: 106 ggagctagcagacaaaaatgtgcccaaccttcatgtaatgaaggccatgcagtctctcaa 165
          ||||||| |||||||||||||||||||||||||||||||||||||||||||||||||||
Sbjct: 125 ggagctggcagacaaaaatgtgcccaaccttcatgtaatgaaggccatgcagtctctcaa 184

Query: 166 gtctcgaggctacgtgaaggaacagtttgcttgagacatttctactggtaccttacgaa 225
          |||||||||||||||||||||||||||||||||||||||||||||||||||
Sbjct: 185 gtctcgaggctacgtgaaggaacagtttgcttgagacatttctactggtaccttacgaa 244

Query: 226 cgagggcatccagtatctccgagactacctgcacctacccccggagatcgtgcccgccac 285
          |||||||||||||||||||||||||||||||||||||||||||||||||||
Sbjct: 245 cgagggcatccagtatctccgagactacctgcacctacccccggagatcgtgcccgccac 304

Query: 286 cctgcgctcgcagccgtcccgagaccggcaggcctcggcccaaagggtccagaggggtgagcg 345
          |||||||||||||||||||||||||||||||||||||||||||||||||||
Sbjct: 305 cctgcgctcgcagccgtcccgagaccggcaggcctcggcccaaagggtccagaggggtgagcg 364

Query: 346 acctgcaagattcacaagaggggaggctgacagagacacctacagaaggagcgctgtgcc 405
          |||||||||||||||||||||||||||||||||||||||||||||||||||
Sbjct: 365 acctgcaagattcacaagaggggaggctgacagagacacctacagaaggagcgctgtgcc 424

Query: 406 ccctggagctgacaagaaagctgaggctgggggctggctcagccactgagttccaggtct 465
          ||||||||||||||||||||||||||||||||||||||||||||| ||| |||
Sbjct: 425 ccctggagctgacaagaaagctgaggct-ggggctggctcagccactgagttcca-gttt 482

Query: 466 agaggccgcttgggtcgtggacgtggtcagccacctcagtgacgtcggagttcatgtcgt 525
          ||||| |||| |||||||||||||||||||||||||||| || ||||| |||| ||
Sbjct: 483 agaggcggcttgggtcgtggacgtggtcagccacctcagtgaaagttggagtttatgttgt 542

Query: 526 attgactaaccttcaaagaa 545
          ||||| ||| ||| |||||
Sbjct: 543 attgaataaactttaagaa 562

```

Figure 3.24. Sequencing comparison between cDNA fragment B8 and ribosomal protein S10. The insert was sequenced using CEQ 2000 dye terminator cycle sequencing system in the presence of M13 sequencing primer. The sequence of cDNA fragment B8 was compared to entire non-redundant sequence database at the National Library of Medicine using BLAST.

Fragment No. & size	Sequence homology	Transcript size (bp)	E-value	Identities
B9 (460 bp)	Fatty acid binding protein, intestine (FABPI)	670	e-142	304/312 (97%)

Query: 98 ctagcagacggaacggagctcactggggcctggaccattgagggaaataaacttattggg 157  
 |||  
 Sbjct: 252 ctagcagacggaacggagctcactggggcctggaccattgagggaaataaacttattggg 311

Query: 158 aaattcacacgtgtagcacaatggaaaggagctgattgctgtccgagaggtttctggtaa 217  
 |||  
 Sbjct: 312 aaattcacacgtgtag-acaatggaaaggagctgattgctgtccgagaggtttctggtaa 370

Query: 218 tgaactaatccagacctacacatatgaaggagttgaggccaagcgattcctttaagaagg 277  
 |||  
 Sbjct: 371 tgaactaatccagacctacacatatgaaggagttgaggccaagcgatt-ctttaagaagg 429

Query: 278 aataagccaacttctcagagcctggagccaacgctgaagagctaagctgtatgtcagatt 337  
 |||  
 Sbjct: 430 aataagtcaacttctcagagcctggag-caacgctgaagagctaagctg-atgtcagatt 487

Query: 338 tctttctccatcatgctaatgccaggctcattcgctcaatcctatccaagcactgggtctcc 397  
 |||  
 Sbjct: 488 tctttctccatcatgctaatgccaggctcattcgctc-atcctatc--agcactgggtctcc 544

Query: 398 agccttgtcaaa 409  
 |||  
 Sbjct: 545 agccttgtcaaa 556

Figure 3.25. Sequencing comparison between cDNA fragment B9 and fatty acid binding protein, intestine (FABPI). The insert was sequenced using CEQ 2000 dye terminator cycle sequencing system in the presence of M13 sequencing primer. The sequence of cDNA fragment B9 was compared to entire non-redundant sequence database at the National Library of Medicine using BLAST.

Fragment No. & size	Sequence homology	Transcript size (bp)	E-value	Identities
B10 (450 bp)	<i>Mus musculus</i> clusterin (CLU)	1669	0.0	365/368 (99%)

Query: 114 agacaagtactaccttcgggtctccaccgtgaccacccattcctctgactcagaggtccc 173  
 |||  
 Sbjct: 1225 agacaagtactaccttcgggtctccaccgtgaccacccattcctctgactcagaggtccc 1284

Query: 174 ctcccgtgtcactgaggtggtggtgaagctgtttgactctgaccccatcacagtgggtgtt 233  
 |||  
 Sbjct: 1285 ctcccgtgtcactgaggtggtggtgaagctgtttgactctgaccccatcacagtgggtgtt 1344

Query: 234 accagaagaagtctctaaggataaccctaagtttatggacacagtggcggagaaggcgct 293  
 |||  
 Sbjct: 1345 accagaagaagtctctaaggataaccctaagtttatggacacagtggcggagaaggcgct 1404

Query: 294 acaggaataaccgcaggaaaagccgtgcggaatgagatagaagcatcaccttcctatatgt 353  
 |||  
 Sbjct: 1405 acaggaataaccgcaggaaaagccgtgcggaatgagatagaagcatcaccttcctatatgt 1464

Query: 354 aggagtgtctgggaggggaatctccagctccccgaggtggctgcagacccttagagaact 413  
 |||  
 Sbjct: 1465 aggagtgtctgggaggggaatctccagctccccgaggtggctgcagacccttagagaact 1524

Query: 414 ccacatgtctccaggcgagtaggcctcccccaagcagcctgccccttctctggattctg 473  
 |||  
 Sbjct: 1525 ccacatgtctccaggcgagtaggcctcacccaagcagcctg-cccttctctggattctg 1583

Query: 474 tacactaa 481  
 |||  
 Sbjct: 1584 tacactaa 1591

Figure 3.26. Sequencing comparison between cDNA fragment B10 and *Mus musculus* clusterin (CLU). The insert was sequenced using CEQ 2000 dye terminator cycle sequencing system in the presence of M13 sequencing primer. The sequence of cDNA fragment B10 was compared to entire non-redundant sequence database at the National Library of Medicine using BLAST.





Fragment No. & size	Sequence homology	Transcript size (bp)	E- value	Identities
B12 (410 bp)	Mouse EST	490	0.0	359/365 (98%)

Query: 110 agcagacagcagtatcatgaggaagctcagtggaactagcagctggcactgtgatacct 169  
 |||  
 Sbjct: 370 agcagacagcagtatcatgaggaagctcagtggaactagcagctggcactgtgatccct 311

Query: 170 gcagcgctgtttgtctgtcatggattgctctatataagcactgtcatggacagcagcttc 229  
 |||  
 Sbjct: 310 gcagcgctgtttgtctgtcatggattgctctatataaacactgtcatggacagcagcttc 251

Query: 230 tagaggattcttgtttctaggtatttattgtatcatttatggggttacatggacaggtga 289  
 |||  
 Sbjct: 250 tagaggattcttgtttctaggtatttattgtatcatttatggggttacatggacaggtga 191

Query: 290 cttggggtttcagaattgcaaatgctagttcctattctggagtgcctgaacacatcc 349  
 |||  
 Sbjct: 190 cttggggtttcagaattgcaaatgctagttcctattctggagtgcctgaacacatcc 131

Query: 350 atattctgcaaagtgaggtcatcagcttgtaaccagggtatgtgtgttctcttagggttg 409  
 |||  
 Sbjct: 130 atattctgcaaagtgaggtcatcagcttgtaaccagggtatgtgtgttctcttagggttg 71

Query: 410 attctccccttta-tggggaaactttaatta-tttttccaaaat-aatcatacatttgt 466  
 |||  
 Sbjct: 70 attctcccctttattgggaaaactttaattattttttccaaaataaatcatacatttgt 11

Query: 467 ctatg 471  
 ||||  
 Sbjct: 10 ctatg 6

Figure 3.28. Sequencing comparison between cDNA fragment B12 and mouse EST. The insert was sequenced using CEQ 2000 dye terminator cycle sequencing system in the presence of M13 sequencing primer. The sequence of cDNA fragment B12 was compared to entire non-redundant sequence database at the National Library of Medicine using BLAST.



Fragment No. & size	Sequence homology	Transcript size (bp)	E-value	Identities
B13 (375 bp)	Mouse cytoplasmic gamma-actin ( $\gamma$ -actin)	4609	e-167	330/335 (98%)

Query: 100 agcagacttccaggatttcctgaggctggcaagggttcctgaaccagttaccactccttc 159  
 |||  
 Sbjct: 3437 agcagacttccaggatttcctgaggctggcaagggttcctgaaccagttaccactccttc 3496

Query: 160 ttgccagtctaacaggggtgggaaagtccgagccttaggaccagtttcagttctggtttc 219  
 |||  
 Sbjct: 3497 ttgccagtctaacaggggtgggaaagtccgagccttaggaccagtttcagttctggtttc 3556

Query: 220 ttccctcctgaccaccatcggttgtagttgccttgagttgggaacgtttgcacgacac 279  
 |||  
 Sbjct: 3557 ttccctcctgaccaccatcggttgtagttgccttgagttgggaacgtttgcacgacac 3616

Query: 280 ctgtaaagtattcattctttaatttatgtaagggtttttgtactcaattctttaagaaa 339  
 |||  
 Sbjct: 3617 ctgtaaagtattcattctttaatttatgtaagggtttttgtactcaattctttaagaaa 3676

Query: 340 tgacaaatthttggthtttctactgthccaatgagaaccatgaggccccagcaaacacgtca 399  
 |||  
 Sbjct: 3677 tgacaaatthttggthtttctactgth-caatgagaa-cattagg-ccccagcaaacacgtca 3733

Query: 400 ttgtgtaaaagaaataaaagtgctgcagtaactga 434  
 |||  
 Sbjct: 3734 ttgtgt-aaagaaataaaagtgctgcagtaactga 3767

Figure 3.29. Sequencing comparison between cDNA fragment B13 and mouse cytoplasmic gamma-actin ( $\gamma$ -actin). The insert was sequenced using CEQ 2000 dye terminator cycle sequencing system in the presence of M13 sequencing primer. The sequence of cDNA fragment B13 was compared to entire non-redundant sequence database at the National Library of Medicine using BLAST.







Fragment No. & size	Sequence homology	Transcript size (bp)	E-value	Identities
C4 (560 bp)	<i>Mus musculus</i> cullin 1 (CUL1)	2986	0.0	453/457 (99%)

Query: 101 ttttcaatcaactttaaacagcatttggttacctgtttattcaatggcctgaacaaaca 160  
 |||  
 Sbjct: 776 ttttcaatcaactttaaacagcatttggttacctgtttattcaatggcctgaacaaaca 717

Query: 161 tctctccatgtcaccaatgcaagtgaatagatttcatatattccttttcgctccttcatca 220  
 |||  
 Sbjct: 716 tctctccatgtcaccaatgcaagtgaatagatttcatatattccttttcgctccttcatca 657

Query: 221 cattcacggcgaaccaatgtctattgaggtaggcacagattccattcagcactttgctg 280  
 |||  
 Sbjct: 656 cattcacggcgaaccaatgtctattgaggtaggcacagattccattcagcactttgctg 597

Query: 281 gagaatcggtaatcttcccactgctgagtgtagaacttcaggacactcccatccattaa 340  
 |||  
 Sbjct: 596 gagaatcggtaatcttcccactgctgagtgtagaacttcaggacactctcatccattaa 537

Query: 341 tcttctccatccttaagaagatttggtcaaataattcttcaaaaattccttcaatcgcttg 400  
 |||  
 Sbjct: 536 tcttctccatccttaagaagatttggtcaaataattcttcaaaaattccttcaatcgcttg 477

Query: 401 tataactccaagccaacaaactgagctccccaggagtctgccccttttttgacttgaa 460  
 |||  
 Sbjct: 476 tataactccaagccaacaaactgagctccccaggagtctgccccttttttgacttgaa 417

Query: 461 ggagggactccagcaccgggctgggttgactgatgcacacctagtagtagttat 520  
 |||  
 Sbjct: 416 ggagggactccagcaccgg-ggcttggttgactgatgcaca-ctagtagtagttat 359

Query: 521 aaacatgagtgtagagttccatgtatctggactttgc 557  
 |||  
 Sbjct: 358 aaacatgagtgtagagttccatgtatctggactttgc 322

Figure 3.32. Sequencing comparison between cDNA fragment C4 and *Mus musculus* cullin 1 (CUL1). The insert was sequenced using CEQ 2000 dye terminator cycle sequencing system in the presence of M13 sequencing primer. The sequence of cDNA fragment C4 was compared to entire non-redundant sequence database at the National Library of Medicine using BLAST.

Fragment No. & size	Sequence homology	Transcript size (bp)	E-value	Identities
C5 (550 bp)	Mouse DNA for virus-like (VL30) retrotransposon BVL-1	5447	0.0	478/515 (92%)

```

Query: 96  ttttttttttttcagcagccacaacatccagg-ccactgacttttcagggaccactcctct 154
          |||
Sbjct: 2250 ttttttttcttcagcagccacaacatccagggccactgacttctcagggaccactcctca 2191

Query: 155  tttgctccggatttccgagctcatttttccctaggctccaggtccatgggcgggaccact 214
          |||
Sbjct: 2190 tttgctccggatttccgagctcatttttccctaggctccaggtccatgggcggg-accact 2132

Query: 215  gtgaccgcgctggctgctctctggagttggagtgaggagcagggcagctgaggatctgaaa 274
          |||
Sbjct: 2131 gtgaccgcgctggctgctctctggagttggagtgaggagcagggcagctggtgatctgaaa 2072

Query: 275  ggaagtggtcagcatagggatctgacaggattcctaggcttatttcagtataggcataac 334
          |||
Sbjct: 2071 ggaagtggtcagcatagggatctgacaggatttttaggcttatttcagaa--ggcataac 2014

Query: 335  ttaaaaacagtcgctcagtcacagtcgaagtcgaacacaaagagacacaaaagacacac 394
          |||
Sbjct: 2013 ttaaaaacagtcgctcagtcacagtcgaagtcgaacacaaagagacacaaaaaagacacac 1954

Query: 395  acaggaaccggttttttaaggcaaccactatagaatcacagtaccacagaaatgacaaac 454
          |||
Sbjct: 1953 acag-aaaccggtttttca-ggcaaccactatagaatcacagtaccacagaaatgacaaac 1896

Query: 455  accagcaagacca-tacaggccatcttacatgacgattttcagagaagcttactgtcacta 513
          ||
Sbjct: 1895 acaagcaagaccaatacagggcatcttacatgacgattttcagagaagcttactgtcacta 1836

Query: 514  tgaccaactcaagtggacctgtctacattgggacggccccagaaacctgaagaaccgc 573
          ||||
Sbjct: 1835 tgacc-aaccctaatggacctgtctccat-gggaaggccc-agaacctga-gaccggc 1780

Query: 574  cttaaaccctaaaaccaggatagtcagtcactcct 608
          ||
Sbjct: 1779 cttaaacc--aaaccaagataatcagtcactcct 1747

```

Figure 3.33. Sequencing comparison between cDNA fragment C5 and mouse DNA for virus-like (VL30) retrotransposon BVL-1. The insert was sequenced using CEQ 2000 dye terminator cycle sequencing system in the presence of M13 sequencing primer. The sequence of cDNA fragment C5 was compared to entire non-redundant sequence database at the National Library of Medicine using BLAST.



Fragment No. & size	Sequence homology	Transcript size (bp)	E-value	Identities
C6 (525 bp)	Mouse EST	516	0.0	447/469 (95%)

Query: 111 gattggctcttctatctcctgaagttactcatggttcttaaaactcctgggactttgttc 170  
 |||  
 Sbjct: 483 gattggctcttctatctcctgaagttactcatggttcttaaaactcctgggactttgttc 424

Query: 171 ttttgccaacgtagaaagcacagtgacgggttggttggcccagccctctctgtaggc 230  
 |||  
 Sbjct: 423 ttttgccaacgtagaaagcacagtgacgggttggttggcccagccctctctgtaggc 364

Query: 231 tgagcagtgacgagcgccacaggtttacacacaagtttggttggtttcttctgttct 290  
 |||  
 Sbjct: 363 tgagcagtgacgagcgccacaggtttacacacaagtttggttggtttcttctgttct 304

Query: 291 gcactttggagtcacctgggtattccacattacaagttgatggtatatttgggggctg 350  
 |||  
 Sbjct: 303 gcactttggagt-ccctgggtattccacattacaagttgatggtata--gggggggctg 247

Query: 351 gaattggtgccctgggatgtggggaccaaggtacaatctaccatgggccccacaaggc 410  
 |||  
 Sbjct: 246 gaattggtgccct-ggatgtggggaccaaggtacaatctaaccatgggccccacaaggc 188

Query: 411 ttctgaaatcaaagttaggtggtgagagtacctgcagtcctcgggataactggtgagtc 470  
 |||  
 Sbjct: 187 ttctgaaatcaaagttaggtggtgagagtacctgcagtcctcgggataactggtgagtc 128

Query: 471 ccctgggtcc-ggaggggtgcaaggtccctg--acagtagtagggatgggga-ctgggctg 526  
 |||  
 Sbjct: 127 ccctgggtcctggaggggtgcaaggtttgtggaacagtagtagggatggggagctgggctg 68

Query: 527 gg-tcatcagaatggcgtgtctgc--tcacagttgctgtcctaagtaa 572  
 ||  
 Sbjct: 67 gg-tcatcagaatggcgtgtctgccttcacag-tgctgtcctaagtaa 20

Figure 3.34. Sequencing comparison between cDNA fragment C6 and mouse EST. The insert was sequenced using CEQ 2000 dye terminator cycle sequencing system in the presence of M13 sequencing primer. The sequence of cDNA fragment C6 was compared to entire non-redundant sequence database at the National Library of Medicine using BLAST.



Fragment No. & size	Sequence homology	Transcript size (bp)	E-value	Identities
C7 (505 bp)	<i>Mus musculus</i> COP9, subunit 3 (COPS3)	1583	0.0	439/446 (98%)

Query: 118 ttaaaca...aaaggtaactttaatgcagtaataacaatctgaggataaataaatccacaac 177  
 |||  
 Sbjct: 1566 ttaaaca...aaaggtaactttaatgcagtaataacaatctgaggataaataaatccacaac 1507

Query: 178 agactctaaagtaggatttttttttctttcctttcctttgcagagaatggttttctgaaagcaa 237  
 |||  
 Sbjct: 1506 agactctaaagtaggatttttttttctttcctttcctttgcagagaatggttttctgaaagcaa 1447

Query: 238 taggactgcagatgttaaactgaatttctgactgtccaggaggaaccggcatggaaccgc 297  
 |||  
 Sbjct: 1446 taggactgcagatgttaaactgaatttctgactgtccaggaggaaccggcatggaaccgc 1387

Query: 298 catggtacttctgctgcgctcttcacacttgccaggccaaggttctgttacctcaagat 357  
 |||  
 Sbjct: 1386 catggtacttctgctgcgctcttcacacttgccaggccaaggttctgttacctcaagat 1327

Query: 358 gggggtagtttcaagagtagctggagggttctgctgagtcattcttctgtgag-cc 416  
 |||  
 Sbjct: 1326 gggggtagtttcaagagtagctggagggttctgctgagtcattcttctgtgagccc 1267

Query: 417 atgctcttttgaacaaactgggggttcaccgtgatctcctgggtccatagccttcagtc 476  
 |||  
 Sbjct: 1266 atgctcttttgaacaaactgggggttcaccgtgatctcctgggtccatagccttcagtcgc 1207

Query: 477 tcat-cagctctatgcatttttagcatctctgggtcgatggtatgaggcatggctgggggtt 535  
 |||  
 Sbjct: 1206 tcatccagctctatgcatttttagcatctctgggtcgatggtatgaagcatggct-ggggtt 1148

Query: 536 attatacttctcaggggttatcatgg 561  
 |||  
 Sbjct: 1147 attatacttctca-ggggttatcatgg 1123

Figure 3.35. Sequencing comparison between cDNA fragment C7 and *Mus musculus* COP9, subunit 3 (COPS3). The insert was sequenced using CEQ 2000 dye terminator cycle sequencing system in the presence of M13 sequencing primer. The sequence of cDNA fragment C7 was compared to entire non-redundant sequence database at the National Library of Medicine using BLAST.

Fragment No. & size	Sequence homology	Transcript size (bp)	E-value	Identities
C9 (485 bp)	Mouse cytoplasmic gamma-actin ( $\gamma$ -actin)	4609	e-139	296/306 (96%)

Query: 108 tcagttactgcagcacttttattttctttacacaatgacgtggtgctggggcctaagtgtc 167  
 |||  
 Sbjct: 3767 tcagttactgcagcacttttattttctttacacaatgacgtggtgctggggcctaagtgtc 3708

Query: 168 tcattgaacagtagaaaacccaaaatttgtcatttcttaagaattgagtacaaaaaacct 227  
 |||  
 Sbjct: 3707 tcattgaacagtagaaaacccaaaatttgtcatttcttaagaattgagtacaaaaaacct 3648

Query: 228 tacataaattaaagaatgaatacatttacaggtgtcgatgcaaacgttcccaactcaagg 287  
 |||  
 Sbjct: 3647 tacataaattaaagaatgaatacatttacaggtgtcgatgcaaacgttcccaactcaagg 3588

Query: 288 caactaacaaccgatggtgggtcaggaggggaagaaactttatgaactgaaactgggtccta 347  
 |||  
 Sbjct: 3587 caactaacaaccgatggtgggtcaggaggggaagaaac---cagaactgaaactgggtccta 3531

Query: 348 aggctcggactttcccaccctgttaagactggccaaagaaggagtggtaactggttcag 407  
 |||  
 Sbjct: 3530 aggctcggacttt-cccaccctgtt-agactggc--aagaaggagtggtaactggttcag 3475

Query: 408 ggaccc 413  
 | |||  
 Sbjct: 3474 gaaccc 3469

Figure 3.36. Sequencing comparison between cDNA fragment C9 and mouse cytoplasmic gamma-actin ( $\gamma$ -actin). The insert was sequenced using CEQ 2000 dye terminator cycle sequencing system in the presence of M13 sequencing primer. The sequence of cDNA fragment C9 was compared to entire non-redundant sequence database at the National Library of Medicine using BLAST.

Fragment No. & size	Sequence homology	Transcript size (bp)	E-value	Identities
C10 (470 bp)	Mouse fibronectin (FN)	905	e-160	317/324 (97%)

Query: 108 atggattggtctgggatcaatagggaaacacaggtagccaactaggaggaaatgtactga 167  
 ||||| |  
 Sbjct: 584 atggtttgggtctgggatcaatagggaaacacaggtagccaactaggaggaaatgtactga 643

Query: 168 atgctagtaccaagaccttgaagcaggaaagtcacccagacacctctgctttcttttgc 227  
 ||||| |  
 Sbjct: 644 atgctagtaccaagacct-gagcaaggaaagtcacccagacacctctgctttcttttgc 702

Query: 228 catctgacctgcagcactgtcaggacatggcctgtggctgtgtgttcaaacacccctccc 287  
 ||||| |  
 Sbjct: 703 catctgacctgcagcactgtcaggacatggcctgtggctgtgtgt-caaacacccctccc 761

Query: 288 acaggactcactttgtccaacaattcagattgcctagaaatacctttctcttacctggt 347  
 ||||| |  
 Sbjct: 762 acagaactcactttgtccaacaattcagattgcctagaaatacctttctcttacctggt 821

Query: 348 tgttatttatcaatttttccagtatattttatacggaaaaaattgtattgaagacacttt 407  
 ||||| |  
 Sbjct: 822 tgttatttatcaatttttccagtatattttatacggaaaaaattgtattgaagacacttt 881

Query: 408 gtatgcagttgataagaggaattc 431  
 ||||| |  
 Sbjct: 882 gtatgcagttgataagaggaattc 905

Figure 3.37. Sequencing comparison between cDNA fragment C10 and mouse fibronectin (FN). The insert was sequenced using CEQ 2000 dye terminator cycle sequencing system in the presence of M13 sequencing primer. The sequence of cDNA fragment C10 was compared to entire non-redundant sequence database at the National Library of Medicine using BLAST.



Fragment No. & size	Sequence homology	Transcript size (bp)	E-value	Identities
C11 (460 bp)	<i>Mus musculus</i> ribosomal protein L3 (RPL3)	1276	e-179	381/395 (96%)

```

Query: 112 agtagaaatattttattggtgagaccccaccatctgcacaaagtggctcctggaatcaagc 171
          |||
Sbjct: 1275 agtagaaatattttattggtgagaccccaccatctgcacaaagtggctcctggaatcaagc 1216

Query: 172 tccttcctccttggcaatgcgatctttcttgagtggccccataaatgctttcttctcctc 231
          |||
Sbjct: 1215 tccttcctccttggcaatgcgatctttcttgagtggccccataaatgctttcttctcctc 1156

Query: 232 catggtctggaagcgaccatggccaaatggaggtgggtgtcaatgaacttcagggtcaat 291
          |||
Sbjct: 1155 catggtctggaagcgaccatggccaaatggaggtgggtgtcaatgaacttcagggtcaat 1096

Query: 292 cttctccagggcccccgcgcttgggtctgaactctagcaaggaccttacgaagagtaagta 351
          |||
Sbjct: 1095 cttctccagggc-ccgacgcttgggtctgaa--ccagcaagga-cttacgaagagtaagta 1040

Query: 352 ctgcttcttgggtcccaccacacagcccttgagcatgatgaagtcattgggtcacctca 411
          |||
Sbjct: 1039 ctgcttcttgggtcccaccacacag-ccttgagcatgatgaagtcattgggtcacctca 981

Query: 412 ccataatgcacaaagccccccagtggttagatgccctgtcagaccagtcatagttagta 471
          |||
Sbjct: 980 ccataatgcacaaagccaccagtggttagatgctcttgtcagacaagtcatagtcagta 921

Query: 472 gatgcattgtccttgaatcagtttgccatccttga 506
          |||
Sbjct: 920 gatgcattgttcttg-atcagtttgccatccttga 887

```

Figure 3.38. Sequencing comparison between cDNA fragment C11 and *Mus musculus* ribosomal protein L3 (RPL3). The insert was sequenced using CEQ 2000 dye terminator cycle sequencing system in the presence of M13 sequencing primer. The sequence of cDNA fragment C11 was compared to entire non-redundant sequence database at the National Library of Medicine using BLAST.



Fragment No. & size	Sequence homology	Transcript size (bp)	E-value	Identities
C12 (440 bp)	<i>Mus musculus</i> ribosomal protein L3 (RPL3)	1276	e-148	301/309 (97%)

```

Query: 105  ttgggtcaaggctacctcatcaaggatggcaaactgatcaagaacaatgcatctactgact 164
           |||
Sbjct: 869  ttgggtcaaggctacctcatcaaggatggcaaactgatcaagaacaatgcatctactgact 928

Query: 165  atgacttgtctgacaagagcatcaaccactgggtggctttgtgcattatggtgaggtga 224
           |||
Sbjct: 929  atgacttgtctgacaagagcatcaaccactgggtggctttgtgcattatggtgaggtga 988

Query: 225  ccaatgacttcatcatgctcaaaggctgtgtggtggggaccaagaagcgagtacttactc 284
           |||
Sbjct: 989  ccaatgacttcatcatgctcaaaggctgtgtggtggggaccaagaagcgagtacttactc 1048

Query: 285  ttcgtaagtcccttgctggttcagaccaaacgtcgggccctggtatттаagattgacctg 344
           |||
Sbjct: 1049 ttcgtaagt-ccttgctggttcagaccaaacgtcgggccctg---gagaagattgacctg 1104

Query: 345  aagttcattgacacccacctccaaatttgccatggtcgcttcagaccatggaggagaa 404
           |||
Sbjct: 1105 aagttcattgaca-ccacctccaaatttgccatggtcgcttcagaccatggaggagaa 1163

Query: 405  gaaagcatt 413
           |||
Sbjct: 1164 gaaagcatt 1172

```

Figure 3.39. Sequencing comparison between cDNA fragment C12 and *Mus musculus* ribosomal protein L3 (RPL3). The insert was sequenced using CEQ 2000 dye terminator cycle sequencing system in the presence of M13 sequencing primer. The sequence of cDNA fragment C12 was compared to entire non-redundant sequence database at the National Library of Medicine using BLAST.



Fragment No. & size	Sequence homology	Transcript size (bp)	E-value	Identities
C14 (360 bp)	<i>Mus musculus</i> PK-120 precursor (ITIH-4)	3030	e-157	306/311 (98%)

```

Query: 106  ttcacactgcccttctttatttgtaacaaggagcatcctcttcccatcaaggctctcggc 165
          |||
Sbjct: 2987 ttcacactgcccttctttatttgtaacaaggagcatcctcttcccatcaaggctctcggc 2928

Query: 166  ctcacaggcgtccctggtggcataagggtgtcatctgcctgcgtacgaggacaacatggca 225
          |||
Sbjct: 2927 ctcacaggcgtccctggtggcataagggtgtcatctgcctgcgtacgaggacaacatggca 2868

Query: 226  gggagtggcgctcctaacagttctatatctccactgtccagcaggaaatctctgctcctg 285
          |||
Sbjct: 2867 gggagcggcgctcctaacagttctatatctccactgtccagcaggaaatctctgctcctg 2808

Query: 286  ggaacccttcttggttaactcaacttgagctctctggtagccaggtagtcaacctccttga 345
          |||
Sbjct: 2807 ggaacccttcttggttaactcaacttgagctctctggtagccaggtagtcaa-ctccttga 2749

Query: 346  actttgactgtccgttttgtataatctaggctcgacgggtggctcccaaacgatgtcccg 405
          |||
Sbjct: 2748 actttgactgtccgttttgtattatct-ggctcgacgggtggctcccaaacgatgtcccg 2690

Query: 406  gtaaaactgac 416
          |||
Sbjct: 2689 gtaaaactgac 2679

```

Figure 3.41. Sequencing comparison between cDNA fragment C14 and *Mus musculus* PK-120 precursor (ITIH-4). The insert was sequenced using CEQ 2000 dye terminator cycle sequencing system in the presence of M13 sequencing primer. The sequence of cDNA fragment C14 was compared to entire non-redundant sequence database at the National Library of Medicine using BLAST.



Fragment No. & size	Sequence homology	Transcript size (bp)	E-value	Identities
C15 (345 bp)	Tcp-1=t-complex polypeptide 1 (TCP1)	10043	e-151	294/297 (98%)

```

Query: 105  tcagcttgctgtactttaatgtgagacacccaaggctacggcattgcacctgacactggt 164
          |||
Sbjct: 9157 tcagcttgctgtactttaatgtgagacacccaaggctacggcattgcacctgacactggt 9098

Query: 165  ataaataagagggaaatccaatcagtcacatcaagggctccagagtgaacagcattttcata 224
          |||
Sbjct: 9097 ataaataagagggaaatccaatcagtcacatcaagggctccagagtgaacagcattttcata 9038

Query: 225  acttccgtgtttatcgtctttgctttctgggtgtaattttatcagatcatcaatccgaag 284
          |||
Sbjct: 9037 acttccgtgtttatcgtctttgctttctgggtgtaattttatcagatcatcaatccgaag 8978

Query: 285  gatggtgattgcagccctctggtgcccgaacttcaggctcttcactttaactatggttgg 344
          |||
Sbjct: 8977 gatggtgattgcag-cctctggtg-cgaacttcaggctcttcactttaactatggttgg 8920

Query: 345  tcaaacacccctgcttgcttgttctcgtgg-ttcccatggaccaaatacaagacca 400
          |||
Sbjct: 8919 tcaaacacccctgcttgcttgttctcgtggtttcccatggaccaaatacaagacca 8863

```

Figure 3.42. Sequencing comparison between cDNA fragment C15 and tcp-1=t-complex polypeptide 1 (TCP1). The insert was sequenced using CEQ 2000 dye terminator cycle sequencing system in the presence of M13 sequencing primer. The sequence of cDNA fragment C15 was compared to entire non-redundant sequence database at the National Library of Medicine using BLAST.



Fragment No. & size	Sequence homology	Transcript size (bp)	E-value	Identities
C16 (320 bp)	Tcp-1=t-complex polypeptide 1 (TCP1)	10043	e-156	298/301 (99%)

Query: 108 tcagcttgctgtactttaatgtgagacacccaaggctacggcattgcacctgacactggt 167  
 |||  
 Sbjct: 9157 tcagcttgctgtactttaatgtgagacacccaaggctacggcattgcacctgacactggt 9098

Query: 168 ataaataagagggaaatccaatcagtcacatcaagggctccagagtgaacagcattttcata 227  
 |||  
 Sbjct: 9097 ataaataagagggaaatccaatcagtcacatcaagggctccagagtgaacagcattttcata 9038

Query: 228 acttccgtgtttatcgtctttgctttctgggtgtaattttatcagatcatcaatccgaag 287  
 |||  
 Sbjct: 9037 acttccgtgtttatcgtctttgctttctgggtgtaattttatcagatcatcaatccgaag 8978

Query: 288 gatggtgattgcagcctctggtgcaacttcaggctcttcactttaactatggttggttc 347  
 |||  
 Sbjct: 8977 gatggtgattgcagcctctggtgcaacttcaggctcttcactttaactatggttggtt- 8919

Query: 348 caaacaccctgctttgcttgttctcgtggtttcccatggaccaaataagaccatc 407  
 |||  
 Sbjct: 8918 caaacaccctgc-ttgcttgttctcgtggtttcccatggaccaaataagaccatc 8860

Query: 408 c 408  
 |  
 Sbjct: 8859 c 8859

Figure 3.43. Sequencing comparison between cDNA fragment C16 and tcp-1=t-complex polypeptide 1 (TCP1). The insert was sequenced using CEQ 2000 dye terminator cycle sequencing system in the presence of M13 sequencing primer. The sequence of cDNA fragment C16 was compared to entire non-redundant sequence database at the National Library of Medicine using BLAST.

Table 3.11 Summary of sequence homology of subcloned cDNA fragments.

Fragment No.	FDD size (bp)	FDD Expression Pattern				Sequencing		Identities (%)
		<i>cyp2e1</i> <sup>+/+</sup>		<i>cyp2e1</i> <sup>-/-</sup>		Sequence Homology		
		CTL	CCl <sub>4</sub>	CTL	CCl <sub>4</sub>			
A1	1500	+++	+	+++	+++		<i>Mus musculus</i> hemopexin	499/527 (94%)
A2	1200	+	+++	+	+		---Sequencing failed---	---
A4	520	+	+++	+	+		<i>Mus musculus</i> t-complex protein 1 (TCP1)	455/468 (97%)
A5	390	+++	+	+++	+++		Mouse major urinary protein (MUP)	333/340 (97%)
B2	990	+	+++	+	+		<i>Mus musculus</i> guanine nucleotide binding protein, beta-2	449/456 (98%)
B4	710	+	+++	+	+		Mouse adipose differentiation-related protein (ADRP)	487/499 (97%)
B5	680	+++	++	+++	+++		His-tagged-multidrug resistance glycoprotein	72/74 (97%)
B6	570	+++	+	+++	+++		Rat GAP-associated protein (P190)	284/326 (87%)
B7	550	+	+++	+	+		<i>Mus musculus</i> integrin linked kinase (ILK)	477/509 (93%)
B8	490	+	+++	+	+		Ribosomal protein S10	425/440 (96%)
B9	460	++	+	++	++		Fatty acid binding protein, intestine (FABPI)	304/312 (97%)
B10	450	++	+	++	++		<i>Mus musculus</i> clusterin (CLU)	365/368 (99%)
B11	420	+++	+	+++	+++		<i>Rattus norvegicus</i> phospholipase C, gamma 1 (PLCG1)	354/378 (93%)
B12	410	+	+++	+	+		Mouse EST	359/365 (98%)
B13	375	-	+	-	-		Mouse cytoplasmic gamma-actin ( $\gamma$ -actin)	330/335 (98%)
C2	800	-	+	-	-		<i>Rattus norvegicus</i> mRNA for acyl-CoA synthetase 5 (ACSS5)	441/487 (90%)
C3	575	-	+	-	-		Mouse EST	371/387 (95%)
C4	560	+++	+	+++	+++		<i>Mus musculus</i> cullin 1 (CUL1)	453/457 (99%)
C5	550	+	+++	+	+		Mouse DNA for virus-like (VL30) retrotransposon BVL-1	478/515 (92%)
C6	525	+	+++	+	+		Mouse EST	447/469 (95%)
C7	505	+	+++	+	+		<i>Mus musculus</i> COP9 subunit 3 (COPS3)	439/446 (98%)
C8	490	+++	+	+++	+++		---Sequencing failed---	---
C9	485	-	+	-	-		Mouse cytoplasmic gamma-actin ( $\gamma$ -actin)	296/306 (96%)
C10	470	+++	+	+++	+++		Mouse fibronectin (FN)	317/324 (97%)
C11	460	+	+++	+	+		<i>Mus musculus</i> ribosomal protein L3 (RPL3)	381/395 (96%)
C12	440	+	+++	+	+		<i>Mus musculus</i> ribosomal protein L3 (RPL3)	301/309 (97%)
C13	410	-	+	-	-		Mouse major histocompatibility complex region	211/222 (95%)
C14	360	+++	+	+++	+++		<i>Mus musculus</i> PK-120 precursor (ITI4-4)	306/311 (98%)
C15	345	+	+++	+	+		Tcp-1 =t-complex polypeptide 1 (TCP1)	294/297 (98%)
C16	320	+	+++	+	+		Tcp-1 =t-complex polypeptide 1 (TCP1)	298/301 (99%)



retrotransposon BVL-1 (C5), *Mus musculus* COP9 subunit 3 (C7), mouse fibronectin (C10), *Mus musculus* ribosomal protein L3 (C11 and C12), mouse major histocompatibility complex region (C13) and *Mus musculus* PK-120 precursor (C14). Three cDNA fragments (B12, C3 and C6) showed remarkable homology to mouse ESTs. It is interesting to note that cDNA fragments A4, C15 and C16 encode the same *Mus musculus* t-complex protein 1 gene, cDNA fragments B13 and C9 encode the same mouse cytoplasmic gamma-actin gene and cDNA fragments C11 and C12 encode the same *Mus musculus* ribosomal protein L3 gene.

### **3.9 Confirmation of differential expression patterns by Northern blot analysis**

Due to the time limitation, Northern blot analysis was performed to confirm the differential expression patterns of only sixteen cDNA fragments including A1, A4, A5, B4, B5, B6, B7, B9, B11, B13, C2, C4, C7, C12, C14 and C15 using liver samples from each treatment group after 24 hr CCl<sub>4</sub> treatment (Table 3.12). Among them, the differential expression patterns of four cDNA fragments (B4, C12, B13 and A5) shown on FDD gels were confirmed by Northern blot analysis (refer to the following section), while the expression patterns of the other five cDNA fragments (A1, A4, B9, C2 and C14) shown on Northern blots (data not shown) did not match with their corresponding expression patterns shown on FDD gels (no differential expression was detected or the difference of expression was not consistent with that of FDD gels). In addition, no expression signals were found on the Northern blots of cDNA fragments B5, B6, B7, B11, C4, C7 and C15 (data not shown).

The expression pattern of cDNA fragment B4 (adipose differentiation-related protein) was shown in Figure 3.44. There was constitutive expression of fragment B4

Table 3.12 Summary of Northern blot analyses on sequenced cDNA fragments.

Fragment No.	FDD size (bp)	FDD Expression Pattern				Sequencing		Results of Northern blot
		<i>cyp2e1</i> <sup>+/+</sup>		<i>cyp2e1</i> <sup>-/-</sup>		Sequence Homology	Identities (%)	
		CTL	CCI <sub>4</sub>	CTL	CCI <sub>4</sub>			
A1	1500	+++	+	+++	+++	<i>Mus musculus</i> hemopexin	499/527 (94%)	x
A4	520	+	+++	+	+	<i>Mus musculus</i> t-complex protein 1 (TCPI1)	455/468 (97%)	x
A5	390	+++	+	+++	+++	Mouse major urinary protein (MUP)	333/340 (97%)	✓
B2	990	+	+++	+	+	<i>Mus musculus</i> guanine nucleotide binding protein, beta-2	449/456 (98%)	/
B4	710	+	+++	+	+	Mouse adipose differentiation-related protein (ADRP)	487/499 (97%)	✓
B5	680	+++	++	+++	+++	His-tagged-multidrug resistance glycoprotein	72/74 (97%)	---
B6	570	+++	+	+++	+++	Rat GAP-associated protein (P190)	284/326 (87%)	---
B7	550	+	+++	+	+	<i>Mus musculus</i> integrin linked kinase (ILK)	477/509 (93%)	---
B8	490	+	+++	+	+	Ribosomal protein S10	425/440 (96%)	/
B9	460	++	+	++	++	Fatty acid binding protein, intestine (FABPI)	304/312 (97%)	x
B10	450	++	+	++	++	<i>Mus musculus</i> clusterin (CLU)	365/368 (99%)	/
B11	420	+++	+	+++	+++	<i>Rattus norvegicus</i> phospholipase C, gamma 1 (PLCG1)	354/378 (93%)	---
B12	410	+	+++	+	+	Mouse EST	359/365 (98%)	/
B13	375	-	+	-	-	Mouse cytoplasmic gamma-actin ( $\gamma$ -actin)	330/335 (98%)	✓
C2	800	-	+	-	-	<i>Rattus norvegicus</i> mRNA for acyl-CoA synthetase 5 (ACSS5)	441/487 (90%)	x
C3	575	-	+	-	-	Mouse EST	371/387 (95%)	/
C4	560	+++	+	+++	+++	<i>Mus musculus</i> cullin 1 (CUL1)	453/457 (99%)	---
C5	550	+	+++	+	+	Mouse DNA for virus-like (VL30) retrotransposon BVL-1	478/515 (92%)	/
C6	525	+	+++	+	+	Mouse EST	447/469 (95%)	/
C7	505	+	+++	+	+	<i>Mus musculus</i> COP9 subunit 3 (COPS3)	439/446 (98%)	---
C9	485	-	+	-	-	Mouse cytoplasmic gamma-actin ( $\gamma$ -actin)	296/306 (96%)	/
C10	470	+++	+	+++	+++	Mouse fibronectin (FN)	317/324 (97%)	/
C11	460	+	+++	+	+	<i>Mus musculus</i> ribosomal protein L3 (RPL3)	381/395 (96%)	/
C12	440	+	+++	+	+	<i>Mus musculus</i> ribosomal protein L3 (RPL3)	301/309 (97%)	✓
C13	410	-	+	-	-	Mouse major histocompatibility complex region	211/222 (95%)	/
C14	360	+++	+	+++	+++	<i>Mus musculus</i> PK-120 precursor (ITI4-4)	306/311 (98%)	x
C15	345	+	+++	+	+	Tcp-1=t-complex polypeptide 1 (TCPI1)	294/297 (98%)	---
C16	320	+	+++	+	+	Tcp-1=t-complex polypeptide 1 (TCPI1)	298/301 (99%)	/

/ Northern blot analyses were not performed on these cDNA fragments.

--- No expression signals were found on the Northern blots of these cDNA fragments.

✓ The differential expression patterns of these cDNA fragments on FDD gels were confirmed by Northern blot analyses.

x The differential expression patterns of these cDNA fragments on FDD gels did not agree with the results from Northern blot analyses.



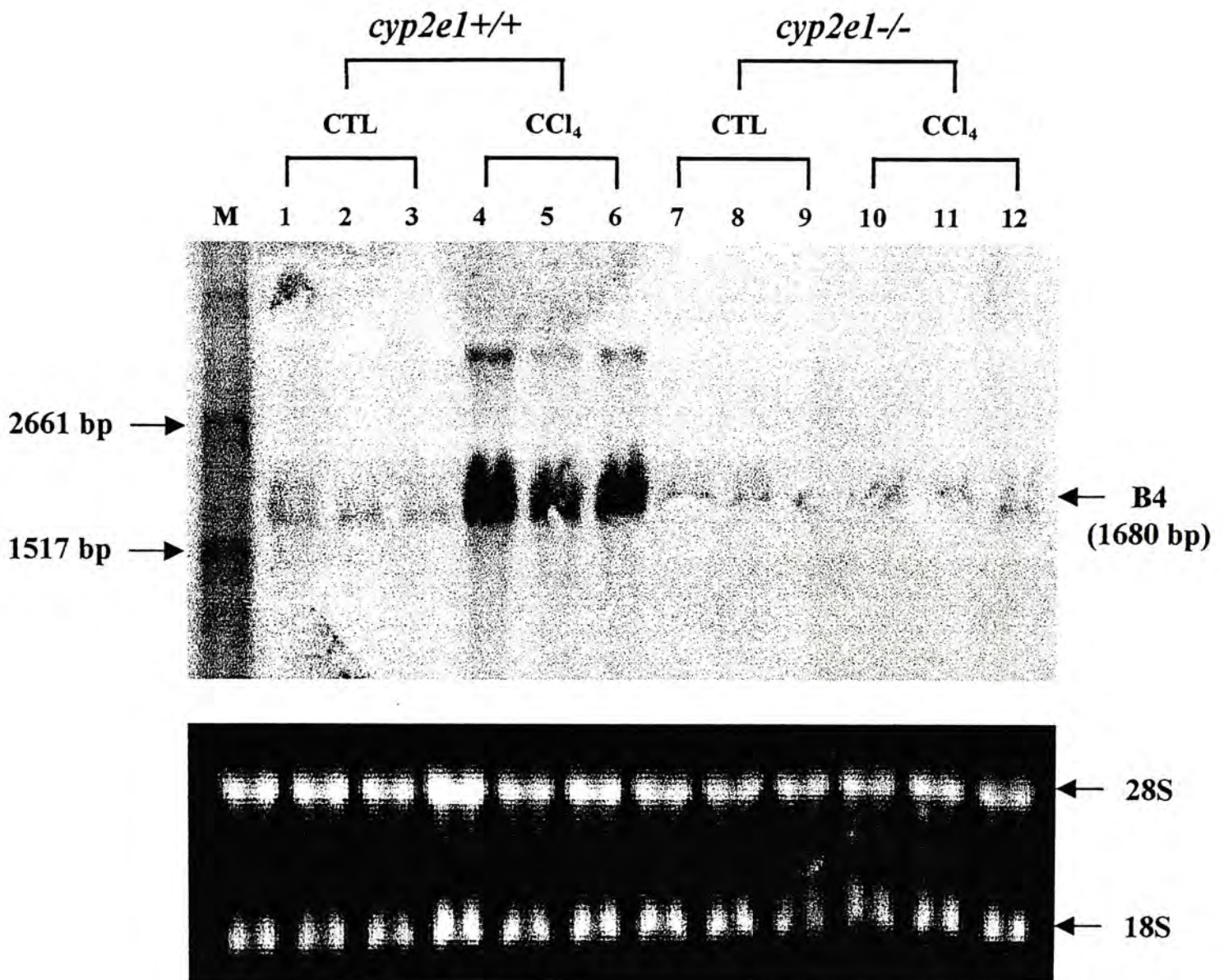


Figure 3.44. Confirmation of FDD expression pattern of cDNA fragment B4 (adipose differentiation-related protein) by Northern blot analysis. Fifteen micrograms of total liver RNA from *cyp2e1*<sup>+/+</sup> and *cyp2e1*<sup>-/-</sup> mice treated with corn oil (CTL) or 1 ml/kg CCl<sub>4</sub> for 24 hr were separated on 1.0% agarose-formaldehyde gel with ethidium bromide staining and transferred to nylon membrane. The membrane was then hybridized with the DIG-labeled cDNA fragment B4 (710 bp) and the signal was detected by colorimetric method with reagents NBT and BCIP. Ethidium bromide stained RNA gel was used for normalization. M, DIG-labeled RNA molecular weight marker I.

(1680 bp) in the livers of both *cyp2e1*<sup>+/+</sup> and *cyp2e1*<sup>-/-</sup> mice treated with corn oil (control). Moreover, fragment B4 was up-regulated in *cyp2e1*<sup>+/+</sup> mice after treatment with 1 ml/kg CCl<sub>4</sub> for 24 hr, while no such induction was observed in *cyp2e1*<sup>-/-</sup> mice with the same treatment. This up-regulated expression pattern of fragment B4 shown on Northern blot was in agreement with the expression pattern shown on the FDD gel (Figure 3.7).

Figure 3.45 illustrated the expression pattern of cDNA fragment C12 (ribosomal protein L3). There was constitutive expression of fragment C12 (1276 bp) in the livers of both *cyp2e1*<sup>+/+</sup> and *cyp2e1*<sup>-/-</sup> mice treated with corn oil (control). Moreover, fragment C12 was up-regulated in *cyp2e1*<sup>+/+</sup> mice after treatment with 1 ml/kg CCl<sub>4</sub> for 24 hr, while only slight induction was observed in *cyp2e1*<sup>-/-</sup> mice with the same treatment. This up-regulation of fragment C12 in *cyp2e1*<sup>+/+</sup> mice shown on Northern blot was consistent with results from FDD gel (Figure 3.8).

The expression pattern of cDNA fragment B13 (cytoplasmic gamma-actin) was shown in Figure 3.46. There was no constitutive expression of fragment B13 (4609 bp) in the livers of both *cyp2e1*<sup>+/+</sup> and *cyp2e1*<sup>-/-</sup> mice treated with corn oil (control). Moreover, fragment B13 was up-regulated in *cyp2e1*<sup>+/+</sup> mice after treatment with 1 ml/kg CCl<sub>4</sub> for 24 hr, while no such induction was observed in *cyp2e1*<sup>-/-</sup> mice with the same treatment. This up-regulated expression pattern of fragment B13 shown on Northern blot was in agreement with the expression pattern shown on the FDD gel (Figure 3.7).

Figure 3.47 illustrated the expression pattern of cDNA fragment A5 (major urinary protein). There was high constitutive expression of fragment A5 (872 bp) in the livers of both *cyp2e1*<sup>+/+</sup> and *cyp2e1*<sup>-/-</sup> mice treated with corn oil (control). Moreover, fragment A5 was down-regulated in *cyp2e1*<sup>+/+</sup> mice after treatment with 1 ml/kg CCl<sub>4</sub> for 24 hr, while



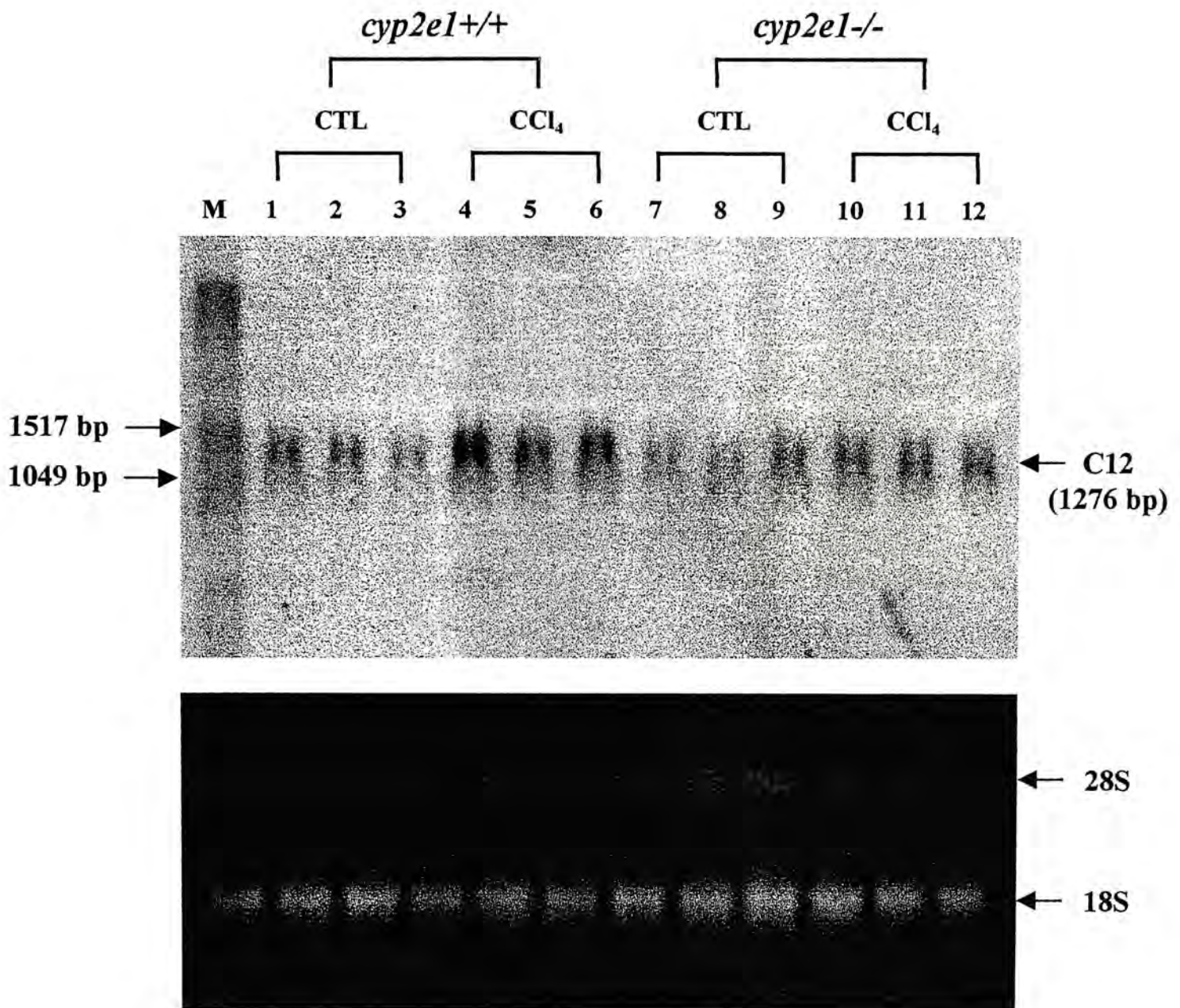


Figure 3.45. Confirmation of FDD expression pattern of cDNA fragment C12 (ribosomal protein L3) by Northern blot analysis. Fifteen micrograms of total liver RNA from *cyp2e1*<sup>+/+</sup> and *cyp2e1*<sup>-/-</sup> mice treated with corn oil (CTL) or 1 ml/kg CCl<sub>4</sub> for 24 hr were separated on 1.0% agarose-formaldehyde gel with ethidium bromide staining and transferred to nylon membrane. The membrane was then hybridized with the DIG-labeled cDNA fragment C12 (440 bp) and the signal was detected by colorimetric method with reagents NBT and BCIP. Ethidium bromide stained RNA gel was used for normalization. M, DIG-labeled RNA molecular weight marker I.

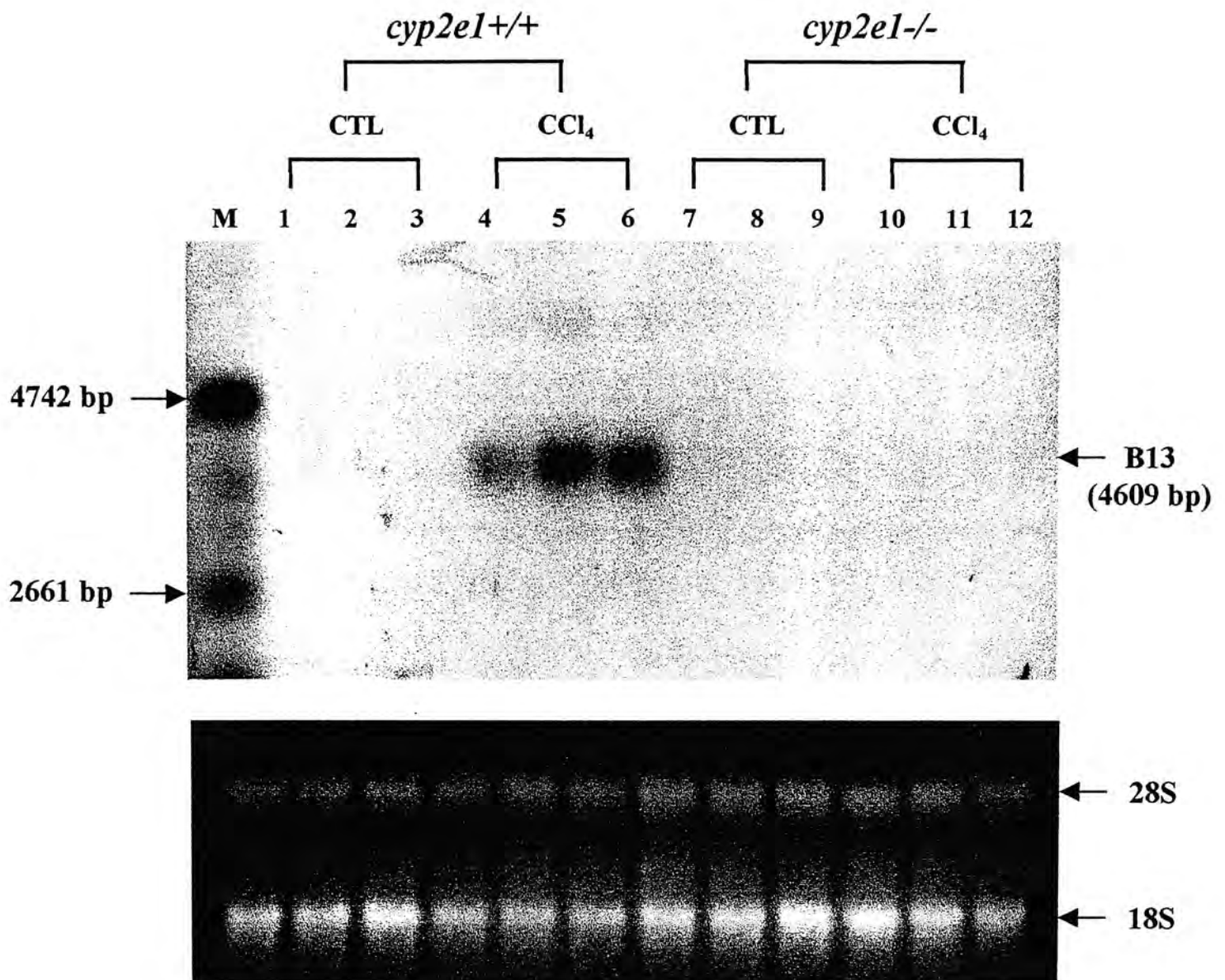


Figure 3.46. Confirmation of FDD expression pattern of cDNA fragment B13 (cytoplasmic gamma-actin) by Northern blot analysis. Fifteen micrograms of total liver RNA from *cyp2e1*<sup>+/+</sup> and *cyp2e1*<sup>-/-</sup> mice treated with corn oil (CTL) or 1 ml/kg CCl<sub>4</sub> for 24 hr were separated on 1.0% agarose-formaldehyde gel with ethidium bromide staining and transferred to nylon membrane. The membrane was then hybridized with the DIG-labeled cDNA fragment B13 (375 bp) and the signal was detected by colorimetric method with reagents NBT and BCIP. Ethidium bromide stained RNA gel was used for normalization. M, DIG-labeled RNA molecular weight marker I.



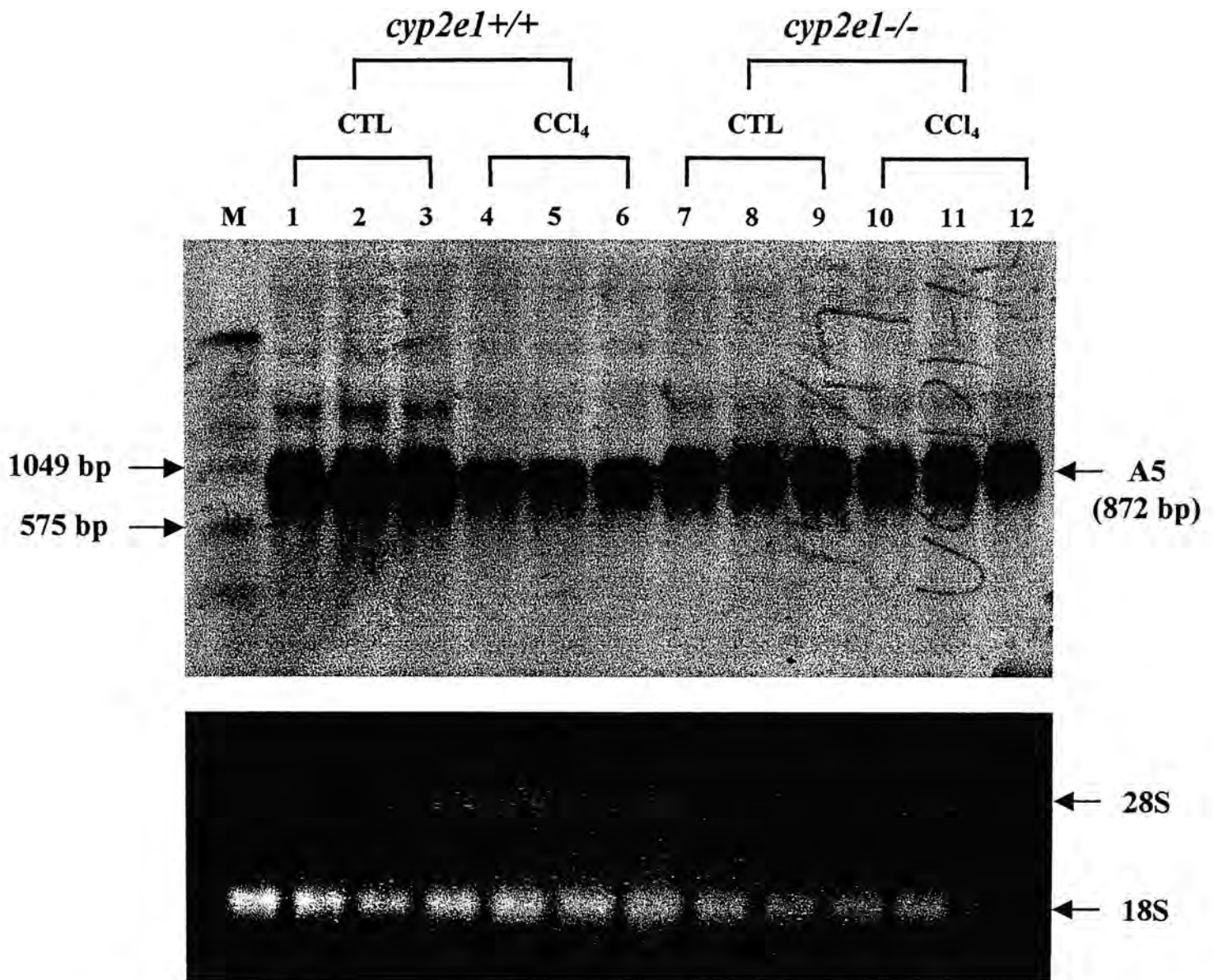


Figure 3.47. Confirmation of FDD expression pattern of cDNA fragment A5 (major urinary protein) by Northern blot analysis. Fifteen micrograms of total liver RNA from *cyp2e1*<sup>+/+</sup> and *cyp2e1*<sup>-/-</sup> mice treated with corn oil (CTL) or 1 ml/kg CCl<sub>4</sub> for 24 hr were separated on 1.0% agarose-formaldehyde gel with ethidium bromide staining and transferred to nylon membrane. The membrane was then hybridized with the DIG-labeled cDNA fragment A5 (390 bp) and the signal was detected by colorimetric method with reagents NBT and BCIP. Ethidium bromide stained RNA gel was used for normalization. M, DIG-labeled RNA molecular weight marker I.

no such suppression was observed in *cyp2e1*<sup>-/-</sup> mice with the same treatment. This down-regulated expression pattern of fragment A5 shown on Northern blot was consistent with the expression pattern shown on the FDD gel (Figure 3.6).

### 3.10 Temporal expression of differentially expressed genes

To explore whether the differential expression of cDNA fragments B4, C12, B13 and A5 in wild-type mice by CCl<sub>4</sub> was time-dependent, time course study was carried out. Since the expression patterns of these five cDNA fragments were not altered in *cyp2e1*<sup>-/-</sup> mice after exposure to CCl<sub>4</sub> comparing with their corresponding controls, only the expression patterns of these four genes in *cyp2e1*<sup>+/+</sup> mice were studied at 2, 6, 12, 24 and 48 hr after CCl<sub>4</sub> i.p. injection.

The time-dependent expression pattern of cDNA fragment B4 was shown in Figure 3.48. Comparing with controls, the induction level of this gene (ADRP) increased as the CCl<sub>4</sub> treatment time increased from 2 to 24 hr. Maximal induction of this gene appeared after 24 hr CCl<sub>4</sub> treatment, and the level of induction declined after 48 hr CCl<sub>4</sub> treatment.

Figure 3.49 illustrated the time-dependent expression pattern of cDNA fragment C12. The expression level of this gene (RPL3) was not altered after 2 and 6 hr CCl<sub>4</sub> treatment. The expression level of RPL3 started to increase after 12 hr CCl<sub>4</sub> treatment and reached to a maximum after 24 hr CCl<sub>4</sub> treatment, and then declined after 48 hr CCl<sub>4</sub> treatment.

The time-dependent expression pattern of cDNA fragment B13 was shown in Figure 3.50. There was no constitutive expression found in controls, while maximal

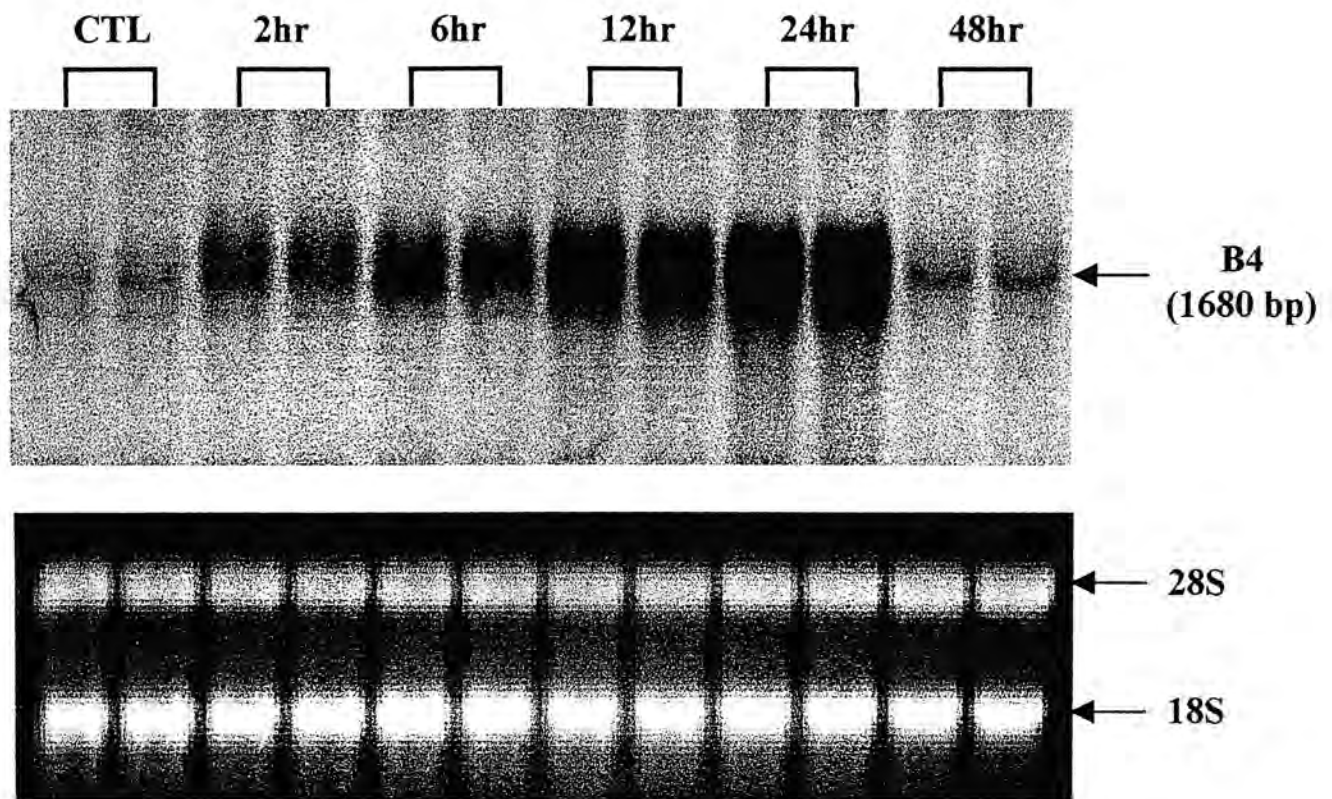


Figure 3.48. Time-dependent expression pattern of cDNA fragment B4 (adipose differentiation-related protein). Fifteen micrograms of total liver RNAs from *Cyp2e1*<sup>+/+</sup> mice treated with corn oil (CTL) or CCl<sub>4</sub> (1 ml/kg) for 2, 6, 12, 24 and 48 hr were separated on a 1.0% agarose-formaldehyde gel and transferred to nylon membrane. The membrane was then hybridized with the DIG-labeled cDNA fragment B4 and the signal was detected by colorimetric method with reagents NBT and BCIP. Ethidium bromide stained RNA gel was used for normalization.

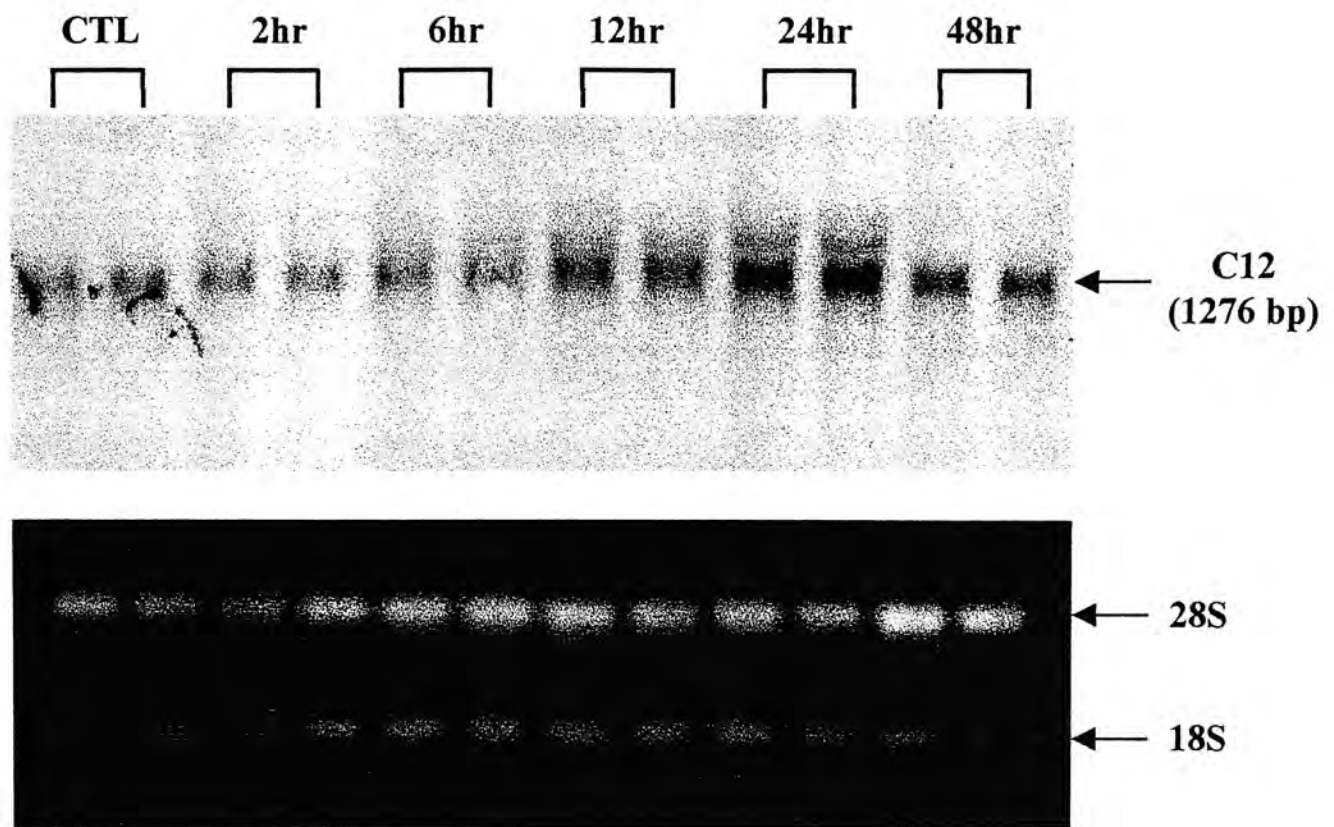


Figure 3.49. Time-dependent expression pattern of cDNA fragment C12 (ribosomal protein L3). Fifteen micrograms of total liver RNAs from *cyp2e1*<sup>+/+</sup> mice treated with corn oil (CTL) or CCl<sub>4</sub> (1 ml/kg) for 2, 6, 12, 24 and 48 hr were separated on a 1.0% agarose-formaldehyde gel and transferred to nylon membrane. The membrane was then hybridized with the DIG-labeled cDNA fragment C12 and the signal was detected by colorimetric method with reagents NBT and BCIP. Ethidium bromide stained RNA gel was used for normalization.



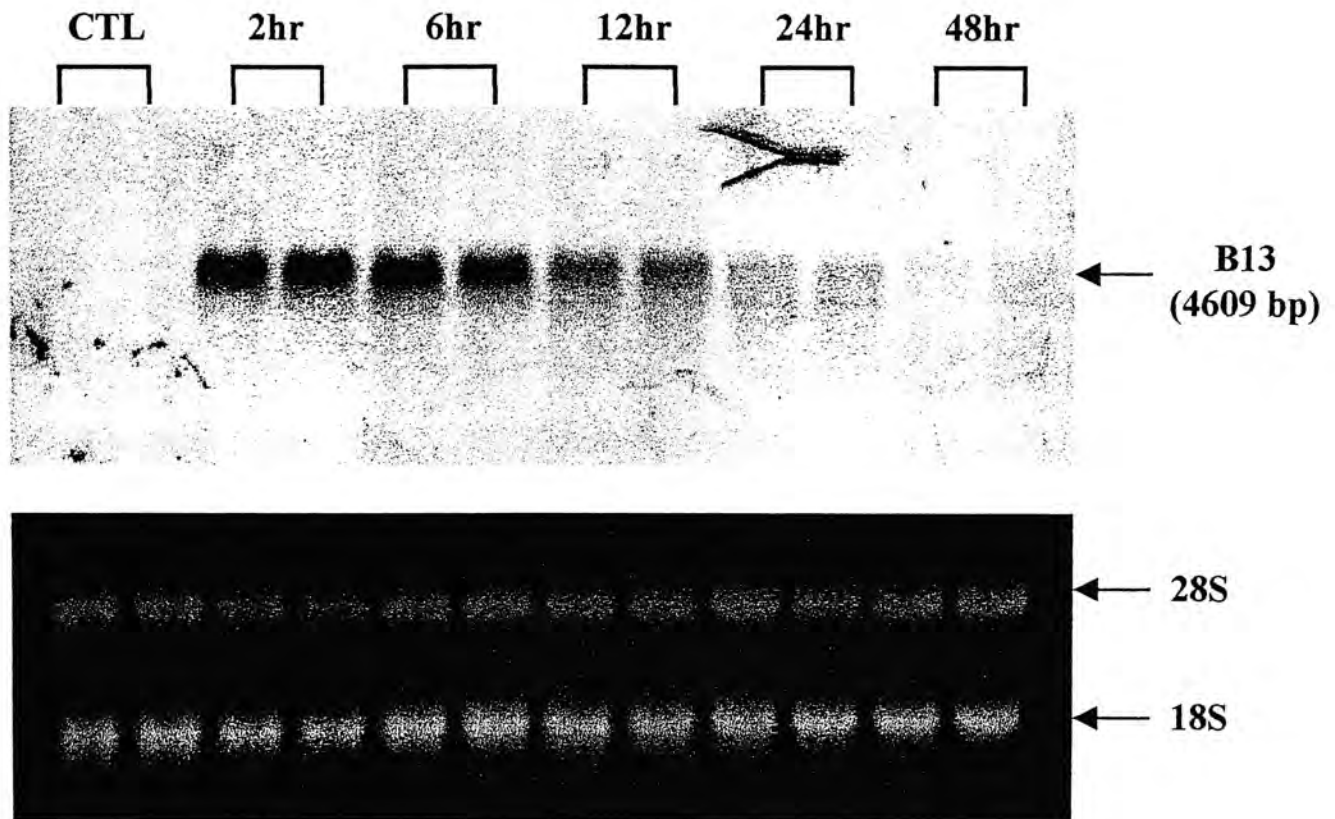


Figure 3.50. Time-dependent expression pattern of cDNA fragment B13 (cytoplasmic gamma-actin). Fifteen micrograms of total liver RNAs from *cyp2e1*<sup>+/+</sup> mice treated with corn oil (CTL) or CCl<sub>4</sub> (1 ml/kg) for 2, 6, 12, 24 and 48 hr were separated on a 1.0% agarose-formaldehyde gel and transferred to nylon membrane. The membrane was then hybridized with the DIG-labeled cDNA fragment B13 and the signal was detected by colorimetric method with reagents NBT and BCIP. Ethidium bromide stained RNA gel was used for normalization.

induction of this gene ( $\gamma$ -actin) appeared after 2 hr CCl<sub>4</sub> treatment, then the level of induction declined as CCl<sub>4</sub> treatment time increased from 6 to 48 hr.

Figure 3.51 illustrated the time-dependent expression pattern of cDNA fragment A5. The suppression level of this gene (MUP) increased as CCl<sub>4</sub> treatment time increased from 2 to 12 hr after CCl<sub>4</sub> treatment. The expression level after 24 hr CCl<sub>4</sub> treatment was slightly higher than that after 12 hr CCl<sub>4</sub> treatment, and then declined again after 48 hr CCl<sub>4</sub> treatment. Maximal suppression of MUP appeared after 48 hr CCl<sub>4</sub> treatment.

### 3.11 Tissue distribution of differentially expressed genes

To investigate the tissue specificity of the four differentially expressed genes, tissue distribution study was conducted. For the cDNA fragment B4, eleven tissues (kidney, heart, spleen, brown fat, white fat, brain, lung, stomach, intestine, muscle and testis) from both *cyp2e1*<sup>+/+</sup> and *cyp2e1*<sup>-/-</sup> mice treated with CCl<sub>4</sub> or corn oil (control) were studied to investigate whether there was differentially expression in these tissues. For the other three cDNA fragments (C12, B13 and A5), due to the requirement of too much tissues, the eleven tissues only from *cyp2e1*<sup>+/+</sup> mice treated with corn oil (control) was studied to investigate the constitutive tissue distribution of these three genes.

Figures 3.52 and 3.53 revealed that cDNA fragment B4 (ADRP) was constitutively expressed in spleen, brown fat, white fat, lung, stomach and intestine. No constitutive expression was observed in kidney, heart, brain, muscle and testis. Besides liver, this gene was up-regulated in kidney, heart, spleen, lung and stomach in *cyp2e1*<sup>+/+</sup> but not *cyp2e1*<sup>-/-</sup> mice after 24 hr CCl<sub>4</sub> treatment.

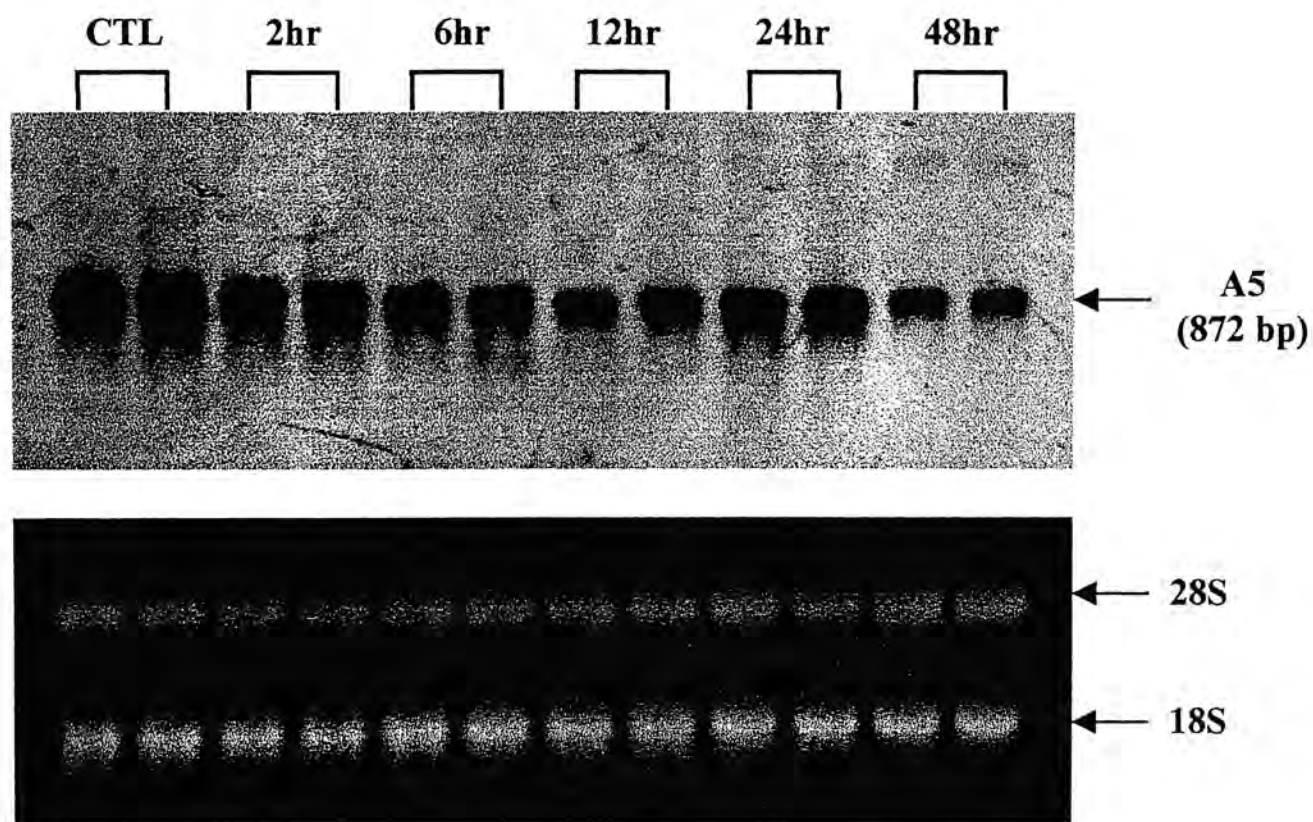


Figure 3.51. Time-dependent expression pattern of cDNA fragment A5 (major urinary protein). Fifteen micrograms of total liver RNAs from *cyp2e1*<sup>+/+</sup> mice treated with corn oil (CTL) or CCl<sub>4</sub> (1 ml/kg) for 2, 6, 12, 24 and 48 hr were separated on a 1.0% agarose-formaldehyde gel and transferred to nylon membrane. The membrane was then hybridized with the DIG-labeled cDNA fragment A5 and the signal was detected by colorimetric method with reagents NBT and BCIP. Ethidium bromide stained RNA gel was used for normalization.

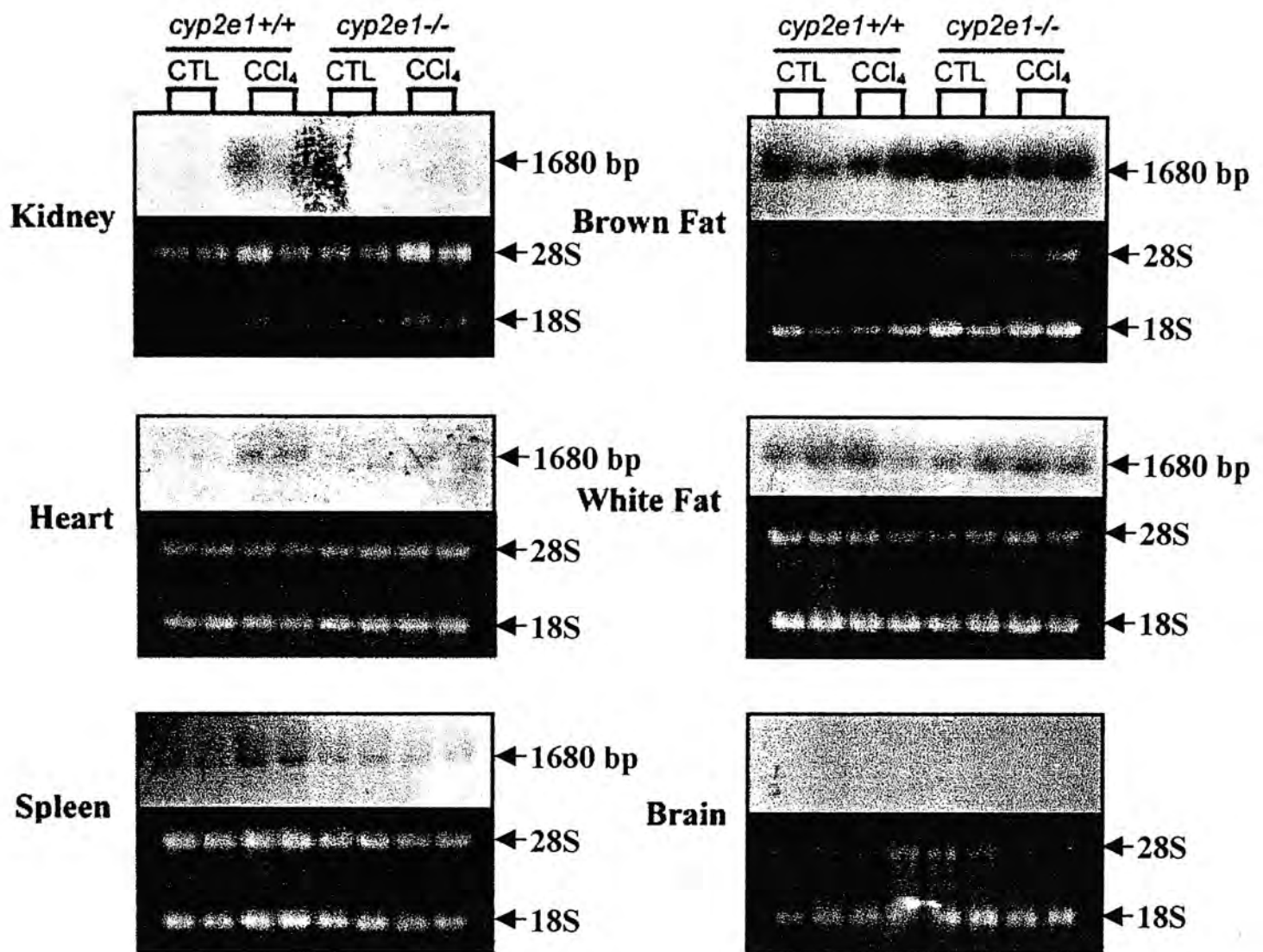


Figure 3.52. Expression pattern of cDNA fragment B4 (adipose differentiation-related protein) in kidney, heart, spleen, brown fat, white fat and brain (Part I). Fifteen micrograms of total RNAs from various tissues of *cyp2e1*<sup>+/+</sup> mice treated with corn oil (CTL) or CCl<sub>4</sub> (1 ml/kg) for 24 hr were separated on six 1.0% agarose-formaldehyde gels and transferred to nylon membranes respectively. The membranes were then hybridized with the DIG-labeled cDNA fragment B4 and the signals were detected by colorimetric method with reagents NBT and BCIP. Ethidium bromide stained RNA gels were used for normalization.



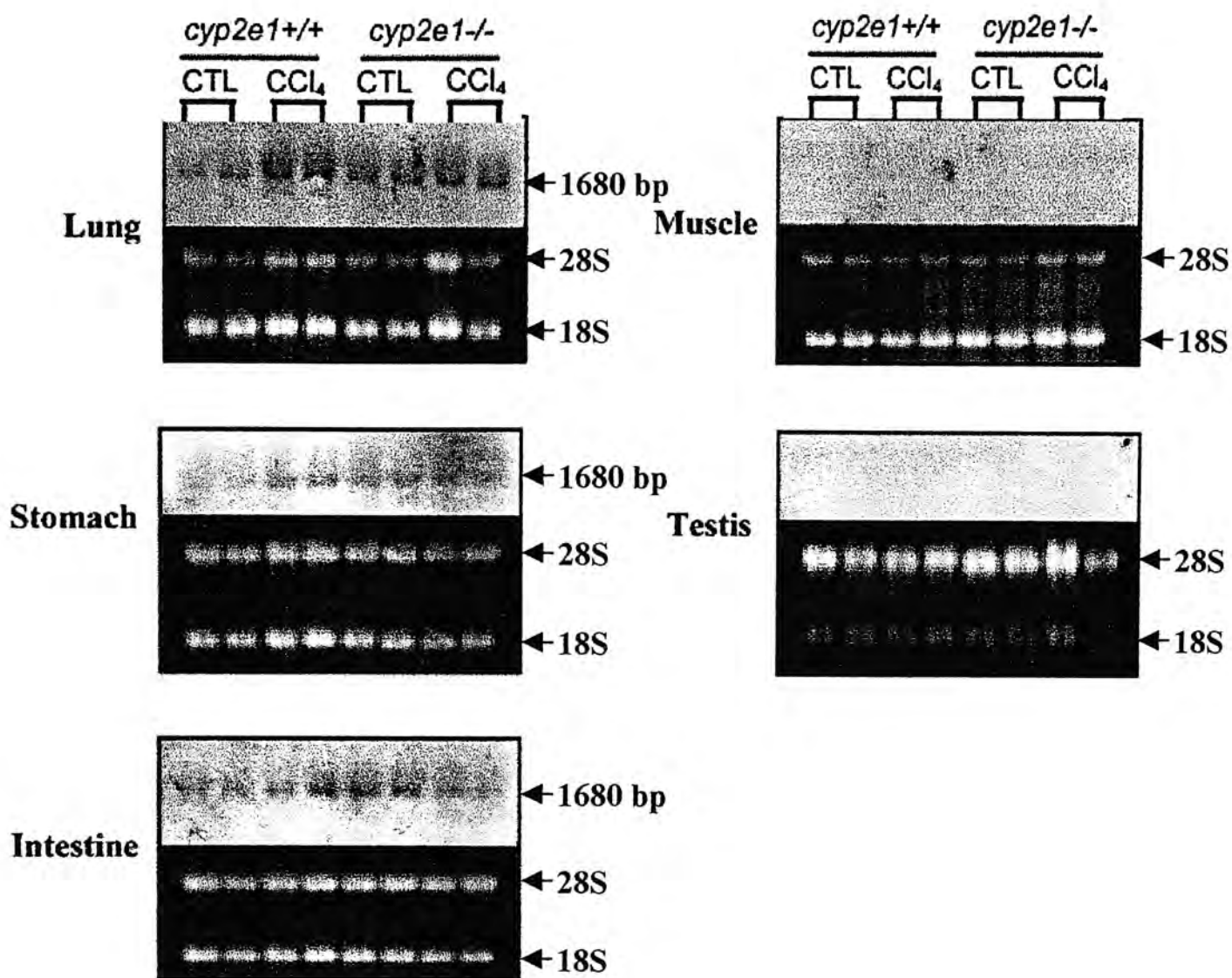


Figure 3.53. Expression pattern of cDNA fragment B4 (adipose differentiation-related protein) in lung, stomach, intestine, muscle and testis (Part II). Fifteen micrograms of total RNAs from various tissues of *cyp2e1*<sup>+/+</sup> mice treated with corn oil (CTL) or CCl<sub>4</sub> (1 ml/kg) for 24 hr were separated on five 1.0% agarose-formaldehyde gels and transferred to nylon membranes respectively. The membranes were then hybridized with the DIG-labeled cDNA fragment B4 and the signals were detected by colorimetric method with reagents NBT and BCIP. Ethidium bromide stained RNA gels were used for normalization.

The expression level of cDNA fragment C12 (RPL3) in various tissues was illustrated in Figure 3.54. There was constitutive expression of RPL3 in all eleven tissues examined including kidney, testis, brain, lung, heart, intestine, stomach, spleen, brown fat, white fat and muscle.

Figure 3.55 revealed that cDNA fragment B13 ( $\gamma$ -actin) was constitutively expressed in kidney, testis, brain, lung, intestine, stomach, spleen and white fat. Barely detectable expression of  $\gamma$ -actin was observed in heart, brown fat and muscle.

The expression level of cDNA fragment A5 (MUP) in various tissues was illustrated in Figure 3.56. No detectable expression of MUP was observed in all eleven tissues examined including kidney, testis, brain, lung, heart, intestine, stomach, spleen, brown fat, white fat and muscle.

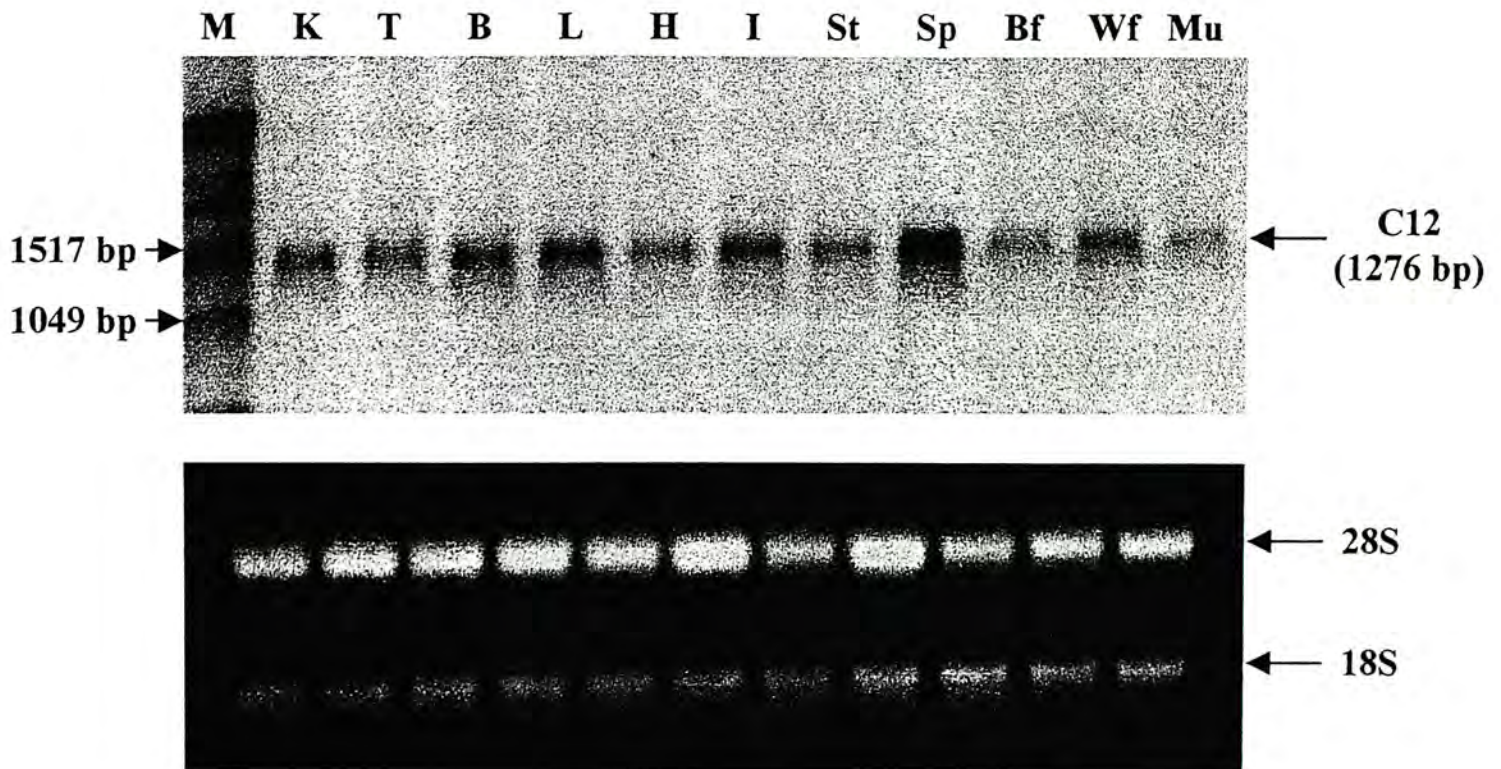


Figure 3.54. Expression pattern of cDNA fragment C12 (ribosomal protein L3) in kidney (K), testis (T), brain (B), lung (L), heart (H), intestine (I), stomach (St), spleen (Sp), brown fat (Bf), white fat (Wf) and muscle (Mu). Fifteen micrograms of total RNAs from various tissues of *cyp2e1*<sup>+/+</sup> mice treated with corn oil (CTL) for 24 hr were separated on a 1.0% agarose-formaldehyde gel and transferred to nylon membrane. The membrane was then hybridized with the DIG-labeled cDNA fragment C12 and the signal was detected by colorimetric method with reagents NBT and BCIP. Ethidium bromide stained RNA gel was used for normalization. M, DIG-labeled RNA molecular weight marker I.



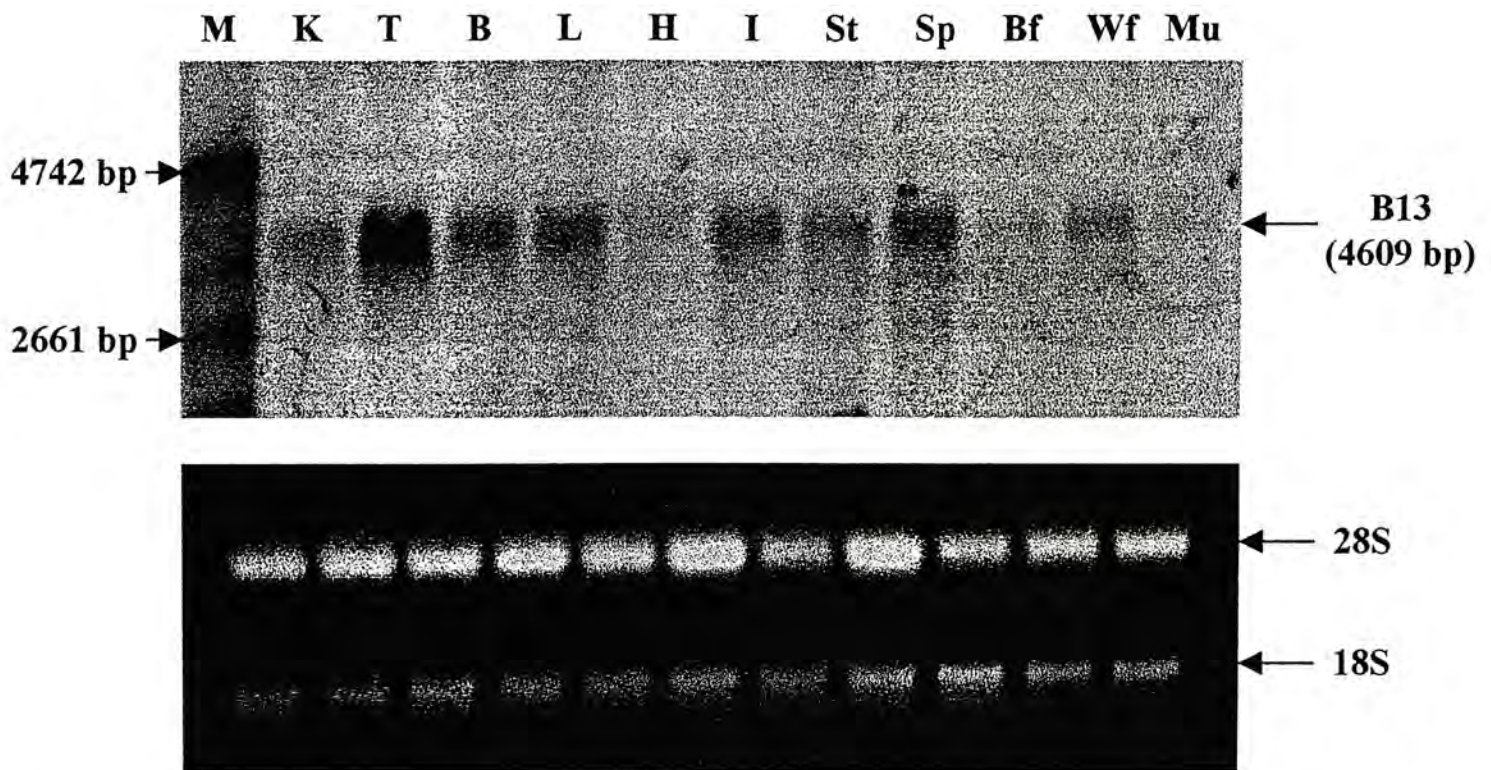


Figure 3.55. Expression pattern of cDNA fragment B13 (cytoplasmic gamma-actin) in kidney (K), testis (T), brain (B), lung (L), heart (H), intestine (I), stomach (St), spleen (Sp), brown fat (Bf), white fat (Wf) and muscle (Mu). Fifteen micrograms of total RNAs from various tissues of *cyp2e1*<sup>+/+</sup> mice treated with corn oil (CTL) for 24 hr were separated on a 1.0% agarose-formaldehyde gel and transferred to nylon membrane. The membrane was then hybridized with the DIG-labeled cDNA fragment B13 and the signal was detected by colorimetric method with reagents NBT and BCIP. Ethidium bromide stained RNA gel was used for normalization. M, DIG-labeled RNA molecular weight marker I.



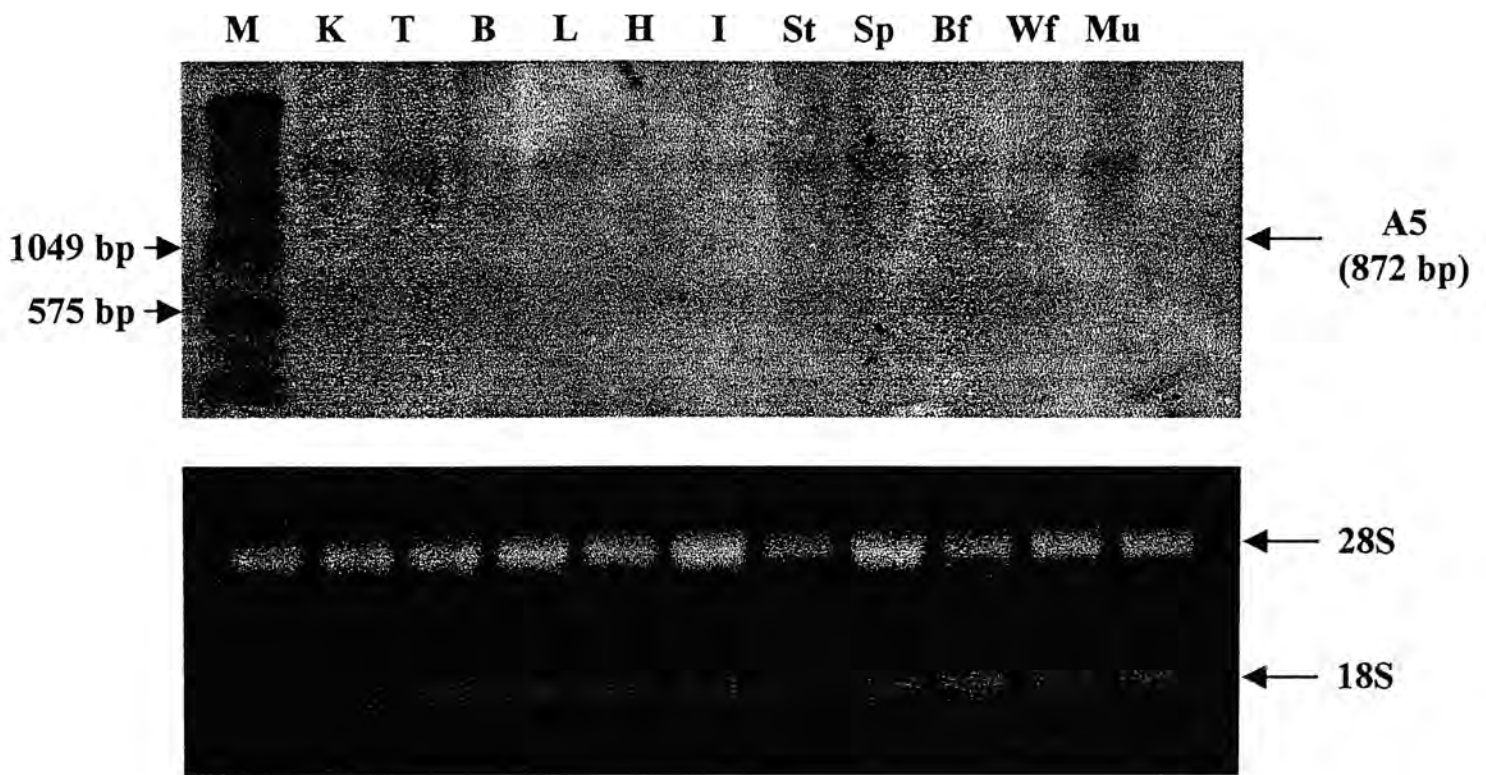


Figure 3.56. Expression pattern of cDNA fragment A5 (major urinary protein) in kidney (K), testis (T), brain (B), lung (L), heart (H), intestine (I), stomach (St), spleen (Sp), brown fat (Bf), white fat (Wf) and muscle (Mu). Fifteen micrograms of total RNAs from various tissues of *cyp2e1*<sup>+/+</sup> mice treated with corn oil (CTL) for 24 hr were separated on a 1.0% agarose-formaldehyde gel and transferred to nylon membrane. The membrane was then hybridized with the DIG-labeled cDNA fragment A5 and the signal was detected by colorimetric method with reagents NBT and BCIP. Ethidium bromide stained RNA gel was used for normalization. M, DIG-labeled RNA molecular weight marker I.

## CHAPTER 4: DISCUSSIONS

The hepatotoxicity of  $\text{CCl}_4$  has been known for a very long time (Hall and Schillinger, 1923). Experimental data from rodents demonstrate that  $\text{CCl}_4$  causes various liver injury, including necrosis, fatty infiltration and decreased activities of microsomal enzymes that catalyse the oxidation of drugs (Chaplin and Mannering, 1970; Tomenson *et al.*, 1995; Padma and Setty, 1999). In the past decades, many researchers investigated the biochemical mechanism of  $\text{CCl}_4$ -induced hepatotoxicity and by now it has already been known that at the beginning of  $\text{CCl}_4$  metabolism,  $\text{CCl}_4$  can be converted to  $\text{CCl}_3\cdot$  by an enzyme system in the smooth endoplasmic reticulum (ER) of liver cells, then  $\text{CCl}_3\cdot$  reacts with the molecular oxygen and destroys the structure of ER membrane. This lipid peroxidation decreases the protein synthesis and lipoprotein secretion, increases the triglyceride content of liver cells and causes fatty liver and finally liver injury (Holman, 1954; Slater, 1982; Huether and McCance, 1996).

Previous studies showed that P450s, an enzyme system in the ER, is mainly responsible for the bioactivation of  $\text{CCl}_4$  and the resulting liver injury (Recknagel and Glende, 1973). Recent studies using CYP2E1-null mice confirmed that cytochrome P450 2E1 (CYP2E1) is the primary P450 isoform involved in  $\text{CCl}_4$ -induced liver injury (Wong *et al.*, 1998). Although it is known that CYP2E1 is involved in  $\text{CCl}_4$ -induced liver injury, the exact molecular mechanism of this process is still not fully understood.

The development of fluorescent differential display (FDD) technique (Liang and Pardee, 1992) and the creation of CYP2E1-null mouse model in 1996 (Lee *et al.*, 1996) provide powerful tools to investigate the mechanism of  $\text{CCl}_4$ -induced hepatotoxicity at

molecular level. FDD permits the detection of differentially expressed genes in a variety of biological processes (Liang and Pardee, 1992). Identification and characterization of differentially expressed genes are the major first step toward the elucidation of molecular mechanisms underlying the CCl<sub>4</sub>-induced hepatotoxicity. The CYP2E1-null mice that lack CYP2E1 expression can help to investigate the involvement of CYP2E1 in various biological processes such as CCl<sub>4</sub>-induced liver injury by comparison of the gene expression profiles in the CCl<sub>4</sub>-resistant CYP2E1-null mice with their corresponding CCl<sub>4</sub>-sensitive wild-type controls. Identification and characterization of the spectrum of CYP2E1-dependent genes involved in CCl<sub>4</sub>-induced hepatotoxicity are the first step to gain insight into the molecular mechanism of this process.

#### **4.1 Liver morphology and serum ALT and AST activities**

It was known for a long time that the CCl<sub>4</sub>-induced liver injury was in a time-dependent manner. In 1985, Smejkalova *et al.* investigated the biochemical and histological changes following CCl<sub>4</sub>-induced liver injury by assessing the ALT, AST, alkaline phosphatase and GMT serum activities after 6, 12, 24, 48 and 72 hr exposure to CCl<sub>4</sub>. They found that the levels of these transaminases increased with the treatment time and reached a maximum after 24 hr CCl<sub>4</sub> treatment. The levels then slowly declined after 48 hr, and were identical with the controls after 72 hr CCl<sub>4</sub> treatment (Smejkalova *et al.*, 1985). By using ALT and SDH as indicators of hepatotoxicity, Steup *et al.* (1993) demonstrated that CCl<sub>4</sub>-induced liver injury was most apparent at 24 hr. At 48 hr after CCl<sub>4</sub> treatment, livers showed a distinctive and uniform pattern of injury with regeneration features predominating over necrosis (Steup *et al.*, 1993). Morigasaki *et al.* (2000)

reported that based on the combination of changes in stability of albumin mRNA and the activity of transcription of its gene, the entire course of CCl<sub>4</sub>-induced liver injury can be classified into three stages, the first stage for aggravation of injury until 9 hr, the second from 9 to 24 hr (reach maximal injury near 24 hr), and the third for repair of injury or regeneration of liver after 48 hr (Morigasaki *et. al.*, 2000).

In the present study, it was found that livers of CCl<sub>4</sub>-treated *cyp2e1*<sup>+/+</sup> mice for 12, 24 and 48 hr were more pale-orange than that observed in CCl<sub>4</sub>-treated *cyp2e1*<sup>-/-</sup> mice and the controls. No such color change was observed in livers of CCl<sub>4</sub>-treated *cyp2e1*<sup>+/+</sup> mice for 2 and 6 hr. In addition, more dramatic color change was observed in livers from 24 hr CCl<sub>4</sub> treatment in comparison to those from 12 and 48 hr after CCl<sub>4</sub> treatment. Using ALT and AST as two indicators of hepatotoxicity, the liver injury was confirmed in a time-dependent manner. It was observed that both ALT and AST activities increased from 6 to 48 hr following CCl<sub>4</sub> treatment and reached a maximum at 24 hr, and then declined at 48 hr after CCl<sub>4</sub> treatment. These results suggested that CCl<sub>4</sub>-induced liver injury reached the maximum at 24 hr and the liver recovery occurred at 48 hr after CCl<sub>4</sub> treatment.

In summary, the present data from liver morphology and ALT and AST activities suggested that CCl<sub>4</sub>-induced liver injury was in a time-dependent manner. The maximum liver injury occurred at 24 hr and liver recovery started at 48 hr after CCl<sub>4</sub> treatment. These data are in good agreement with those previous studies.

#### **4.2 Identification of CYP2E1-dependent genes involved in CCl<sub>4</sub>-induced hepatotoxicity**



In the present study, livers from mice after 24 hr CCl<sub>4</sub> treatment were chosen to conduct the FDD experiments since the anticipated maximum liver injury took place at that time point after CCl<sub>4</sub> treatment as reported by many investigators (Letteron *et. al.*, 1990; Hong and Park, 1997; Wong *et. al.*, 1998). After comparing the gene expression patterns in livers of *cyp2e1*<sup>+/+</sup> and *cyp2e1*<sup>-/-</sup> mice after 24 hr CCl<sub>4</sub> (1 ml/kg) treatment with corn oil (control), thirty-four cDNA fragments which were differentially expressed (either up or down) in *cyp2e1*<sup>+/+</sup> but not *cyp2e1*<sup>-/-</sup> mice were obtained from three FDD gels. Thirty of them were reamplified and subcloned successfully. Among these thirty subcloned cDNA fragments, twenty-eight (93%) of them were successfully sequenced. Twenty-five cDNA fragments (83%) were identified as known genes including *Mus musculus* hemopexin, *Mus musculus* t-complex protein 1 (TCP1), mouse major urinary protein (MUP), *Mus musculus* guanine nucleotide binding protein, beta-2, mouse adipose differentiation-related protein (ADRP), his-tagged-multidrug resistance glycoprotein, rat GAP-associated protein (P190), *Mus musculus* integrin linked kinase (ILK), ribosomal protein S10, fatty acid binding protein (FABPI), intestine, *Mus musculus* clusterin (CLU), *Rattus norvegicus* phospholipase C, gamma 1 (PLCG1), mouse cytoplasmic gamma-actin ( $\gamma$ -actin), *Rattus norvegicus* mRNA for acyl-CoA synthetase 5 (ACS5), *Mus musculus* cullin 1 (CUL1), mouse DNA for virus-like (VL30) retrotransposon BVL-1, *Mus musculus* COP9 subunit 3 (COPS3), mouse fibronectin (FN), *Mus musculus* ribosomal protein L3 (RPL3), mouse major histocompatibility complex region and *Mus musculus* PK-120 precursor (ITIH-4). Three cDNA fragments (10%) showed remarkable homology to mouse ESTs. It is necessary to perform cDNA library screening or 5' or 3' RACE to obtain the full-length cDNA of these three cDNA fragments.

In the present study, livers from mice after 24 hr CCl<sub>4</sub> treatment were chosen to conduct the FDD experiments since the anticipated maximum liver injury took place at that time point after CCl<sub>4</sub> treatment as reported by many investigators (Letteron *et. al.*, 1990; Hong and Park, 1997; Wong *et. al.*, 1998). After comparing the gene expression patterns in livers of *cyp2e1*<sup>+/+</sup> and *cyp2e1*<sup>-/-</sup> mice after 24 hr CCl<sub>4</sub> (1 ml/kg) treatment with corn oil (control), thirty-four cDNA fragments which were differentially expressed (either up or down) in *cyp2e1*<sup>+/+</sup> but not *cyp2e1*<sup>-/-</sup> mice were obtained from three FDD gels. Thirty of them were reamplified and subcloned successfully. Among these thirty subcloned cDNA fragments, twenty-eight (93%) of them were successfully sequenced. Twenty-five cDNA fragments (83%) were identified as known genes including *Mus musculus* hemopexin, *Mus musculus* t-complex protein 1 (TCP1), mouse major urinary protein (MUP), *Mus musculus* guanine nucleotide binding protein, beta-2, mouse adipose differentiation-related protein (ADRP), his-tagged-multidrug resistance glycoprotein, rat GAP-associated protein (P190), *Mus musculus* integrin linked kinase (ILK), ribosomal protein S10, fatty acid binding protein (FABPI), intestine, *Mus musculus* clusterin (CLU), *Rattus norvegicus* phospholipase C, gamma 1 (PLCG1), mouse cytoplasmic gamma-actin ( $\gamma$ -actin), *Rattus norvegicus* mRNA for acyl-CoA synthetase 5 (ACS5), *Mus musculus* cullin 1 (CUL1), mouse DNA for virus-like (VL30) retrotransposon BVL-1, *Mus musculus* COP9 subunit 3 (COPS3), mouse fibronectin (FN), *Mus musculus* ribosomal protein L3 (RPL3), mouse major histocompatibility complex region and *Mus musculus* PK-120 precursor (ITIH-4). Three cDNA fragments (10%) showed remarkable homology to mouse ESTs. It is necessary to perform cDNA library screening or 5' or 3' RACE to obtain the full-length cDNA of these three cDNA fragments.

The FDD patterns of the four identified CYP2E1-dependent genes including adipose differentiation-related protein (B4), ribosomal protein L3 (C12), cytoplasmic gamma-actin (B13) and major urinary protein (A5) were confirmed by Northern blot analysis. The data here clearly demonstrated that these four identified genes are all CYP2E1-dependent involved in CCl<sub>4</sub>-induced liver injury.

Although thirty-four differentially expressed cDNA fragments were characterized in the present study, there were some other differentially expressed cDNA fragments needed to be reamplified, subcloned, sequenced and confirmed by Northern blot analysis in the future study. Since only three pairs of AP and ARP primers were selected to perform the FDD RT-PCR analysis in the present study, other AP and ARP primer combinations should be used to identify the spectrum of CYP2E1-dependent genes involved in CCl<sub>4</sub>-induced hepatotoxicity.

### **4.3 Functional roles of the identified differentially expressed genes**

#### **4.3.1 Fragment B4**

cDNA fragment B4 was identified as adipose differentiation-related protein (ADRP). Both the FDD expression pattern and Northern blot analysis showed that ADRP was up-regulated in *cyp2e1*<sup>+/+</sup> mice but not *cyp2e1*<sup>-/-</sup> mice after CCl<sub>4</sub> treatment indicating that ADRP was a CYP2E1-dependent gene involved in CCl<sub>4</sub>-induced liver injury.

Adipose differentiation-related protein (ADRP) is a 50-kDa membrane-associated protein cloned from a mouse 1246 adipocyte cDNA and rapidly induced during adipocyte differentiation (Jiang and Serrero, 1992). Recent experiments demonstrated that ADRP is a fatty acid binding protein that specifically facilitates the uptake of long-chain fatty acids

(Gao *et. al.*, 2000). Besides expression in adipocytes, ADRP is also found in livers of rats treated with etomoxir, an inhibitor of carnithine palmitoyltransferase (Steiner *et. al.*, 1996), which may induce lipid accumulation in liver. Since fatty liver can be induced by CCl<sub>4</sub>, and lipid accumulation might be involved in the generation of fatty liver, ADRP might have the similar function role in CCl<sub>4</sub>-induced liver injury as in that of etomoxir-induced lipid accumulation in liver.

#### 4.3.2 Fragment C12

cDNA fragment C12 was identified as ribosomal protein L3 (RPL3). Both the FDD expression pattern and Northern blot analysis found that RPL3 was up-regulated in *cyp2e1*<sup>+/+</sup> mice while only slight induction was observed in *cyp2e1*<sup>-/-</sup> mice after CCl<sub>4</sub> treatment indicating that RPL3 was a CYP2E1-dependent gene involved in CCl<sub>4</sub>-induced liver injury.

Ribosomal protein L3 (RPL3) is a component of the 60S ribosome subunit. The ubiquitous expression of RPL3 message is consistent with its role in general protein translation (Chan *et. al.*, 1998). RPL3 has 403 amino acids and has a molecular weight of 46,106 and the mRNA for the protein is about 1,400 nucleotides in length. Rat L3 is homologous to ribosome proteins from other eukaryotes and to proteins from eubacterial, archaebacterial, and chloroplast ribosomes (Kuвано and Wool, 1992). Previous study indicated that RPL3 gene, of which the expression is regulated along with the development or cell division cycle, is so ubiquitous that all eukaryotic organisms may have such gene for ribosomal protein. This gene is essential for the ribosome synthesis which is closely correlated with protein synthesis, metabolic activity and cell division (Jeong *et. al.*, 2001).



Since the data in the present study showed that CCl<sub>4</sub> treatment resulted in the up-regulation of many gene expressions (i.e. increase in gene transcription), the up-regulation of RPL3 in CCl<sub>4</sub>-induced liver injury seemed to support the idea that RPL3 was required for the increased protein translations from those up-regulated genes during the CCl<sub>4</sub>-induced liver injury process.

#### 4.3.3 Fragment B13

cDNA fragment B13 was identified as cytoplasmic gamma-actin ( $\gamma$ -actin). Both the FDD expression pattern and Northern blot analysis showed that  $\gamma$ -actin was up-regulated in *cyp2e1*<sup>+/+</sup> but not *cyp2e1*<sup>-/-</sup> mice after CCl<sub>4</sub> treatment indicating that  $\gamma$ -actin was a CYP2E1-dependent gene involved in CCl<sub>4</sub>-induced liver injury.

$\gamma$ -actin is an isoform of actin families which are ubiquitous proteins in eukaryotic cells and play a crucial role in muscle contraction, cell motility, cytoskeletal structure, cell division, intracellular transport, and cell differentiation (Herman, 1993).  $\gamma$ -actin is expressed by a greater degree in actively replicating smooth muscle cell versus stationary cells (Sundy, 1995). The upregulation of the  $\gamma$ -actin gene is consistent with the switching of actin isoforms found *in vitro* (Thakker-Varia *et. al.*, 1999). Previous research work suggested that there were multiple regulatory mechanisms of cytoskeletal actin genes and were consistent with the argument that  $\gamma$ -actin might have functional diversity in mammalian cells (Tokunaga, 1988). Early studies demonstrated that alpha-actin mRNA expression increased following CCl<sub>4</sub> treatment in cultured stellate cells (Ikeda *et. al.*, 1998) and in skeletal muscle (Kim *et. al.*, 2000) while beta-actin mRNA expression increased after CCl<sub>4</sub> treatment in liver (Armendariz-Borunda *et. al.*, 1990). Besides alpha- and beta-

actins, the present data showed that  $\gamma$ -actin mRNA expression also increased after CCl<sub>4</sub> treatment in liver suggesting that the actin families might play significant roles in CCl<sub>4</sub>-induced liver injury.

#### 4.3.4 Fragment A5

cDNA fragment A5 was identified as major urinary protein (MUP). Both the FDD expression pattern and Northern blot analysis found that MUP was down-regulated in *cyp2e1*<sup>+/+</sup> but not *cyp2e1*<sup>-/-</sup> mice after CCl<sub>4</sub> treatment indicating that MUP was a CYP2E1-dependent gene involved in CCl<sub>4</sub>-induced liver injury.

The mouse MUP is a family of at least three major proteins which are synthesized in the liver of all strains of mice. The relative levels of synthesis of these proteins with respect to each other in the presence of testosterone are regulated by the MUP-a locus located on chromosome 4 (Krauter *et. al.*, 1982). The multigene family coding for the mouse MUP consists of approximately 35 genes. Most of these are members of two different groups, Group 1 and Group 2. Short mRNA is approximately 750 bp containing six exons and is the main product of the Group 2 genes, and long mRNA is approximately 880 bp containing seven exons and is the main product of the Group 1 genes (Clark *et. al.*, 1984). It was reported that the immunocytochemistry analysis using a goat antibody to MUP on histologic liver sections containing diethylnitrosamine-induced liver nodules have showed that the decrease in MUP levels occurred in microscopic nodules, which revealed that MUP decrease represents an early event in the development of mouse liver tumors, and it may be used as a tumor marker in mouse hepatocarcinogenesis (Dragani *et. al.*, 1989). Similarly, the observed down-regulation of MUP gene expression in livers of

CCl<sub>4</sub>-treated *cyp2e1*<sup>+/+</sup> but not *cyp2e1*<sup>-/-</sup> mice in the present study seemed to suggest that the decrease of MUP expression was related to the cause of CCl<sub>4</sub>-induced liver injury and MUP might be used as an early marker in mouse liver injury.

In summary, four CCl<sub>4</sub>-responsive and CYP2E1-dependent genes (adipose differentiation-related protein, ribosomal protein L3, cytoplasmic gamma-actin and major urinary protein) were identified in the present study. These four genes might play some roles in the etiology of CCl<sub>4</sub>-induced liver injury.

#### **4.4 Temporal expression of differentially expressed genes**

Since the CCl<sub>4</sub>-induced liver injury was in a time-dependent manner (Smejkalova *et. al.*, 1985; Steup *et. al.*, 1993; Morigasaki *et. al.*, 2000), the temporal expression of the four identified CYP2E1-dependent genes involved in CCl<sub>4</sub>-induced hepatotoxicity was investigated to determine whether the gene expression patterns of these genes parallel the severity of CCl<sub>4</sub>-induced liver injury.

##### **4.4.1 Fragment B4**

Previous investigation provides evidence that ADRP mRNA and protein expression in preadipocytes is stimulated by fatty acids in a time- and dose-dependent fashion/manner (Brasaemle *et. al.*, 1997). Since the elevation of fatty acids were observed to be involved in CCl<sub>4</sub>-induced liver injury (Szlanka *et. al.*, 1975), the induction of ADRP by CCl<sub>4</sub> may be also time-dependent. This speculation was verified in the present study.

At present, it was found that induction of ADRP gene expression by CCl<sub>4</sub> in *cyp2e1*<sup>+/+</sup> mice was in a time-dependent manner. ADRP gene expression increased as the

CCl<sub>4</sub> treatment time increased from 2 to 24 hr and reached a maximum at 24 hr, then declined dramatically at 48 hr after CCl<sub>4</sub> treatment. The time-dependent manners of ADRP gene expression and ALT and AST activities following CCl<sub>4</sub> treatment are so similar that ADRP might serve as a molecular marker for the severity of CCl<sub>4</sub>-induced liver injury.

#### 4.4.2 Fragment C12

As mentioned in 5.3.2, RPL3 plays a role in general protein translation (Chan *et. al.*, 1998) and is essential for the ribosome synthesis which is closely correlated with protein synthesis, metabolic activity and cell division (Jeong *et. al.*, 2001). Since protein synthesis and metabolic activity and cell division are common events occur in liver all the time, during CCl<sub>4</sub>-induced liver injury, these activities might have relationships with the CCl<sub>4</sub> treatment time. Therefore, the induction of RPL3 gene expression might be also related to the CCl<sub>4</sub> treatment time.

In the present study, it was found that the induction of RPL3 gene expression by CCl<sub>4</sub> in *cyp2e1*<sup>+/+</sup> mice was in a time-dependent manner. The expression of RPL3 did not change at 2 and 6 hr, then increased from 12 to 24 hr and reached a maximum at 24 hr, and declined to normal level at 48 hr after CCl<sub>4</sub> treatment. It seemed that the induction of RPL3 gene expression only appeared in severe CCl<sub>4</sub>-liver injury (12 to 24 hr) suggesting that high demand of RPL3 was required for protein translations during liver injury.

#### 4.4.3 Fragment B13

Actins are a group of general cellular and housekeeping genes (Panduro *et. al.*, 1986). Previous research showed there was an increased expression of actin-like protein in



regenerating hepatocytes and granulation tissue fibroblasts in CCl<sub>4</sub>-induced liver injury (Toh *et. al.*, 1977). Early studies showed that the induction of alpha-actin by CCl<sub>4</sub> treatment in skeletal muscle was in a time-dependent manner (Kim *et. al.*, 2000) suggesting that the induction of  $\gamma$ -actin may be also time-dependent.

In the present study, it was found that the induction of  $\gamma$ -actin gene expression by CCl<sub>4</sub> in *cyp2e1*<sup>+/+</sup> mice took place at very early stage following CCl<sub>4</sub> treatment. The maximum induction of  $\gamma$ -actin appeared at 2 and 6 hr, and then declined gradually from 12 to 48 hr after CCl<sub>4</sub> treatment. Since the induction of  $\gamma$ -actin occurred and reached to the maximum very early (2 to 6 hr) after CCl<sub>4</sub> treatment while the CCl<sub>4</sub>-induced liver injury just began at that time, it seemed that  $\gamma$ -actin might play a role in the beginning of CCl<sub>4</sub>-induced liver injury.

#### 4.4.4 Fragment A5

Former studies demonstrated that MUP was involved in mouse hepatocellular carcinomas and tumors (Dragani *et. al.*, 1989; Yamada *et. al.*, 1999). Therefore, the time course study of MUP may enable us to estimate the possibility to use MUP as the cancer marker at early stage.

The present results showed that the suppression of MUP gene expression by CCl<sub>4</sub> in *cyp2e1*<sup>+/+</sup> mice was in a time-dependent manner. The expression of MUP decreased as the CCl<sub>4</sub> treatment time increased from 2 to 12 hr and reached a minimum at 48 hr after CCl<sub>4</sub> treatment. During the suppression, it was interesting to observe that the expression of MUP was a little higher at 24 hr than that at 12 hr after CCl<sub>4</sub> treatment. Although the exact reason for this unanticipated result was unknown, it seemed that there might be some new

factors appeared and affected the MUP gene expression from 12 to 24 hr after CCl<sub>4</sub> treatment. Further studies are needed to find the truth beyond this phenomenon.

## 4.5 Tissue distribution of differentially expressed genes

### 4.5.1 Fragment B4

Previous research demonstrated that ADRP mRNA is expressed in various tissues and cultures cell lines (Brasaemle *et. al.*, 1997). High level of expression of ADRP mRNA appeared in adipose tissue (Jiang and Serrero, 1992); moderate levels were observed in lung, liver, and testis; and reduced levels were observed in spleen, brain, heart, skeletal muscle, and kidney, in order of decreasing abundance (Brasaemle *et. al.*, 1997). In the present study, the tissue distribution of ADRP was slightly different from previous papers. Constitutive expression of ADRP was found in liver, lung, intestine, stomach, white fat and brown fat in *cyp2e1*<sup>+/+</sup> mice (wild-type). It is interesting to note that ADRP was differentially expressed in kidney and heart besides liver in *cyp2e1*<sup>+/+</sup> but not *cyp2e1*<sup>-/-</sup> mice. Since no constitutive expression of ADRP was found in kidney and heart, the up-regulation of ADRP in CCl<sub>4</sub>-treated *cyp2e1*<sup>+/+</sup> mice suggested that this gene is related to the CCl<sub>4</sub>-induced injury in these two tissues.

### 4.5.2 Fragment C12

Previous studies showed that RPL3 was expressed in hypothalamus and brown adipose tissue of mice and bats (Allan *et. al.*, 2000). For other tissues, no reports could be found at this moment. However, since RPL3 is generally involved in RNA and protein synthesis, metabolic activity and cell division (Jeong *et. al.*, 2001), it may be expressed in

various tissues. The present data showed that RPL3 was expressed in all of the eleven tissues tested including kidney, testis, brain, lung, heart, intestine, stomach, spleen, brown fat, white fat and muscle suggesting that RPL3 might have functions in various organs. The wide distribution of RPL3 in a variety of tissues may be related to its role in general protein translation and synthesis processes.

#### 4.5.3 Fragment B13

Early studies demonstrated that  $\gamma$ -actin was expressed in various mouse tissues and cell types (Tokunaga, 1988). The present data showed that in the eleven tissues of wild-type mice (*cyp2e1*<sup>+/+</sup>),  $\gamma$ -actin was expressed in a tissue-specific manner in kidney, testis, brain, lung, intestine, stomach, spleen and white fat, which was in agreement with the previous studies. Surprisingly, barely detectable expression was observed in heart, brown fat and muscle. This might be due to the low abundance of this gene presented in these three tissues.

#### 4.5.4 Fragment A5

Early studies showed that MUP mRNAs are present in several secretory tissues in addition to the liver, in which they were originally identified. The regulation of MUP is in a tissue-specific manner (Shahan and Derman, 1984). The differential expression of MUP genes in six tissues, mammary, parotid, sublingual, lachrymal, submaxillary glands and liver was found. The tissue-specific synthesis of MUP mRNAs could be through two major mechanisms: the expression, in different tissues, of different members of the family and the expression of a single gene at various levels in different tissues (Shahan *et. al.*, 1987). The

present data showed that in the eleven tissues tested including kidney, testis, brain, lung, heart, intestine, stomach, spleen, brown fat, white fat and muscle, no detectable expression of MUP was observed in all these tissues. To make sure no mistake was made, the experiments were repeated and the same results were obtained suggesting that MUP might be not expressed in all these tissues.

#### 4.5.5 Roles of the identified genes involved in CCl<sub>4</sub>-induced hepatotoxicity

To further study the functional roles of the identified genes, some experimental strategies could be taken. These include overexpression of the identified genes using sense or inducible sense expression vectors (Augustine, 1997), inhibition of the expression of the identified genes using antisense technology (Alama *et. al.*, 1997) and generation of transgenic mice with target disruption of specific genes.

#### 4.6 Normalization of Northern blot analysis

In the present study, ethidium bromide stained total RNA was used for normalization in Northern blot analysis. The house-keeping genes such as GAPDH,  $\beta$ -actin or albumin was not used for normalization in our experiments because the expression of these genes can be induced by CCl<sub>4</sub> (Goldsworthy *et. al.*, 1993). Accurate quantification of mRNA levels required the normalization of the gene of interest with transcriptional level that do not vary through the cell cycle or with a particular treatment. Therefore, ethidium bromide stained total RNA was used for normalization in this study.

#### 4.7 Limitations of FDD technique to identify differentially expressed genes



The limitation of FDD technique is the generation of false positives which may be due to the contamination of trace amounts of genomic DNA, errors in band excision, and the subcloning of wrong cDNA fragments having same size as target one. Therefore, Northern blot analysis should be carried out to confirm the FDD patterns of identified cDNA fragments. In the present study, Northern blot analyses were performed on sixteen cDNA fragments and the FDD patterns of four cDNA fragments were confirmed by Northern blots. The expression patterns of five cDNA fragments on the Northern blots did not match with their corresponding differential expression patterns on the FDD gels. No expression signals could be detected in Northern blots of seven cDNA fragments. This might be due to the inadequate amounts of probes used for hybridization during Northern blot analysis or low abundance of genes.

#### **4.8 Future studies**

##### **4.8.1 Investigation of the differential expression patterns of the identified genes in acetaminophen-induced liver injury**

Acetaminophen (APAP) is an active ingredient in panadol/tylenol and is widely used to treat headache and fever. APAP could lead to liver necrosis in both human and rodents under the conditions of overdose. It has been demonstrated that CYP2E1 mediates the APAP-induced liver injury (Lee *et. al.*, 1996). Since both CCl<sub>4</sub>- and APAP-induced liver injury are mediated by CYP2E1, further studies will be carried out to determine if the same differential expression patterns of the four identified genes will be obtained in APAP-induced liver injury.

#### 4.8.2 Dot blot analysis

Due to the great possibility of missing positives during the long course of reamplification, subcloning and Northern blot analysis, dot-blot techniques are preferred to be used to overcome this shortcoming and speed up the experimental progress in the future. Dot-blot methods allow the rapid analysis of numerous samples for the sequence of interest and is less time consuming than the gel electrophoresis methods (Sambrook *et. al.*, 1989). In the further study of this project, “dots” of excised FDD cDNA fragments will be made onto a filter using a manifold and the filter will be then hybridized with the DIG-labeled RNA probes made directly from the RNA samples.

#### 4.8.3 DNA microarray

DNA microarray technique, another powerful tool for gene expression studies, was developed during the past several years. Microarray technology allows us to look at many genes at once and determine which are expressed in the animals with a particular treatment (DeRisi *et. al.*, 1997; Lashkari *et. al.*, 1997). To analyze differential gene expression in different treatment groups, probes are made from the cDNA samples from each treatment group with fluorescent labeling. Then the probes, each labeled with a different fluorescent dye, are simultaneously hybridized to a microarray. The gene expression differences will be obtained after signal detection. In the future, DNA microarray can speed up the investigation of the gene expression changes involved in CCl<sub>4</sub>-induced liver injury.

## REFERENCES

- Abraham, P., Wilfred, G., and Cathrine, S. P. (1999) Oxidative damage to the lipids and proteins of the lungs, testis and kidney of rats during carbon tetrachloride intoxication. *Clin. Chim. Acta*, **289**, 177-179.
- Adams, M. D., Soares, M. B., Kerlavage, A. R., Fields, C., and Venter, J. C. (1993) Rapid cDNA sequencing (expressed sequence tags) from a directionally cloned human infant brain cDNA library. *Nature*, **4**, 373-380.
- Agency for Toxic Substances and Disease Registry (1994) Toxicological Profile for Carbon tetrachloride. United States Public Health Service.
- Alama, A., Barbieri, F., Cagnoli, M., and Schettini, G. (1997) Antisense oligonucleotides as therapeutic agents. *Pharmacol. Res.*, **36**, 171-178.
- Allan, M. F., Nielsen, M. K., and Pomp, D. (2000) Gene expression in hypothalamus and brown adipose tissue of mice divergently selected for heat loss. *Physiol. Genomics*, **3**, 149-156.
- Anders, M. W. (1988) Bioactivation mechanisms and hepatocellular damage. In: *The liver: biology and pathobiology*, 389-400, Raven Press, New York.
- Armendariz-Borunda, J., Seyer, J. M., Kang, A. H., and Raghov, R. (1990) Regulation of TGF beta gene expression in rat liver intoxicated with carbon tetrachloride. *FASEB J.*, **4**, 215-221.
- Augustine, K. (1997) Antisense approaches for investigating mechanisms of abnormal development. *Mutation Res.*, **396**, 175-193.
- Bauer, D., Müller, H., Reich, J., Riedel, H., Ahrenkiel, V., Warthoe, P., and Strauss, M. (1993) Identification of differentially expressed mRNA species by an improved display technique (DDRT-PCR). *Nucleic Acids Res.*, **21**, 4272-4280.
- Bergmeyer, H. U., Scheibe, P., Wahlefeld, A. W. (1978) Optimization of methods for aspartate aminotransferase and alanine aminotransferase. *Clin. Chem.*, **24**, 58.
- Brady, J. F., Xiao, F., Wang, M. H., Li, Y., Ning, S. M., Gapac, J. M., and Yang, C. S. (1991) Effects of disulfiram on hepatic P450IIE1, other microsomal enzymes, and hepatotoxicity in rats. *Toxicol. Appl. Pharmacol.*, **108**, 366-373.
- Brasaemle, D. L., Barber, T., Wolins, N. E., Serrero, G., Blanchette-Mackie, E. J., and Londos, C. (1997) Adipose differentiation-related protein is an ubiquitously expressed lipid storage droplet-associated protein. *J. Lipid Res.*, **38**, 2249-2263.

- Bruckner, J. V., MacKenzie, W. F., Muralidhara, S., Luthra, R., Kyle, G. M., and Acosta, D. (1986) Oral toxicity of carbon tetrachloride: acute, subacute, and subchronic studies in rats. *Fund. Appl. Toxicol.*, **6**, 16-34.
- Castro, J. A., De Ferreyra, E. C., De Castro, C. R., De Fenos, O. M., Sasame, H., and Gillette, J. R. (1974) Prevention of carbon tetrachloride-induced necrosis by inhibitors of drug metabolism--further studies on their mechanism of action. *Biochem. Pharmacol.*, **23**, 295-302.
- Chan, H. Y., Zhang, Y., Hoheisel, J. D., and O'Kane, C. J. (1998) Identification and characterization of the gene for *Drosophila* L3 ribosome protein. *Gene*, **212**, 119-125.
- Chaplin, M. D., and Mannering, G. J. (1970) Role of phospholipids in the hepatic microsomal drug-metabolizing system. *Mol. Pharmacol.*, **6**, 631-640.
- Cho, Y. J., Meade, J. D., Walden, J. C., Chen, X., Guo, Z., and Liang, P. (2001) Multicolor fluorescent differential display. *Biotechniques*, **30**, 562-572.
- Chopra, P., Roy, S., Ramalingaswamin, V., and Nayak, N. C. (1972) Mechanism of carbon tetrachloride hepatotoxicity: an *in vivo* study of its molecular basis in rats and monkeys. *Lab. Invest.*, **26**, 716-727.
- Clark, A. J., Clissold, P. M., A. Shawi, R., Beattie, P., and Bishop, J. (1984) Structure of mouse major urinary protein genes: different splicing configurations in the 3'-non-coding region. *EMBO. J.*, **3**, 1045-1052.
- Denison, M. S., and Whitlock, J. P. (1995) Xenobiotic-inducible transcription of cytochrome P450 genes. *J. Biol. Chem.*, **270**, 18175-18178.
- DeRisi, J. L., Iyer, V. R., and Brown, P. O. (1997) Exploring the metabolic and genetic control of gene expression on a genomic scale. *Science*, **278**, 680-686.
- Dragani, T. A., Manenti, G., Sacchi, M. R., Colombo, B. M., and Della Porta, G. (1989) Major urinary protein as a negative tumor marker in mouse hepatocarcinogenesis. *Mol. Carcinog.*, **2**, 355-360.
- Environmental Protection Agency (1984) Health assessment document for carbon tetrachloride. EPA-600/8-82-001F, Cincinnati, OH.
- Fleming, L. E., Hodgson, M., Ambre, J., Becker, C., Borak, J., Cannella, J., Kipen, H., Jackson, R. J., Rodnick, J., and Wummer, B. A. (1995) Case studies in environmental medicine: carbon tetrachloride toxicity. *Environmental Medicine*, **8**, 251, National Academic Press, Washington, D. C.
- Franco, G. R., Adams, M. D., Soares, M. B., Simpson, A. J., Venter, J. C., and Pena, S. D. (1995) Identification of new *Schistosoma mansoni* genes by the EST strategy using a directional cDNA library. *Gene*, **152**, 141-147.



- Gao, J., Ye, H., and Serrero, G. (2000) Stimulation of adipose differentiation related protein (ADRP) expression in adipocyte precursors by long-chain fatty acids. *J. Cell. Physiol.*, **182**, 297-302.
- Goldsworthy, S. M., Goldsworthy, T. L., Sprankle, C. S., and Butterworth, B. E. (1993) Variation in expression of genes used for normalization of Northern blots after induction of cell proliferation. *Cell Prolif.*, **26**, 511-517.
- Gram, T. E., and Gillette, J. R. (1971) Bio-transformation of drugs. In: Fundamentals of biochemical pharmacology, 571-609, Pergamen Press, New York.
- Hall, M., and Schillinger, J. (1923) Miscellaneous tests of carbon tetrachloride as an anthelmintic. *J. Agric. Res.*, **23**, 163-192.
- Herman, I. M. (1993) Actin isoforms. *Curr. Opin. Cell Biol.*, **5**, 48-55.
- Holman, R. T. (1954) Autooxidation of fats and related substances. In: Progress in the chemistry of fats and other lipids. Vol. 2, 251-265, Academic Press, New York.
- Hong, S. W., and Park, C. (1997) The effect of aflatoxin B1 on the expression of early response genes and transforming growth factor-alpha in CCl<sub>4</sub> induced rat liver injury. *Yonsei. Med. J.*, **38**, 167-177.
- Huether, S. E., and McCance, K. L. (1996) Altered cellular and tissue biology. In: Understanding pathophysiology, 73-74, Von Hoffmann Press, St. Louis, Missouri.
- Ikeda, K., Kawada, N., Wang, Y. Q., Kadoya, H., Nakatani, K., Sato, M., and Kaneda, K. (1998) Expression of cellular prion protein in activated hepatic stellate cells. *Am. J. Pathol.*, **153**, 1695-1700.
- Ito, T., Kito, K., Adati, N., Mitsui, Y., Hagiwara, H., and Sakaki, Y. (1994) Fluorescent differential display: arbitrarily primed RT-PCR fingerprinting on an automated DNA sequencer. *FEBS Lett.*, **351**, 231-236.
- Janbaz, K. H., and Gilani, A. H. (1999) Potentiation of paracetamol and carbon tetrachloride-induced hepatotoxicity in rodents by the food additive vanillin. *Food and Chem. Toxicol.*, **37**, 603-607.
- Jeong, H. Y., Cho, G. B., Han, K. Y., Kim, J., Han, D. M., Jahng, K. Y., and Chae, K. S. (2001) Differential expression of house-keeping genes of *Aspergillus nidulans* during sexual development. *Gene*, **262**, 215-219.
- Jiang, H. P., and Serrero, G. (1992) Isolation and characterization of a full-length cDNA coding for an adipose differentiation-related protein. *Proc. Natl. Acad. Sci.*, **89**, 7856-7860.

- Juchau, M. R., Boutelet-Bochan, H., and Huang, Y. (1998) Cytochrome-P450-dependent biotransformation of xenobiotics in human and rodent embryonic tissues. *Drug Metab. Rev.*, **30**, 541-568.
- Kim, K. Y., Choi, I., and Kim, S. S. (2000) Progression of hepatic stellate cell activation is associated with the level of oxidative stress rather than cytokines during CCl<sub>4</sub>-induced fibrogenesis. *Mol. Cells*, **30**, 289-300.
- Klaassen, C. D., and Plaa, G. L. (1966) Relative effects of various chlorinated hydrocarbons on liver and kidney function in mice. *Toxicol. Appl. Pharmacol.*, **9**, 139-151.
- Kluwe, W. M., Hook, J. B., and Bernstein, J. (1982) Synergistic toxicity of carbon tetrachloride and several aromatic organohalide compounds. *Toxicology*, **23**, 321-336.
- Krauter, K., Leinwand, L., D'Eustachio, P., Ruddle, F., and Darnell, J. E. (1982) Structural genes of the mouse major urinary protein are on chromosome 4. *J. Cell. Biol.*, **94**, 414-417.
- Kuwano, Y., and Wool, I. G. (1992) The primary structure of rat ribosome protein L3. *Biochem. Biophys. Res. Commun.*, **187**, 58-64.
- Laird, P. W., Zijderveld, A., Linders, K., Rudnicki, M. A., Jaenisch, R., and Berns, A. (1991) Simplified mammalian DNA isolation procedure. *Nucleic Acids Res.*, **19**, 4293.
- Lamson, P. D., and Wing, R. (1926) Early cirrhosis of the liver produced in dogs by carbon tetrachloride. *J. Pharmacol. Exp. Ther.*, **29**, 191-202.
- Lashkari, D. A., DeRisi, J. L., McCusker, J. H., Namath, A. F., Gentile, C., Hwang, S. Y., Brown, P. O., and Davis, R. W. (1997) Yeast microarrays for genome wide parallel genetic and gene expression analysis. *Proc. Natl. Acad. Sci.*, **94**, 13057-13062.
- Lee, S. S. T., Buters, J. T. M., Pineau, T., Fernandez-Salguero, P., and Gonzalez, F. J. (1996) Role of CYP2E1 in the hepatotoxicity of acetaminophen. *J. Biol. Chem.*, **271**, 12063-12067.
- Lee, W. S. (2000) Identification of peroxisome proliferator-activated receptor alpha (PPAR  $\alpha$ )-dependent genes involved in peroxisome proliferator-induced pleiotropic responses using fluorescent differential display. MPhil. thesis, 60, The Chinese University of Hong Kong, Hong Kong.
- Letteron, P., Labbe, G., Degott, C., Berson, A., Fromenty, B., Delaforge, M., Larrey, D., and Pessayre, D. (1990) Mechanism for the protective effects of silymarin against carbon tetrachloride-induced lipid peroxidation and hepatotoxicity in mice. Evidence that silymarin acts both as an inhibitor of metabolic activation and as a chain-breaking antioxidant. *Biochem. Pharmacol.*, **39**, 2027-2034.

- Liang P., and Pardee, A. B. (1992) Differential display of eukaryotic messenger RNA by means of the polymerase chain reaction. *Science*, **257**, 967-971.
- Lindros, K. O., Cai, Y. A., and Penttila, K. E. (1990) Role of ethanol-inducible cytochrome P-450 IIE1 in carbon tetrachloride-induced damage to centrilobular hepatocytes from ethanol-treated rats. *Hepatology*, **12**, 1092-1097.
- Manno, M., Rezzadore, M., Grossi, M., and Sbrana, C. (1996) Potentiation of occupational carbon tetrachloride toxicity by ethanol abuse. *Hum. Exp. Toxicol.*, **15**, 294-300.
- Martin, K. J., Kwan, C. P. and Sager, R. (1997) A direct-sequencing-based strategy for identifying and cloning cDNAs from differential display gel. In: *Methods in molecular biology, differential display methods and protocols*, 77-85, Human Press, Totowa, New Jersey.
- McGregor, D., and Lang, M. (1996) Carbon tetrachloride: genetics effects and other modes of action. *Mutat. Res.*, **366**, 181-195.
- McLean, E. K., McLean, A. E., and Sutton, P. M. (1969) Instant cirrhosis: an improved method for producing cirrhosis of the liver in rats by simultaneous administration of carbon tetrachloride and phenobarbitone. *Br. J. Exp. Pathol.*, **50**, 502-506.
- Morigasaki, S., Li, F., Kawai, A., Yamazaki, K., Sikdar, D., Hibino, Y., and Hiraga, K. (2000) Interaction of albumin mRNA with protein from rat liver with CCl<sub>4</sub>-induced injury. *Biochem. Biophys. Res. Commun.*, **273**, 261-266.
- Mou, L., Miller, H., Li, J., Wang, E., and Chalifour, L. (1994) Improvements to the differential display method for gene analysis. *Biochem. Biophys. Res. Comm.*, **199**, 564-569.
- Murakawa, K., Matsubara, K., Fukushima, A., Yoshii, J., and Okubo, K. (1994) Chromosomal assignments of 3'-directed partial cDNA sequences representing novel genes expressed in granulocytoid cells. *Genomics*, **23**, 379-389.
- Nebert, D. W. (1990) Drug metabolism. Growth signal pathways. *Nature*, **25**, 709-710.
- Nebert, D. W., Nelson, D. R., and Feyereisen, R. (1989) Evolution of the cytochrome P450 genes. *Xenobiotica*, **19**, 1149-1160.
- Ohyama, T., Tagashira, H., and Tsujibayashi, H. (1997) Easy screening of recombinant plasmids. *Elsevier Trends Journals Technical Tips Online*, **96**, 40073-40077.
- Padma, P., and Setty, O. H. (1999) Protective effect of *Phyllanthus fraternus* against carbon tetrachloride-induced mitochondrial dysfunction. *Life Sci.*, **64**, 2411-2417.
- Panduro, A., Shalaby, F., Weiner, F. R., Biempica, L., Zern, M. A., and Shafritz, D. A. (1986) Transcriptional switch from albumin to alpha-fetoprotein and changes in



transcription of other genes during carbon tetrachloride induced liver regeneration. *Biochemistry*, **25**, 1414-1420.

Pencil, S. D., Brattin, W. J., Glende, E. A., and Recknagel, R. O. (1984) Evidence against involvement of calcium in carbon tetrachloride-dependent inhibition of lipid secretion by isolated hepatocytes. *Biochem. Pharmacol.*, **33**, 2425-2429.

Raucy, J. L., Kraner, J. C., and Lasker, J. M. (1993) Bioactivation of halogenated hydrocarbons by cytochrome P4502E1. *Crit. Rev. Toxicol.*, **23**, 1-20.

Ray, S. D., and Mehendale, H. M. (1990) Potentiation of CCl<sub>4</sub> and CHCl<sub>3</sub> hepatotoxicity and lethality by various alcohols. *Fund. Appl. Toxicol.*, **15**, 429-440.

Recknagel, R. O. (1967) Carbon tetrachloride hepatotoxicity. *Pharmacol. Rev.*, **19**, 145-208.

Recknagel, R. O., and Ghoshal, A. K. (1966) Lipoperoxidation as a vector in carbon tetrachloride hepatotoxicity. *Lab Invest.*, **15**, 132-48.

Recknagel, R. O., and Glende, E. A. (1973) Carbon tetrachloride hepatotoxicity: an example of lethal cleavage. *CRC Crit Rev. Toxicol.*, **2**, 263-297.

Recknagel, R. O., Glende, E. A., Dolak, J. A., and Waller, R. L. (1989) Mechanisms of carbon tetrachloride toxicity. *Pharmacol. Ther.*, **43**, 139-154.

Rubin, E., and Popper, H. (1967) The evolution of human cirrhosis deduced from observations in experimental animals. *Medicine*, **46**, 163-183.

Ruprah, M., Mant, T. G., and Flanagan, R. J. (1985) Acute carbon tetrachloride poisoning in 19 patients: implications for diagnosis and treatment. *Lancet*, **1**, 1027-1029.

Sambrook, J., Fritsch, E. F., and Maniatis, T. (1989). Molecular cloning, a laboratory manual, Cold Spring Harbor Laboratory Press, Cold Spring Harbor, New York.

Seidegard, J., and DePierre, J. W. (1982) The effect of trans-stilbene oxide and other structurally related inducers of drug-metabolizing enzymes on glucuronidation. *Chem. Biol. Interact.*, **40**, 15-25.

Shahan, K., Denaro, M., Gilmartin, M., Shi, Y., and Derman, E. (1987) Expression of six mouse major urinary protein genes in the mammary, parotid, sublingual, submaxillary, and lachrymal glands and in the liver. *Mol. Cell. Biol.*, **7**, 1947-1954.

Shahan, K., and Derman, E. (1984) Tissue-specific expression of major urinary protein (MUP) genes in mice: characterization of MUP mRNAs by restriction mapping of cDNA and by in vitro translation. *Mol. Cell. Biol.*, **4**, 2259-2265.

Shibayama, Y. (1988) Hepatotoxicity of carbon tetrachloride after chronic ethanol consumption. *Exp. Mol. Pathol.*, **49**, 234-242.



- Sinclair, P. R., Gorman, N., Walton, H. S., Bement, W. J., Szakacs, J., Gonzalez, F. J., Dalton, T. P., Nebert, D. W., and Sinclair, J. F. (2000) Relative roles of CYP2E1 and CYP1A2 in mouse uroporphyrin caused by acetone. *Arch Biochem. Biophys.*, **384**, 383-390.
- Slater, T. F. (1982) Lipid peroxidation. *Biochem. Soc. Trans.*, **10**, 70-71.
- Smejkalova, J., Simek, J., Rouchal, J., and Dvorackova, I. (1985) The time course of biochemical and histological changes following carbon tetrachloride-induced liver damage in rats of both sexes. *Physiol. Bohemoslov.*, **34**, 494-501.
- Steiner, S., Wahl, D., Mangold, B. L., Robinson, R., Raymakers, J., Meheus, L., Anderson, N. L., and Cordier, A. (1996) Induction of the adipose differentiation-related protein in liver of etomoxir-treated rats. *Biochem. Biophys. Res. Commun.*, **18**, 777-782.
- Stenger, R. J. (1966) Hepatic sinusoids in carbon tetrachloride-induced cirrhosis. An electron microscopic study. *Arch. Pathol.*, **81**, 439-447.
- Steup, D. R., Hall, P., McMillan, D. A., and Sipes, I. G. (1993) Time course of hepatic injury and recovery following coadministration of carbon tetrachloride and trichloroethylene in Fischer-344 rats. *Toxicol. Pathol.*, **21**, 327-334.
- Sundy, M. E. (1995) Differential display RT-PCR for identifying novel gene expression in the lung. *Am. J. Physiol.*, **269**, 273-284.
- Szlamka, I., Menyhart, J., and Somogyi, J. (1975) Relationship between lysosomal damage, fatty infiltration and hepatocellular necrosis in the course of acute liver injury induced by carbon tetrachloride in the rat. *Acta Physiol. Acad. Sci. Hung.*, **46**, 51-57.
- Tamayo, R. P. (1983) Is cirrhosis of the liver experimentally produced by CCl<sub>4</sub> an adequate model of human cirrhosis? *Hepatology*, **3**, 112-120.
- Thakker-Varia, S., Tozzi, C. A., Chari, S., Tiku, K., and Riley, D. J. (1999) Isolation of differentially expressed genes in hypertensive pulmonary artery of rats. *Exp. Lung Res.*, **25**, 689-699.
- Timbrell, J. A. (1991) Biochemical mechanisms of toxicity: specific examples. In: *Principles of biochemical toxicology*, 296-299, Taylor and Francis Press, London.
- Toh, B. H., Cauchi, M. N., and Muller, H. K. (1977) Actin-like contractile protein in carbon tetrachloride-induced cirrhosis in the rat. *Pathology*, **9**, 187-194.
- Tokunaga, K., Takeda, K., Kamiyama, K., Kageyama, H., Takenaga, K., and Sakiyama, S. (1988) Isolation of cDNA clones for mouse cytoskeletal gamma-actin and differential expression of cytoskeletal actin mRNAs in mouse cells. *Mol. Cell Biol.*, **8**, 3929-3933.

- Tomenson, J. A., Baron, C. E., O'Sullivan, J. J., Edwards, J. C., Stonard, M. D., Walker, R. J., and Fearnley, D. M. (1995) Hepatic function in workers occupationally exposed to carbon tetrachloride. *Occup. Environ. Med.*, **52**, 508-514.
- Travis, G. H., Milner, R. J., and Sutcliffe, J. G. (1989) Molecular neurobiological techniques. In: *Neuromethods*, Vol. 16, 49-78, Humana Press, Clifton, New Jersey.
- Tuchweber, B., Werringloer, J., and Kourounakis, P. (1974) Effect of phenobarbital or pregnenolone-16 $\alpha$ -carbonitrile (PCN) pretreatment on acute carbon tetrachloride hepatotoxicity in rats. *Biochem. Pharmacol.*, **1**, 513-518.
- Ugazio, G., Koch, R. R., and Recknagel, R. O. (1973) Reversibility of liver damage in rats rendered resistant to carbon tetrachloride by prior carbon tetrachloride administration: bearing on the lipoperoxidation hypothesis. *Exp. Mol. Pathol.*, **18**, 281-289.
- Velculescu, V. E., Zhang, L., Vogelstein, B., and Kinzler, K. W. (1995) Serial analysis of gene expression. *Science*, **270**, 484-487.
- Watson, J. B. and Margulies, J. E. (1996) Differential cDNA screening strategies to identify novel stage-specific proteins in the developing mammalian brain. *Develop. Neuro.*, **15**, 77-86.
- Wong, F. W., Chan, W. Y., and Lee, S. S. (1998) Resistance to carbon tetrachloride-induced hepatotoxicity in mice which lack CYP2E1 expression. *Toxicol. Appl. Pharmacol.*, **153**, 109-118.
- Yamada, Y., Karasaki, H., Matsushima, K., Lee, G. H., and Ogawa, K. (1999) Expression of an IL-1 receptor antagonist during mouse hepatocarcinogenesis demonstrated by differential display analysis. *Lab Invest.*, **79**, 1059-1067.
- Zangar, R. C., Benson, J. M., Burnett, V. L., and Springer, D. L. (2000) Cytochrome P450 2E1 is the primary enzyme responsible for low-dose carbon tetrachloride metabolism in human liver microsomes. *Chem. Biol. Interact.*, **125**, 233-243.
- Zhang, J. S., Duncan, E. L., Chang, A. C. M., and Redde, R. R. (1998) Differential display of mRNA. *Mol. Biotech.*, **10**, 155-165.
- Zhao, S., Ooi, S. L., and Pardee, A. B. (1995) New primer strategy improves precision of differential display. *Biotechniques*, **18**, 842-850.



CUHK Libraries



003871600